7-2018

Type 2 Bovine Viral Diarrhea Virus N^{pro} Suppresses Type I Interferon Pathway Signaling in Bovine Cells and Augments Bovine Respiratory Syncytial Virus Replication

Abdulrahman Abdulaziz A. Alkheraif
University of Nebraska-Lincoln, aaboyousef@hotmail.com

TYPE 2 BOVINE VIRAL DIARRHEA VIRUS N^{pro} SUPPRESSES TYPE I INTERFERON PATHWAY SIGNALING IN BOVINE CELLS AND AUGMENTS BOVINE RESPIRATORY SYNCYTIAL VIRUS REPLICATION

by

Abdulrahman Abdulaziz A. Alkheraif

A DISSERTATION

Presented to the Faculty of

The Graduate College at the University of Nebraska

In Partial Fulfillment of Requirements

For the Degree of Doctor of Philosophy

Major: Integrative Biomedical Sciences

Under the Supervision of Professor Clayton L. Kelling

Lincoln, Nebraska

July, 2018

TYPE 2 BOVINE VIRAL DIARRHEA VIRUS N^{pro} SUPPRESSES TYPE I INTERFERON PATHWAY SIGNALING IN BOVINE CELLS AND AUGMENTS BOVINE RESPIRATORY SYNCYTIAL VIRUS REPLICATION

Abdulrahman Abdulaziz A. Alkheraif, Ph.D.

University of Nebraska, 2018

Advisor: Clayton L. Kelling, Ph.D.

Bovine viral diarrhea virus (BVDV) and bovine respiratory syncytial virus (BRSV) infections contribute to the bovine respiratory disease complex (BRDC), which is a multi-factorial disorder involving co-infections of viruses and bacteria including mycoplasma. BRDC causes great economic losses to the United States feedlot industry. BVDV infection induces immunosuppression in infected animals. BVDV N^{pro} binds and degrades the transcription factor interferon regulatory factor-3 (IRF-3) and effectively blocks type I interferon (type I IFN) expression in host cells. BRSV nonstructural proteins, NS1 and NS2, block activation of IRF-3. In calves, concurrent infection with BVDV and BRSV resulted in more severe clinical signs of disease and extensive lung lesions than infection with either virus alone. The objective of this study was to extend the understanding of the role of the N^{pro} of noncytopathic BVDV-2 (pestivirus B) on type I IFN pathway signaling in bovine turbinate (BT) cells during single and co-infection with BRSV.

Based on real-time quantitative-reverse transcription-polymerase chain reaction, the BVDV-2 mutant with dysfunctional N^{pro} (BVDV2-E) significantly up-regulated protein kinase R (PKR), TANK-Binding Kinase 1, IRF-3, IRF-7, and interferon-β (IFN-β) mRNAs compared to BVDV-2 wild-type (BVDV2-wt) and BRSV in single and co-infected BT cells. BRSV-infected cells expressed significantly up-regulated PKR, IRF-3,

IRF-7, and IFN-β mRNAs, whereas BVDV2-wt, but not BVDV2-E, abolished this up-regulation in co-infection. No significant differences were observed in mitochondrial antiviral signaling, Nuclear Factor-κB (NF-κB), and NIMA-Interacting 1 mRNAs. A dual-luciferase reporter assay showed that BVDV2-wt significantly increased NF-κB activity compared to BVDV2-E, while BVDV2-E significantly increased IFN-β activity compared to BVDV2-wt. BT cells infected with BVDV2-E produced more IRF-3 protein compared to cells infected with BRSV or BVDV2-wt. The BRSV titer and RNA levels significantly increased in cells co-infected with BRSV/BVDV2-wt compared to cells co-infected with BRSV/BVDV2-E or infected with BRSV alone. BVDV2-E single and co-infected cells synthesized type I IFN significantly higher than BVDV2-wt single and co-infected BT cells. These findings are useful in defining the role of the intact BVDV-2 N^{pro} on type I IFN pathway signaling and support the understanding of the mechanism underlying the synergistic action of BVDV2-wt and BRSV inhibition of type I IFN. The inhibition of BRSV-induced signals by BVDV augments BRSV infection.

In the name of Allah (God) the most beneficent the most merciful

This Degree of Doctor of Philosophy (Ph.D.)

in Major: Integrative Biomedical Sciences

is Dedicated to

My extended family, Alkheraif.

The family of Kheraif bin Fawaz bin Abdullah Alkheraif.

From Al-Sabakh in the city of Buraydah, Al-Qassim, Saudi Arabia.

Thul-Qa'dah, 1439 for the noble Prophet's migration.
July, 2018.

Dedicated by\ Abo-Yousef Al-lobida.
Your son\ Abdulrahman bin Abdulaziz bin Abdulrahman Al-Abdullah (Al-lobida) Alkheraif.

ACKNOWLEDGMENTS

First of all, I thank God, Allah, for finishing my Ph.D. degree. With my loving memory of my mother, Norah Alothim, I would like to thank my father, Abdulaziz Alkheraif, who permitted me to leave him for continuous years to continue my study overseas. I am grateful for him.

I would also like to thank Dr. Jay Reddy, Dr. Matthew Wiebe, Dr. Samodha Fernando, and Dr. Christina Topliff, my Ph.D. committee members, for their suggestions and support. My deepest gratitude goes to my graduate advisor, Dr. Clayton Kelling, for extensive support, guidance, and the opportunity to work in his laboratory.

Special appreciation and thanks to Dr. Christina Topliff who spent numerous hours training, explaining, and editing my writing. I am grateful to the second reader. Dr. Reddy's reading and suggestions were very helpful. Thanks to the staff and students of the School of Veterinary Medicine and Biomedical Sciences, University of Nebraska – Lincoln. Also, thanks to the University of Qassim in my hometown for awarding me the scholarship.

I would finally like to thank my family, my wife Mona Almushayti, my sons Yousef, Albara, and Osayd, and our daughter Wujude, who have lived with me in Lincoln for years. Since they were with me here, I felt that living in Lincoln was just like living in my hometown Buraydah, Al-Qassim, Saudi Arabia. Thanks to the lovely people of this beloved city, Lincoln, Nebraska and I hope to have the chance to visit Lincoln again and again in the future.

PREFACE

Chapter 2 has been published in *Virology*. (Alkheraif AA, Topliff CL, Reddy J, Massilamany C, Donis RO, Meyers G, Eskridge KM, Kelling CL. Type 2 BVDV N(pro) suppresses IFN-1 pathway signaling in bovine cells and augments BRSV replication. *Virology*. 2017 Jul; 507:123-134. doi: 10.1016/j.virol.2017.04.015. Epub 2017 Apr 19. PubMed PMID: 28432927).

TABLE OF CONTENTS

TABLE OF FIGURES

TABLE OF ABBREVIATIONS

ACTB: actin-β (Beta-actin, β-Actin)
AEC Solution: 3-amino-9-ethyl-carbazole solution
AMP: Ampicillin
AT: alpaca testicular
avSG: antiviral stress granule
BRDC: bovine respiratory disease complex
BRSV: bovine respiratory syncytial virus
BRV: bovine rotavirus
BSA: bovine serum albumin
BT: bovine turbinate
BVDV: bovine viral diarrhea virus
BVDV-1: bovine viral diarrhea virus 1
BVDV-2: bovine viral diarrhea virus 2
BVDV2-E: BVDV-2 mutant with dysfunctional N^{pro}
BVDV2-wt: BVDV-2 wild-type
CA: State of California
CAT: chloramphenicol acetyltransferase
cDNA: complementary DNA
CMF-PBS: calcium and magnesium-free phosphate-buffered saline
Cp: cytopathic
CPE: cytopathic effects
Cq: quantification cycle
CSFV: classical swine fever virus
DC: dendritic cells
DENV2: dengue virus serotype 2
DMEM: Dulbecco's modified eagle medium (high glucose)
DMSO: dimethyl sulfoxide
DNA: deoxyribonucleic acid
DPI: days post-infection
dsRNA: double-stranded RNA
EGFP: enhanced green fluorescent protein

ELISA: enzyme-linked immunosorbent assay

FA: fluorescent antibody

GAPDH: Glyceraldehyde 3-phosphate dehydrogenase

gDNA: genomic DNA

H_2O_2: Hydrogen peroxide

HPI: hours post-infection

HRSV: human respiratory syncytial virus

HS: horse serum (equine serum)

IA: State of Iowa

IFN-1: type I interferon α/β

IFN-λ: type III interferon

IgG: immunoglobulin G

IHC: immunohistochemistry

IRF-3: interferon regulatory factor-3

IRF-7: interferon regulatory factor-7

IRF-9: interferon regulatory factor-9

ISGF3: IFN-stimulated gene factor 3

ISRE gene: IFN stimulated response element gene

kb: kilobases

LB: Luria-Bertani

mAb: monoclonal antibody

mAb 348: primary monoclonal antibody directed against BVDV-1 & BVDV-2 E2 (gp53)

mAb 8G12: primary monoclonal antibody directed against BRSV F protein

MAVS: mitochondrial antiviral signaling

MDBK: Madin-Darby bovine kidney

MD: mucosal disease

MDA5: melanoma-differentiation-associated gene 5

NC: State of North Carolina

NCL1-ISRE-Luc-Hygro cells: modified bovine uterus cells ISRE-Luc-Hygro

Ncp: noncytopathic

NF-κB: nuclear Factor-κB

NK: natural killer cells

No-RT: without reverse transcriptase

OAS 1: 2',5'-oligoadenylate synthetase 1

ORF: open reading frame

PBS: phosphate buffered saline

PI: persistently infected

PIN-1: NIMA-interacting 1

PKR: protein kinase R

pmol: picomolar (= 10^{-12} mol/L)

Poly I:C: polyinosinic-polycytidylic acid

PRRs: pattern-recognition receptors

PTC12: phenyl thiophene carboxamide derivative 12

Q-RT-PCR: quantitative-reverse transcription-polymerase chain reaction

QC-RT-PCR quantitative competitive-reverse transcription-polymerase chain reaction

Real-time Q-RT-PCR: Real-time quantitative-RT-PCR

RIG: retinoic acid-inducible gene

RLR: (RIG)-like receptors

RLU: relative light units

RNA: ribonucleic acid

RPS18: ribosomal protein S18 (bovine)

RSV: respiratory syncytial virus

RT: reverse transcriptase

RT-PCR: reverse transcription-polymerase chain reaction

SDS: sodium dodecyl sulfate

SH: small hydrophobic

STAT1: signal transducer and activator of transcription 1

STAT2: signal transducer and activator of transcription 2

TBK-1: TANK-binding kinase 1

TBS-T: Tris buffer saline with 0.1% Tween® 20

Th1: T helper1 cells

Type I IFN: type I interferon α/β

UI cells: uninfected cells

upH_2O: Ultrapure water

UPW: Ultrapure water

UT: State of Utah

UTR: untranslated region

VI: virus isolation

INTRODUCTION

Bovine viral diarrhea virus (BVDV) is a significant pathogen of cattle worldwide and an endemic virus in North America causing continuous economic losses to the cattle industry primarily due to decreased reproductive performance. BVDV infections are associated with gastrointestinal, respiratory, and reproductive diseases and because of its ability to cross the placenta during early pregnancy, it can result in the birth of persistently infected (PI) calves. BVDV N^{pro} prevents the production of type I interferon α/β (type I IFN) by suppressing levels of interferon regulatory factor-3 (IRF-3) to avoid host antiviral responses (Hilton *et al.,* 2006; Horscroft *et al.,* 2005). Bovine respiratory syncytial virus (BRSV) is the major cause of pneumonia in calves, especially during the first year of life but reinfection can occur at any age. Nonstructural proteins, NS1 and NS2, of BRSV block activation of IRF-3.

BVDV and BRSV infections contribute to the bovine respiratory disease complex (BRDC), which has a major negative impact on animal well-being. Concurrent infection with BVDV and BRSV in cattle causes more severe respiratory tract disease compared to single infection with either virus alone (Brodersen and Kelling, 1998). Type I IFN activates many genes that transcribe new proteins that inhibit virus replication. Viruses can interfere with components of the type I IFN induction and signaling pathway to subvert the innate immune system. We recently determined that enhancement of BRSV replication by BVDV co-infection was associated with BVDV N^{pro} antagonism of type I IFN production (Alkheraif *et al.,* 2017).

Type I IFN induction is mediated by IFN regulatory factors that are transmitted via a pathway dependent upon intracellular receptors known as retinoic acid-inducible gene (RIG)-like receptors (RLR), located in the cell cytoplasm. These receptors bind viral dsRNA resulting in activation of type I IFN induction cell signals, including mitochondrial antiviral signaling (MAVS), TANK-Binding Kinase 1 (TBK-1), protein kinase R (PKR), interferon regulatory factor-3 (IRF-3), IRF-7, and Nuclear Factor-κB (NF-κB). These signals activate transcription and play key roles among numerous adaptor molecules in complex pathways that culminate in the production of type I IFN (Peterhans and Schweizer, 2013). The interaction of viral dsRNA and RLRs induces interaction with their adaptor protein, MAVS, activating TBK-1, which induces the phosphorylation of IRF-3 and IRF-7. Homodimers and heterodimers of IRF-3/7 translocate to the nucleus to activate the transcription of type I IFN genes.

The effects of BVDV N^{pro} on type I IFN pathway signaling in cells infected with BVDV or co-infected with BVDV and another viral pathogen, such as BRSV, has not been previously studied. In this study, we hypothesized that BVDV-2 N^{pro} enhances virulence and modulates host cell innate immune responses which augment BRSV replication during co-infection with BVDV. Our main objectives were:

1. To characterize the effects of BVDV N^{pro} on type I IFN induction cell signals in IFN antagonism during BVDV infections. These cell signals include MAVS, PKR, TBK-1, IRF-3, IRF-7, IFN, NF-κB and NIMA-Interacting 1 (PIN-1).

2. To identify BVDV immunomodulatory proteins and host cell responses which are important to increased virulence of BRSV and the effects of BVDV N^{pro} on type I IFN cell signaling in IFN antagonism and enhancement of BRSV replication during co-infections with BVDV.

To elucidate the BRSV effects and the role of BVDV N^{pro} on these type I IFN induction cell signals and the mechanisms by which BVDV infection enhances the effects of BRSV infection, we propose to characterize type I IFN pathway signaling in bovine turbinate (BT) cells infected with BRSV, BVDV-2 wild-type (BVDV2-wt), or BVDV-2 mutant with dysfunctional N^{pro} (BVDV2-E) or co-infected with BRSV/BVDV2-wt or BRSV/BVDV2-E. To evaluate the mRNA levels of the cell signals, total RNA was extracted from these infected and co-infected BT cells and real-time quantitative-reverse transcription-polymerase chain reaction (Q-RT-PCR) was performed. The results were normalized against two reference genes, glyceraldehyde 3-phosphate dehydrogenase (GAPDH) and bovine ribosomal protein S18 (RPS18). IFN-β and NF-kB activities were determined using a Dual-luciferase reporter assay. Synthesized type I IFN and IRF-3 protein production were evaluated.

CHAPTER 1:

LITERATURE REVIEW

Bovine Viral Diarrhea Virus (BVDV)

Bovine viral diarrhea virus (BVDV) is a member of the genus *Pestivirus* within the family *Flaviviridae.* The genus *Pestivirus* also includes classical swine fever virus (CSFV, pestivirus C) and border disease virus (pestivirus D) of sheep (Simmonds *et al.*, 2017; Smith *et al.*, 2017; Wengler, 1991). BVDV is commonly associated with cattle, but infection has also been reported in pigs (Liess and Moennig, 1990; Løken, 1995), deer (Frölich and Hofmann, 1995; Raizman *et al.*, 2009), other domesticated and exotic ungulates including sheep (Løken, 1995; Silveira *et al.*, 2018), and new world camelids (Belknap *et al.*, 2000), such as alpacas (Topliff *et al.*, 2009). BVDV was first identified in New York State from cattle with gastroenteritis, diarrhea, and abortion (Olafson *et al.*, 1946). BVDV infection is endemic and causes economic loss. In BVDV infected herds, 60-85% of the cattle are antibody positive and 1-2% of the cattle are persistently-infected (PI). Persistently-infected animals are the common source of the virus and spread the virus by direct contact to other susceptible animals (Houe, 1999). Estimates of economic losses due to BVDV vary depending on the immune status of the animal and the virulence of the infecting virus strains. Annual losses due to BVDV are estimated at $20 per calving due to a low-virulent BVDV strain with an estimated annual incidence of acute infections of 34%. Annual losses are estimated at $75 per calving due to a high-virulent BVDV strain at the same incidence of infection (Houe, 1999). BVDV infection

in dairies decreases milk production, reproductive performance and growth while increasing occurrence of other diseases and mortality among calves. At the national level, it is estimated that the losses in dairies due to BVDV infection range between $10 and $40 per calving (Houe, 2003). The mortality rates associated with infectious disease are significantly higher in feedlot cattle positive for BVDV-1 (Booker *et al.*, 2008).

BVDV Types and Genome

BVDV isolates belong to one of two species, pestivirus A (bovine viral diarrhea virus 1, BVDV-1) or pestivirus B (BVDV-2), within the genus *Pestivirus*. Within each BVDV species, there are two biotypes, cytopathic (cp) and noncytopathic (ncp), based on their effects in cell culture (Mendez *et al.*, 1998). The genus *Pestivirus* has four species, pestivirus A, B, C, and D, but it has been recently proposed to create seven new species in addition to the current four species. The new designation includes pestivirus E, F, G, H, I, J, and K (Smith *et al.*, 2017). There are currently more than thirty BVDV genomes that have been completely sequenced. Recently in Italy, Colitti *et al.*, 2018 sequenced the complete genome of ncp BVDV-2 strain CN10.2015.821, which was isolated from a PI calf (Colitti *et al.*, 2018). BVDV species are designated based on sequence differences of the 5' untranslated region (UTR). Antigenic and pathological differences exist between BVDV-1 and BVDV-2 species (Ridpath *et al.*, 1994). Monoclonal antibodies specific for BVDV-2 demonstrated no or weak cross-reaction with BVDV-1 (Deregt *et al.*, 1998). In the 5' UTR, two nucleotide substitutions were identified distinguishing between eight isolates of low and high virulence BVDV-2. A cytosine at position 219 and a uracil at position 278 was present in the low virulence isolates, while the opposite was observed in

the high virulence isolates (Topliff and Kelling, 1998). Cp strains of BVDV induce apoptosis of cells *in vitro*, whereas ncp strains do not (Hoff and Donis, 1997; Yamane *et al.*, 2006). Viral proteins of ncp BVDV protect cells from induction of apoptosis by other factors, such as synthetic molecules or other viral infections. Ncp BVDV strains decrease type I interferon (type I IFN) *in vitro* more effectively than cp strains (Schweizer and Peterhans, 2001). Unlike cp BVDV strains, ncp BVDV strains may cause persistent infection in calves that get infected early in gestation. These PI calves will be immunotolerant and shed virus throughout their lifetime (Bolin *et al.*, 1990).

BVDV has a single-stranded, positive-sense RNA genome of approximately 12.5 kilobases (kb). It consists of a large open reading frame (ORF) with a UTR on both the 5' and 3' ends (Ridpath and Bolin, 1995). The BVDV viral proteins from 5' to 3' are: N^{pro} – C – E^{rns} – E1 – E2 – P7 – NS2 – NS3 – NS4A – NS4B – NS5A – NS5B (Collett *et al.*, 1991; Tautz *et al.*, 2015). The BVDV genome encodes four structural (C, E^{rns}, E1, and E2) and eight non-structural (N^{pro}, P7, NS2, NS3, NS4A, NS4B, NS5A, and NS5B) proteins (Collett *et al.*, 1988; Donis *et al.*, 1988; Meyers and Thiel, 1996; Thiel *et al.*, 1991). The main differences in genomic organization between ncp and cp BVDV are rearrangements in the NS2/NS3 region of the genome. By a variety of mechanisms, such as cellular RNA insertions, cp BVDV arises by RNA recombination of ncp BVDV (Qi *et al.*, 1992; Ridpath and Bolin, 1995; Tautz *et al.*, 1994). Unlike in cp BVDV, the NS2/NS3 region is not cleaved in ncp BVDV (Greiser-Wilke *et al.*, 1992). The soluble form of the envelope glycoprotein E^{rns} of pestivirus degrades immunostimulatory viral single- and double-stranded RNA and inhibits ss- and dsRNA-induced type I IFN synthesis (Lussi and Schweizer, 2016).

N^{pro} of BVDV and Host Interferon

The autoprotease, N^{pro}, is a NS protein that has proteolytic properties and cleaves itself from the capsid protein between Cys_{168} and Ser_{169} of the polyprotein (Stark *et al.*, 1993). Only pestiviruses within the family *Flaviviridae* have a NS protein at the N-terminus of the polyprotein. The essential amino acids for the proteolytic activity of N^{pro} are Cys_{69}, His_{49}, and Glu_{22} (Rumenapf *et al.*, 1998). Viruses can be attenuated by deleting or mutating the N^{pro} (Tratschin *et al.*, 1998). The growth kinetics of a BVDV chimeric virus in which the N^{pro} region was replaced with the hepatitis C virus (genus *Hepacivirus* in the family *Flaviviridae*) NS3 gene, resulting in the N^{pro} enzymatic activity with a serine protease, were similar to the wild-type BVDV. However, the growth kinetics and replication of an N^{pro}-null BVDV virus (entire N^{pro} region deleted) were much lower than the wild-type BVDV, but still viable (Lai *et al.*, 2000). A ncp BVDV, attenuated by deleting N^{pro}, showed reduced virulence in experimentally infected calves compared to wild-type BVDV, however, no difference in type I IFN induction was observed (Henningson *et al.*, 2009).

Interferons (IFNs), inducible cytokines, are a major component of innate immunity and a bridge between innate and adaptive immunity. They are produced by almost every type of nucleated cell, especially immunological cells including B and T cells. There are three types of IFNs classified as type I, including subtypes α and β, type II, including subtype γ, and type III, including subtype λ. Type I IFN is the innate immune response to viral infection or dsRNA exposure of cells and activates cellular factors to degrade viral RNA and shut down viral mRNA synthesis (Bautista *et al.*, 2005; Castelli *et al.*, 1997). Type I IFN has control effects on viral infection through its action

on cells to assist in the production and activation of constitutively expressed cellular protein kinase R (PKR) (Clemens and Elia, 1997; Wang *et al.*, 2003). In addition, type I IFN controls some cellular functions such as inducing dendritic cell (DC) differentiation and stimulating proliferation and class switching of B cells (Jego *et al.*, 2003; Litinskiy *et al.*, 2002; Paquette *et al.*, 2002; Tough, 2004). Type I IFN also stimulates the motility, differentiation, and cross-priming of T cells, enhances the cytotoxicity of natural killer (NK) cells, stimulates the production of inflammatory cytokines or nitric oxide, and affects the capacity of type II IFN to activate phagocytes (Biron, 2001; Bogdan, 2000; Foster *et al.*, 2004; García-Sastre and Biron, 2006; Le Bon *et al.*, 2003; Rogge *et al.*, 1998; Sato *et al.*, 2001). DC, NK, and T helper1 (Th1) cells produce type II IFN. Unlike type I IFN, type II IFN is not directly inducible by viral infection (Munder *et al.*, 1998). The first characterization of type III IFN (IFN-λ) was in 2002 with similar activity to, but independent of, type I IFN. In several human cell lines and tissues, type III IFN RNA, like type I IFN RNA, was inducible by viral infection (Kotenko *et al.*, 2003). Type III IFN also has antiviral activity in viral infected animals preventing them from sickness and weight loss (Bartlett *et al.*, 2005).

In both BVDV and CSFV, the amino-terminal cysteine protease, N^{pro}, prevents the production of type I IFN by suppressing levels of interferon regulatory factor-3 (IRF-3) to avoid host antiviral responses (Horscroft *et al.*, 2005). Even though IRF-3 can be relocated from the cytoplasm to the nucleus in BVDV-infected cells, N^{pro} blocks IRF-3 protein binding to DNA and directs the degradation of the protein IRF-3 by proteasomes, but not IRF-3 mRNA. The autoprotease activity of N^{pro} is not required for IFN inhibition (Hilton *et al.*, 2006; Seago *et al.*, 2007). Infection of cells with ncp BVDV having a

functional N^{pro} interferes with type I IFN production *in vitro*, while *in vivo* BVDV induces a sustained IFN (alpha, beta, and gamma) production in postnatal animals (Charleston *et al.*, 2002).

Many studies have evaluated the role of N^{pro} on evasion of the innate immune response of host cells infected with CSFV or BVDV. Host cells produce type I IFN in response to viral infection, and macrophages are important IFN producers (Roberts *et al.*, 1979). Studies using polyinosinic-polycytidylic acid (poly I:C), a synthetic dsRNA that induces IFN, have shown a novel function of N^{pro} against the cellular innate immune system. Wild-type CSFV protects macrophages and the porcine kidney cells, PK-15, stimulated with poly I:C from poly I:C-induced apoptosis and prevents poly I:C-induced type I IFN production; in contrast, N^{pro}-deleted mutants did not (Ruggli *et al.*, 2003). Preventing type I IFN production requires the presence of BVDV N^{pro} in cell culture. Infection of DCs, a major link between innate and adaptive immunity, with cp and ncp N^{pro}-deleted CSFV mutants resulted in increased type I IFN production and DC maturation with decreased replication of these mutants (Bauhofer *et al.*, 2005). In macrophages, monocytes, DCs, and calf testicle cells *in vitro*, type I IFN production was induced in cp BVDV infection; however, in ncp BVDV infection, type I IFN was suppressed (Adler *et al.*, 1997; Baigent *et al.*, 2002; Glew *et al.*, 2003; Perler *et al.*, 2000). Other studies have reported that in infected cells, BVDV N^{pro} prevented IFN-β mRNA production (Chen *et al.*, 2007; Hilton *et al.*, 2006). In pregnant cows, experimentally infected with ncp BVDV-2 at gestation day 75, type I IFN was increased and virus was cleared in approximately two weeks; however, fetuses were persistently infected (Smirnova *et al.*, 2008). By antagonism of type I INF, N^{pro} of BVDV plays a role

in evasion of the innate immune response. The N-terminal region of N^{pro} is necessary for this antagonism. Abolition of the ability of N^{pro} to suppress production of IFN was achieved by substituting amino acids E22 and H49. A mutant BVDV-1 strain NADL with modified N^{pro} fused with enhanced green fluorescent protein (EGFP) showed reduced antagonism of type I IFN synthesis indicating that the structural integrity of the BVDV N^{pro} amino terminus was important for type I IFN suppression, but not the enzymatic activity of the protein (Gil *et al.*, 2006a; Alkheraif *et al.*, 2017).

BVDV and Innate Immunity

Innate immunity is the first line of the host's immune system defying viral infection. Recombinant type I IFN inhibited CSFV replication in multiple cell lines (Xia *et al.*, 2005). Viruses, intracellular pathogens, have developed mechanisms to avoid the innate immunity and allow virus propagation and survival. BVDV double-stranded RNA (dsRNA) is a trigger of the innate immune response. Cp and ncp BVDV strains have different effects on the cell pathways of apoptosis and type I IFN production. Cp BVDV produces large amounts of dsRNA during viral replication *in vitro*, which stimulates activation of transcriptional factors and increases type I IFN production, while ncp BVDV does not (Alexopoulou *et al.*, 2001; Gil and Esteban, 2000; Yamane *et al.*, 2006). BVDV infection in alpaca testicular (AT) cells resulted in a 3 – 4 log $TCID_{50}$ decrease in infectivity compared to bovine cells. The limited permissiveness of BVDV infection in AT cells may be a result of greater type I IFN expression in the AT cells inhibiting replication. BVDV-1 infected alpaca cells synthesized greater levels of type I IFN following poly I:C stimulation compared to bovine cells (Samson *et al.*, 2011). In

experimentally infected pregnant heifers, ncp BVDV-2 induces IFN-gamma (IFN-γ) secretion during acute infection in fetuses while the BVDV RNA concentrations were decreased in PI fetal blood and tissues (Smirnova *et al.*, 2014). Between two and three weeks post maternal inoculation, IFN-γ mRNA was significantly elevated in fetal lymphatic tissues. Ncp BVDV titer in infected fetuses was reduced by the induction of type I IFN and IFN-γ (Hansen *et al.*, 2015).

Ncp BVDV prevents apoptosis to ensure its intracellular survival, while cp BVDV induces apoptosis to insure its spread (Grummer *et al.*, 1998; Hoff and Donis, 1997; Lambot *et al.*, 1998; Schweizer and Peterhans, 1999; Zhang *et al.*, 1996). During cp BVDV infection, the major population of cells undergoing apoptosis is monocytes (Lambot *et al.*, 1998). NS3 protein of cp BVDV plays a role in induction of apoptosis initiated by caspase-8 activation (St-Louis *et al.*, 2005). The NS3 protein of cp BVDV is present in its uncleaved form, NS23, in ncp BVDV. In cells stimulated with poly I:C, a potent inducer of apoptosis, ncp BVDV proteins were necessary to protect cells from apoptosis (Schweizer and Peterhans, 2001). A study examining the role of BVDV dsRNA showed that ncp BVDV suppressed apoptosis by inhibiting two dsRNA reactive cellular factors, dsRNA-dependent protein kinase R (PKR) and 2',5'-oligoadenylate synthetase 1 (OAS 1). PKR regulates RNA translation in the cell by inactivating the RNA translation factor, eIF2, through phosphorylation (Chawla-Sarkar *et al.*, 2003; Yamane *et al.*, 2006). In cp BVDV infection *in vitro,* initiation of apoptosis was correlated with the inhibition of the anti-apoptotic Bcl-2 protein, induction of the expression of caspase-12, and a decrease in intracellular glutathione levels (Jordan *et al.*, 2002). Ncp BVDV upregulates Bcl-2 anti-apoptosis protein and TNF-α (Bendfeldt *et al.*, 2003; Yamane *et al.*, 2005).

Cp BVDV-1 significantly up-regulated the radiation-inducible immediate-early response protein (IER3) and A20 (TNFAIP3), which may lead to blocking the NF-κB pathway. This possible blocking of NF-κB signaling pathway could partly explain the immunosuppression observed in cattle during BVDV infection (Villalba *et al.*, 2016). Prostaglandin A_1 (PGA_1) is capable of blocking the replication of CSFV and a wide variety of RNA and DNA viruses. A recent study reported that PGA_1 in MDBK cells inhibits the replication of BVDV. PGA_1 activity is attributed to the induction of heat shock proteins, HSP-70, and a mechanism targeting the small ribosomal subunit (40S) and the eukaryotic initiation factors eIF3s (Caldas *et al.*, 2018; Tsukimoto *et al.*, 2015). In enteric infection of neonatal calves, BVDV had direct and indirect roles. Host immunosuppression caused by BVDV enhances other infections. Calves with concurrent infection with BVDV and bovine rotavirus (BRV) had more severe enteric infection (villus atrophy and submucosal inflammation) than calves infected with either virus alone (Kelling *et al.*, 2002a).

BVDV Infections

BVDV infections range from subclinical to highly fatal clinical forms, which depend on host immune status, pregnancy status, fetal gestational age, and the influence of concurrent environmental stress factors. BVDV can cause a variety of syndromes including subclinical infections, clinical BVDV with enteric or respiratory disease, hemorrhagic syndrome, reproductive failure, congenital defects, persistent infection, and mucosal disease (Ames, 1986; Baker, 1995; Brownlie, 1990a; Brownlie, 1990b). Ruminant fetuses (calves and lambs) are very susceptible to transplacental BVDV

infection since they are agammaglobulinemic, immunologically immature, and have many immature organ systems with undifferentiated cells. BVDV can cause early embryonic death, abortion, stillbirth, malformation, congenital defects in the central nervous and ocular systems of fetuses, immunotolerance, and birth of seropositive animals (Done *et al.*, 1980; Kirkbride, 1992). Newborn calves and lambs can have low birth weights, may be weak, persistently viremic, and immunologically tolerant following exposure of the dam with ncp BVDV during gestation (Done *et al.*, 1980; Hewicker-Trautwein and Trautwein, 1994; Osburn and Castrucci, 1991).

Approximately 70-90% of BVDV infections are subclinical (Ames, 1986). Subclinically-infected dairy cows may exhibit a decrease in milk yield with more severe respiratory disease in their calves (Moerman *et al.*, 1994). During acute experimental clinical infection with BVDV-1, calves developed leukopenia, high fever, increased respiratory rates, viremia, and infection of the thymus (Kelling *et al.*, 2005). Calves acutely infected with BVDV developed mild clinical signs, including varying degrees of fever and anorexia, and lymphoid depletion in Peyer's patch. BVDV and its specific antigen were detected with high concentrations in the thymus, Peyer's patch, mesenteric lymph node, and the bone marrow. Platelet counts were significantly reduced and may result in thrombocytopenia during infection (Marshall *et al.*, 1996).

Hemorrhagic syndrome is due to infections with high virulence ncp BVDV-2 isolates. The syndrome is characterized by thrombocytopenia, hemorrhage, leukopenia, fever, diarrhea, and death (Carman *et al.*, 1998; Kelling *et al.*, 2002b; Pellerin *et al.*, 1994; Ridpath *et al.*, 1994). Common clinical findings include: diarrhea with blood and mucous, fever, anorexia, depression, dyspnea, and continued bleeding form injection

sites. Pathologically, findings may include leukopenia, and thrombocytopenia, but this is not consistently observed in every study (Kelling *et al.*, 2002b; Stoffregen *et al.*, 2000). Changes in platelet function were seen in animals infected with BVDV-1 and BVDV-2, and the platelet percentage, especially with BVDV-2, was decreased over time up to 12 DPI. Altered platelet function may be an important contributing factor for the hemorrhagic syndrome and for the increased virulence of some BVDV-2 isolates (Walz *et al.*, 2001).

Persistent Infection (PI)

Ncp BVDV strains can cross the placenta from the pregnant dam to the fetus (Fredriksen *et al.*, 1999; Harding *et al.*, 2002). Usually the fetus, infected *in utero* between 42-114 days of gestation, recognizes the viral antigens as a part of its immune system, and becomes persistently-infected and immunotolerant (Malmquist, 1968; McClurkin *et al.*, 1984) specifically to that BVDV strain, but immunocompetent to other heterologous BVDV strains (Bolin *et al.*, 1985a; Steck *et al.*, 1980). At day 97 of gestation, the IFN-γ concentrations increased at the peak of viremia in the PI fetus (Hansen *et al.*, 2015). PI calves are important BVDV reservoirs in the environment and shed BVDV lifelong, infecting healthy animals (Houe, 1995). In one recent clinical study, however, it was demonstrated that BVDV-1 transmission from PI neonate lamb to naïve sheep and cattle is limited (Evans *et al.*, 2018). Fetal PI was identified in 0.5% of calves in two dairy herds (Muñoz-Zanzi *et al.*, 2003) and 0.3% in feedlot herds (Loneragan *et al.*, 2005). In recent years, it has become evident that evasion of the innate immune response is essential to induce and maintain persistent infection (Lussi and

Schweizer, 2016). PI animals often show no lesions (Liebler-Tenorio *et al.*, 2004) and may not be distinguishable from other healthy calves. Some PI animals have increased secondary infections, growth retardation (Barber *et al.*, 1985; Stokstad and Løken, 2002) and increased mortality rates particularly in the first year of life (Duffell and Harkness, 1985; Houe, 1993). A wide spectrum of pathologic lesions in epithelial and non-epithelial cells may be caused by PI BVDV infections. Histopathological lesions are often rare, but may be seen in the kidneys, hepatic portal triads, lymphatic nodes, and mammary gland. PI calves also may display an abnormal hair coat and have shallow erosions, ulcers, and hemorrhage in the gastrointestinal tract. Oral and abomasal ulcers in cattle with PI have been reported (Bielefeldt-Ohmann, 1995; Shin and Acland, 2001). However, the architecture of lymphoid tissues and number of lymphoid cells are normal (Bielefeldt-Ohmann, 1988). BVDV infects many cell types of most organ systems including neural, epithelial, and lymphoid tissues (Bielefeldt-Ohmann, 1987; Hewicker *et al.*, 1990). In PI lymphoid cells, BVDV is detected in monocytes and T cells, but not in B cells (Lopez *et al.*, 1993). In the central nervous system of PI calves, BVDV has been found in the thalamic nuclei, hippocampus, entorhinal cortex, basal nuclei, and piriform cortex (Montgomery, 2007). BVDV has also been detected in the epithelial and non-epithelial cells of the gastrointestinal tract, liver, pancreas, spleen, lymph nodes, lung, kidney, adrenal gland, thymus, mammary glands, macrophages, ovary, uterus, placenta, fetal fluids, and semen (Bielefeldt-Ohmann, 1983; Confer *et al.*, 2005; Niskanen *et al.*, 2002; Shin and Acland, 2001).

Mucosal Disease (MD)

Recombination events between ncp and cp BVDV strains can generate new cp BVDV strains within PI animals (Becher *et al.*, 1999; Becher *et al.*, 2001; Bolin, 1995b; Ridpath and Bolin, 1995). These new cp BVDV strains superinfect PI animals causing a fatal disease called mucosal disease (MD). Clinical signs of MD include: fever, depression, anorexia, mucous nasal discharge, hemorrhage, weakness, elevated heart and respiratory rates, lesions in the mucosa of the digestive tract, and death (Bolin *et al.*, 1985b; Brownlie *et al.*, 1984; Dabak *et al.*, 2007). Even though MD can be seen in animals of all ages, it is commonly seen between 6 months and two years (Bolin, 1995b).

There are early onset and late onset MDs, depending on the duration between superinfection and the development of MD. If the cp BVDV isolate is closely related to the ncp BVDV isolate present in the PI animal, infection with the cp isolate will result in a rapid, early onset MD, which can occur within two weeks post inoculation (Moennig *et al.*, 1990). On the other hand, if there is less antigenic homology between ncp and cp isolates, a recombination event between them must occur to develop a late onset MD, which can occur months post inoculation (Fritzeneier *et al.*, 1995; 1997). There are minor pathological differences between the two forms of MD. Vascular lesions have been observed in late onset MD, but were absent in early onset MD. Histological lesions are similar in both forms of MD, but are different in distribution. Severe depletion of Peyer's patches has been observed in both courses, with a complete loss of lymphoid architecture in late onset MD only (Liebler-Tenorio *et al.*, 2000).

BVDV Transmission and Control

PI animals are immunotolerant to BVDV and harbor BVDV throughout their life. The main source of BVDV infection in herds are PI animals that shed virus in the environment and transmit it to healthy animals by direct contact; however, acutely infected animals also secrete and transmit virus, but only for a short period of time. Also, other species of animals infected with BVDV can transmit virus. Transmission by indirect contact may happen through the use of contaminated equipment, such as needles and gloves (Fulton *et al.*, 2005; Houe, 1999). BVDV transmission can also occur through insemination with BVDV infected semen that has normal quality. Seronegative dams inseminated with semen from PI bulls results in poor rates of conception and may result in PI calves (Givens *et al.*, 2003; Kirkland *et al.*, 1994; Niskanen *et al.*, 2002; Paton *et al.*, 1990). Furthermore, the exchange of embryos, gametes, semen, and somatic cells may provide an unnatural way to transmit BVDV between herds of cattle over the world (Gard *et al.*, 2007).

Identification and elimination of PI animals and vaccination are important to prevent BVDV infections (Moennig *et al.*, 2005). Quarantine of new animals and testing them for BVDV PI status before accepting them is very important to maintain a BVDV-free closed herd (Brock, 2004; Kelling *et al.*, 2000). Modified live and inactivated vaccines are widely used and because of the antigenic variability, contain BVDV-1 and BVDV-2 strains (Beer *et al.*, 1997; Bolin, 1995a). The timing of BVDV vaccination depends on factors that include: immune response, crossreactivity, fetal protection, immunosuppression, duration of immunity, reversion to virulence, effect of maternal

antibody on immune responses and purity. There is no single BVDV vaccine that provides complete fetal protection (Kelling, 2004).

Several methods are used to diagnose BVDV infections or to confirm vaccine efficacy in live animals or to identify contamination in biological products. These tests include: reverse transcription-polymerase chain reaction (RT-PCR), antigen detection by fluorescent antibody (FA) testing, enzyme-linked immunosorbent assay (ELISA), antigen capture ELISA (ACE), immunohistochemistry (IHC), and virus isolation (VI). Virus isolation is considered the best for BVDV diagnosis (Saliki and Dubovi, 2004; Sandvik, 2005). Real-time PCR and RT-PCR are used to detect BVDV and for taxonomy (Ridpath and Bolin, 1998). IHC and ACE rarely miss a PI animal. They detected nearly 100% of PI calves. Since the tests sometimes were positive for acute infections, virus isolation or RT-PCR is recommended 30 days after the initial test to confirm PI infections (Cornish *et al.*, 2005). A study evaluating the diagnostic proficiency of methods for the detection of BVDV in infected cattle using comparisons among tests and laboratories determined that the test that provided the greatest consistency in detecting positive animals is ACE. It also has a very good agreement among diagnostic laboratories (Edmondson *et al.*, 2007).

Antiviral targeting of virus envelope proteins is an effective strategy against viral infections. A multiwell antibody ELISA based on the recombinant E2 protein of BVDV species was developed and evaluated (Nogarol *et al.*, 2017). In a study, chickens were immunized with the BVDV structural protein E2. IgY antibodies against the BVDV-E2 protein were extracted from egg yolk and used in IgY-based ELISA and immuno-chromatographic assays (ICA) (Zhang *et al.*, 2016). Recent *in vitro* studies identified BVDV inhibitors using structure-based virtual screening on the BVDV structural protein

E2. One drug that was designed for BVDV-E2 and emerged as a specific BVDV inhibitor of replication is phenyl thiophene carboxamide derivative 12 (PTC12). In MDBK cells, PTC12 was identified as a potent inhibitor of BVDV entry (Bollini *et al.*, 2018; Pascual *et al.*, 2018).

Bovine Respiratory Disease Complex (BRDC)

One of the most costly diseases in the feedlot cattle industry is bovine respiratory disease complex (BRDC, aka shipping fever) (Snowder *et al.*, 2006). The pathogenesis factors of BRDC include contributions from not only microbial pathogens but also host, environmental, and animal management factors. Microbial pathogens include *Mannheimia haemolytica*, *Mycoplasma bovis*, BVDV, bovine herpesvirus-1, BRSV, parainfluenza-3 virus, bovine rhinitis A and B virus, bovine coronavirus, and influenza D virus (Mitra *et al.*, 2016; Ridpath, 2010). BRDC is of major economic importance to the global cattle industries. The United States feedlot industry estimates a loss as high as 1 billion dollars every year because of bovine respiratory disease, loss of production, increased labor expenses, drug costs, and death (Fulton *et al.*, 2002a; Sacco *et al.*, 2014).

BVDV is a significant contributor to BRDC. BVDV infection results in immunosuppression, leading to secondary infections by other pathogens, such as BRSV (Brodersen and Kelling, 1998; Gagea *et al.*, 2006). BVDV potentiates the severity of disease in cattle when concurrently infected with other respiratory tract and gastrointestinal pathogens (Kelling *et al.*, 2002a). Similarly, immunosuppression during BVDV infection in alpacas may contribute to secondary bacterial and viral infections (Topliff *et al.*, 2017). Experimentally, calves concurrently infected with BVDV and

BRSV had more severe clinical signs of disease and extensive lung lesions, and shed virus in greater concentration for longer duration compared to calves infected with either virus alone (Brodersen and Kelling, 1999). BVDV plays an indirect role by causing host immunosuppression while BRSV acts directly causing bronchopneumonia. BVDV and BRSV possibly act synergistically during co-infection of calves and as a result of synergism, respiratory and digestive tract diseases are enhanced (Brodersen and Kelling, 1998). BVDV strains are different in causing pneumonia. A ncp BVDV-1 (subtype Ib) was the predominant isolate in feedlot cattle with respiratory disease (Fulton *et al.*, 2002b).

Bovine Respiratory Syncytial Virus (BRSV)

Bovine respiratory syncytial virus (BRSV) is a member of the genus *Pneumovirus* within the family *Paramyxoviridae* (Murphy *et al.*, 1995). BRSV is closely related to human respiratory syncytial virus (HRSV), the leading cause of severe acute lower respiratory tract infection in infants and children all over the world. Respiratory syncytial virus (RSV) is enveloped and has a single-stranded, negative-sense RNA genome of 15,222 nucleotides encoding 11 proteins (Huang and Wertz, 1982). RSV was first reported in 1955 as a respiratory disease in chimpanzees (Blount *et al.*, 1956) and called chimpanzee coryza agent. It was subsequently renamed RSV, due to its ability to form syncytia (Chanock *et al.*, 1957). BRSV is a pathogen of the bovine respiratory system (Paccaud and Jacquier, 1970) and infection commonly occurs during the first year of life in calves, but reinfection is common and can occur at any age (Gershwin, 2012; Van der Poel *et al.*, 1993). Related RSV isolates cause respiratory tract diseases in small

ruminants, such as sheep and goats (Mallipeddi and Samal, 1993; Oberst *et al.*, 1993; Yeşilbağ and Güngör, 2009).

The BRSV genome has 11 genes that encode for 11 mRNAs. The viral-specific mRNAs from BRSV-infected cells have electrophoretic mobilities similar to those of HRSV mRNAs. Nine proteins specific to BRSV-infected cells correspond to those of HRSV proteins. The BRSV viral proteins are: non-structural proteins, NS1 and NS2, glycoprotein (G), fusion (F), small hydrophobic (SH), nucleoprotein (N), phosphoprotein (P), viral RNA-dependent polymerase (L), and the matrix proteins, M, M2-1, and M2-2. Unlike F, N, P, and M proteins, only G glycoprotein of BRSV shows major antigenic differences from the G glycoprotein of HRSV (Lerch *et al.*, 1989; Valarcher and Taylor, 2007). The major determinants of BRSV host range are NS1 and NS2. Together, these proteins inhibit the phosphorylation and transcriptional activity of IRF-3 reducing type I IFN production by infected host cells. The SH protein is not essential for virus replication and exists as different forms, SHg, SHp, SH0, and SHt. The G protein is a large glycoprotein and is the major attachment protein. Antibodies specific to the G protein block cell-virus binding. The F protein mediates the cell-virus binding and is responsible for the fusion between the virus and the host's cells (viral penetration) and among infected cells (syncytium formation). The N, P, and L proteins are nucleocapsid proteins. L protein is responsible for viral transcription and replication. (Bossert and Conzelmann, 2002; Bossert *et al.*, 2003; Guzman and Taylor, 2015; Valarcher and Taylor, 2007). It has been suggested that blocking the induction of host type I IFN gene expression increases the virulence of BRSV. Recombinant BRSV (rBRSV) lacking the NS1 or NS2 protein is a strong inducer of type I IFN in bovine cells compared to wild-type BRSV. The

replication of NS protein deletion mutants was severely attenuated in bovine cells and young calves because of increased type I IFN production (Valarcher *et al.*, 2003). The inhibition of type I IFN production by NS proteins of BRSV in the Madin Darby Bovine Kidney (MDBK) cells compared to cell lines of other origins suggests an adaptation of the virus to host-specific antiviral responses (Schlender *et al.*, 2000).

The suppressor of cytokine signaling (SOCS) family utilizes a feedback loop to inhibit the type I IFN dependent antiviral signaling pathway. SOCS1 and SOCS3 can inhibit NF-κB and JNK/p38 pathways. By disrupting the JAK/STAT pathway and decreasing the production of IRF7, SOCS3 inhibits both the production and signal transduction of type I IFN (Akhtar and Benveniste, 2011). Induction of SOCS3 by some viruses, such as hepatitis C virus and human immunodeficiency virus 1, suggests an important role for SOCS3 in suppressing anti-viral signal transduction (Mahony *et al.*, 2016). Gene expression analysis of nasal samples from infants with severe RSV bronchiolitis confirmed the reduction of type I IFN gene expression (Thwaites *et al.*, 2018). During RSV infection, NS1 upregulates both SOCS1 and SOCS3 proteins while NS2 upregulates SOCS1 expression. This induced expression of SOCS1 and SOCS3 inhibited the IFN-inducible antiviral response (Zheng *et al.*, 2015). The BRSV genome encodes a SH protein, which has a viroporin activity altering host cell membrane permeability. It has been reported that recombinant BRSV lacking the SH gene (rBRSVΔSH) was attenuated and induced protective immunity in calves (Taylor *et al.*, 2014). In response to BRSV infection, SH inhibits NF-κB p65 phosphorylation and reduces the production of pro-inflammatory cytokines while rBRSVΔSH does not inhibit

NF-κB p65 phosphorylation leading to increased expression of pro-inflammatory cytokines in bovine cells (Pollock *et al.*, 2017).

Clinical symptoms of natural BRSV infection include: fever, cough, and increased respiratory rates. Lung lesions include bronchitis, bronchiolitis, fibrosis, emphysema, and severe edema (Bryson *et al.*, 1983; Kimman *et al.*, 1989). Calves experimentally infected with BRSV had fever, diarrhea and developed a lobular suppurative and necrotic bronchointerstitial pneumonia and diffuse cilia loss with mild necrosuppurative inflammatory changes (Brodersen and Kelling, 1998). Colostrum-fed 17- to 24-day-old calves experimentally infected with BRSV developed severe chronic bronchiolitis and bronchiolitis obliterans. Secretions filled the bronchiolar lumina and alteration of the ciliogenesis was observed with partial loss of cilia (Philippou *et al.*, 2000). In calves with BRDC, concurrent infections with BVDV and BRSV causes more severe respiratory and digestive tract diseases than infections with either virus alone (Brodersen and Kelling, 1998).

Killed and modified live BRSV vaccines are available as part of multivalent products. Although there is widespread use of BRSV vaccines in calves, their efficacy is not optimal. Some studies have developed BRSV mutants or anti-BRSV antibodies that may provide protection to calves against infection. Experimentally, calves vaccinated with BRSV NS1- or NS2-deletion-mutants exhibited a robust BRSV-specific antibody (Valarcher *et al.*, 2003). BRSV immunostimulating complexes (BRSV-ISCOMs) used in 3 to 8-week-old calves induced BRSV-specific cellular and humoral responses and calves were protected from virulent BRSV infection (Hägglund *et al.*, 2011). Furthermore, it has been reported that IgG purified from bovine milk binds to human RSV, which may

contribute to immune protection against RSV (den Hartog *et al.*, 2014). Anti-RSV G monoclonal antibodies (anti-G mAbs) reduce lung inflammation and viral titers when evaluated using a mouse model (Caidi *et al.*, 2018). Recently, McGill *et al.*, 2018 developed a mucosal nanovaccine and determined the efficacy of the vaccine against RSV infection. Vaccinated calves challenged with BRSV infection exhibited reduced lesions and decreased virus shedding compared to unvaccinated control calves, indicating the potential of the BRSV-F/G nanovaccine to significantly reduce the disease burden associated with HRSV and BRSV infections (McGill *et al.*, 2018).

Cellular Signal Transduction

While BVDV and BRSV are responsible for significant economic losses in the cattle industry, little is known about the pathological responses of the host's cells and the signaling pathways mediated by BVDV and/or BRSV infections. When cells are infected with a RNA virus, the viral dsRNA will be recognized by cytosolic pattern-recognition receptors (PRRs) which will trigger innate immune responses and activate stress responses. Cytosolic PRRs, called RIG-I-like receptors (RLRs), include retinoic-acid-inducible gene I (RIG-I) and melanoma-differentiation-associated gene 5 (MDA5). The interaction of dsRNA and RLRs induces interaction with their adaptor protein on the mitochondrial membrane, mitochondrial antiviral signaling (MAVS, also known as IFN-β-promoter stimulator 1, IPS-1/VISA/Cardif) protein. MAVS activates TANK-binding kinase 1 (TBK-1) which induces the phosphorylation of interferon regulatory factor 3 (IRF-3) and IRF-7 leading to their homo- or hetero-dimerization and their translocation to the nucleus to activate the transcription of type I IFN genes and increase type I IFN

production (Fig. 1.1). Produced type I IFN binds to the type I IFN receptor on the cellular membrane causing a positive-feedback regulation of type I IFN genes. This binding activates a heterotrimeric transcriptional activator, IFN-stimulated gene factor 3 (ISGF3), which consists of IRF-9 and signal transducer and activator of transcription 1 (STAT1) and STAT2. ISGF3 increases the induction of the IRF-7 gene and subsequently increases the type I IFN production (Fig. 1.2). In the nucleus, the phosphorylated IRF-3 interacts with the cis–trans peptidylprolyl isomerase, NIMA-interacting 1 (PIN-1), which facilitates proteasome-dependent degradation of IRF-3 in the cytoplasm. MAVS also contributes in the NF-κB-activation pathway, which induces pro-inflammatory cytokine genes (Fig. 1.1). Double-stranded RNA-dependent protein kinase R (PKR) can detect the viral dsRNA and initiates antiviral stress granule (avSG) formation in the cytoplasm which then triggers innate immunity (Honda *et al.*, 2005; Honda and Taniguchi, 2006; Onomoto *et al.*, 2012; Yoneyama *et al.*, 2015).

Mitochondrial Antiviral Signaling (MAVS)

Mitochondria have emerged as critical cellular organelles for antiviral innate immune signaling. This is due in large part to the innate immune signaling adaptor MAVS, which coordinates signals received from two independent cytosolic PRRs (retinoic acid-inducible gene-I, RIG-I, or melanoma differentiation-associated gene 5, MDA5) to induce antiviral genes. MAVS is essential for type I IFN production in viral infections through the IRF-3 and NF-κB pathways. Through alteration of MAVS expression and signaling, the host cell can control inflammation and prevent cellular damage (Jacobs and Coyne, 2013). The mitochondria-associated endoplasmic reticulum

membrane (MAM) protein Gp78 modulates type I IFN induction by both decreasing MAVS protein levels and by inhibiting MAVS signaling via physical interactions (Jacobs *et al.,* 2014). The importance of MAVS in the type I IFN pathway was studied in mammalian (feline) cells. Inhibiting MAVS by using siRNA inhibited the IFN-β promoter activation during Sendai virus infection. In contrast, MAVS over-expression activated IRF-3 and NF-κB pathway signaling and induced IFN-β production (Wu *et al.,* 2016). Poliovirus significantly reduced the IFN-β mRNA levels. A study reported that MAVS was largely intact in HEC-1B cells infected with poliovirus suggesting that the suppression of the host type I IFN during poliovirus infection is not mediated by MAVS (Kotla and Gustin, 2015).

TANK-Binding Kinase 1 (TBK-1)

TANK-binding kinase 1 (TBK-1, also known as NF-κB-activating kinase (NAK) or T2K) regulates the IRF-3 and NF-κB pathways. Phosphorylated (activated) TBK-1 phosphorylates the transcription factors IRF-3 and IRF-7 (Zhao, 2013). The NS3 protein of hepatitis C virus binds to TBK-1 and inhibits the interaction between TBK-1 and IRF-3 leading to the inhibition of the cellular antiviral response (Otsuka *et al.,* 2005). Dengue virus serotype 2 (DENV2) is a member of the family *Flaviviridae*. When HepG2 cells were treated with a TBK-1 inhibitor (BX795) and stimulated with poly I:C, the type I IFN pathway signaling was inhibited. TBK-1 inhibitor decreased the IFN-β mRNA expression and increased the viral mRNA expression of DENV2 (Zhang *et al.*, 2013).

Interferon Regulatory Factor 3 (IRF-3) and IRF-7

The mammalian interferon-regulatory factor (IRF) family includes nine members named from one to nine. They have different roles in the gene regulatory networks in the immune system. Interferon regulatory factor 3 (IRF-3) and IRF-7 are closely related to each other and are important cellular transcription factors targeting the type I IFN gene and increasing type I IFN production in infected cells. IRF-3 and IRF-7 monomers are activated into phosphorylated homo- and heterodimers and translocated to the nucleus of virus-infected cells (Taniguchi *et al.*, 2001). IRF-3 is an essential antiviral signaling molecule and is important in IFN regulation and development of the immune system. IRF-3 is expressed in a variety of tissue cells, such as mature DCs. IRF-3 is found in an inactive cytoplasmic form and is posttranslationally-modified following virus infection by protein phosphorylation. This virus-dependent phosphorylation of IRF-3 alters protein conformation causing the translocation of IRF-3 from the cytoplasm to the nucleus. Phosphorylation also stimulates DNA binding with IRF-3, and increases IRF-3 transcriptional activation and primary activation of IFN-responsive genes to produce type I IFN and establish early innate immunity (Gabriele and Ozato, 2007; Hiscott *et al.*, 1999). It was reported that the N^{pro} protein of pestivirus prevented IFN production by directly interacting with the monomer and dimer forms of IRF-3 (Gottipati *et al.*, 2016). In infected cells, the N^{pro} of both BVDV and CSFV suppress IRF-3 levels by blocking IRF-3 binding to DNA and mediates the degradation of the protein IRF-3, but not IRF-3 mRNA (Hilton *et al.*, 2006; Horscroft *et al.*, 2005; Seago *et al.*, 2007). BVDV N^{pro} interacts with IRF-3 before virus-induced phosphorylation of IRF-3 leading to polyubiquitination and proteasomal degradation of IRF-3 (Chen *et al.*, 2007). In infected

MDBK cells, NS1 and NS2 proteins of BRSV inhibit the phosphorylation and transcriptional activity of IRF-3 and IFN induction (Bossert and Conzelmann, 2002; Bossert *et al.,* 2003). The production of IRF-7 in MDBK cells was induced by cp BVDV-1 (Fredericksen *et al.,* 2015). Both cp and ncp BVDV inhibit the full function of IRF-3 but do not affect the nuclear uptake of IRF-7 (Baigent *et al.*, 2004).

NIMA-Interacting 1 (PIN-1)

The phosphorylated IRF-3 in the nucleus interacts with the peptidylprolyl isomerase (cis–trans peptidylprolyl isomerase, NIMA-interacting 1, PIN-1) to terminate the action of IRF-3 and facilitate the IRF-3 degradation in the cytoplasm (Saitoh *et al.,* 2006). The role of PIN-1 during BVDV infection is not clear. It was suggested that BVDV N^{pro} induces IRF-3 degradation via a PIN-1-independent mechanism (Chen *et al.*, 2007).

Protein Kinase R (PKR)

The IFN-induced double-stranded RNA-dependent protein kinase R (PKR) is a serine/threonine kinase and is induced by interferon (Meurs *et al.,* 1990). PKR is a component of signal transduction pathways mediating cell growth control and is activated in response to dsRNA, viral infection, and a wide range of activators and cell stresses. Phosphorylated (activated) PKR can activate NF-κB, phosphorylate the alpha-subunit of eukaryotic translation initiation factor 2 (eIF2α), and induce apoptosis (Gabel *et al.,* 2006; García *et al.,* 2006; Lee *et al.,* 1997; Taylor *et al.,* 2005). The multiple functions of PKR during viral infection include inhibiting the translation initiation and protein synthesis through the transcription factor eIF2α and induction of apoptosis. PKR controls

the activation of many transcription factors including NF-κB, p53, and STATs (Gil and Eseban, 2000; Pathak *et al.,* 1988; Wong *et al.,* 1997). PKR detects viral dsRNA and initiates antiviral stress granule (avSG) formation in the cytoplasm which triggers innate immunity. Removal of PKR diminished IFN production and enhanced viral replication (Onomoto *et al.*, 2012). Type I IFN binds to type I IFN receptor on neighboring cells triggering a variety of genes including PKR, which can be induced by IFN treatment (García *et al.,* 2007). CSFV activates PKR which phosphorylates eIF2α and inhibits translation in viral infected cells leading to apoptosis (Hsu *et al.,* 2014). At 5 DPI *in vivo*, both ncp BVDV-1 and BVDV-2, increased PKR mRNA in spleen and tracheo-bronchial lymph nodes of infected beef calves (Palomares *et al.,* 2013). On the other hand, unlike cp BVDV, ncp BVDV-1 inhibited the signaling pathway of PKR resulting in enhanced protein synthesis and cell survival (Gil *et al.,* 2006b).

Nuclear Factor-κB (NF-κB)

The transcription factor, nuclear factor-κB (NF-κB), induces the expression of immune and inflammatory genes and type I IFN production. Viruses activate three main transcription factor complexes involved in type I IFN production: NF-κB, IRF3/IRF7 and ATF2/c-jun. In the cytoplasm of resting cells, NF-κB inhibitor (IκBα) holds NF-κB as an inactive complex. When cells are infected with viruses, NF-κB will be released and translocated to the nucleus inducing target genes and increasing IFN production (Taylor and Mossman, 2013). NF-κB signaling pathway maintains immune homeostasis in cells. A20 (TNFAIP3) molecule is a target ubiquitin-editing enzyme of NF-κB and a key regulatory factor in the immune response, hematopoietic differentiation, and

immunomodulation. The expression of the negative regulator of the immune response A20 (TNFAIP3) is mediated by the NF-κB pathway. Through NF-κB pathway, BVDV modulates bovine A20 activation (Fredericksen *et al.,* 2016). In MDBK cells, cp BVDV-1 was able to induce the production of cytokines and modulate transcriptional factors, including BCL3, IL-1β, IL-8, IL-15, IL-18, Mx-1, IRF-1, and IRF-7, through activating NF-κB. The pharmacological inhibitor of NF-κB signaling pathway (BAY-117085) blocks the BVDV-1 activities (Fredericksen *et al.,* 2015). In cells infected with cp BVDV NADL, the N^{pro} does not affect the NF-κB activation of gene expression (Chen *et al.,* 2007). A study *in vitro* reported that respiratory syncytial virus (RSV) is a potent activator of NF-κB (Jamaluddin *et al.,* 1998). NF-κB p65 phosphorylation is a main step in the regulation of pro-inflammatory cytokines. In BRSV-infected bovine cells, SH inhibits NF-κB p65 phosphorylation and decreases pro-inflammatory cytokine production (Pollock *et al.*, 2017). However, it was reported that the immediate early response 3 (IER3) overexpression in bovine cells blocked the NF-κB pathway activity leading to down-regulation of interleukin-8 (IL-8) during BVDV-1 infection (Villalba *et al.*, 2017).

Hypothesis and Goals

Based on our review of the literature, there is a lack of information regarding the type I IFN signaling pathways during BVDV infection, in particular, the effects of N^{pro} on these pathways. The effect of BVDV N^{pro} on the IFN pathway signals in cells co-infected with BVDV and other viral pathogens, such as BRSV, has not been previously evaluated. This study investigates the effects of BVDV N^{pro} during BVDV single and co-infection with BRSV on the type I IFN pathway in BT cells infected with BRSV,

BVDV2-wt, or BVDV2-E or co-infected with BRSV/BVDV2-wt or BRSV/BVDV2-E. We hypothesized that BVDV-2 N^{pro} enhances virulence and modulates host cell innate immune responses which augment BRSV replication during co-infection with BVDV. The long term goal of our study is to develop new strategies to control BRDC in cattle. Our research is centered on studying BVDV virulence determinants and mechanisms of enhanced disease from BRSV/BVDV2 co-infection. We proposed to undertake the study to identify and characterize pathogen-specific genes that inhibit immune responses. Specifically, we proposed to characterize the functional role of enhancement of BRSV replication during co-infection. The objectives include (1) characterization of the effects of BVDV N^{pro} on type I IFN induction cell signals in IFN antagonism during BVDV infections and (2) identifying the BVDV immunomodulatory proteins and host cell responses which are important to increased virulence of BRSV and the effects of BVDV N^{pro} on type I IFN cell signaling in IFN antagonism and enhancement of BRSV replication during co-infections with BVDV. The investigated cell signals are MAVS, PKR, TBK-1, IRF-3, IRF-7, IFN, NF-κB, and PIN-1 using real-time Q-RT-PCR for signal mRNA and western blotting for signal proteins (Fig. 1.3). A reporter cell line and Dual-luciferase reporter assays were also used in this study.

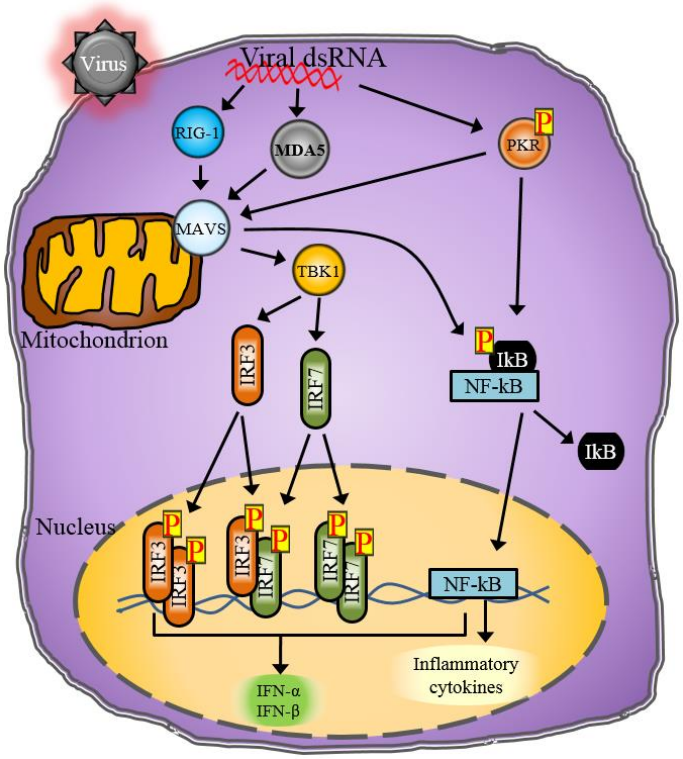

Fig. 1.1. Virus-dependent type I IFN signaling pathways. Cytosolic pattern-recognition receptors (PRRs), called RIG-I-like receptors (RLRs), which include RIG-I and MDA5, recognize viral dsRNA and interacts with MAVS protein. MAVS activates TBK-1 which induces the phosphorylation of IRF-3 and IRF-7 leading to their dimerization and their translocation to the nucleus to activate the transcription of type I IFN genes and increase type I IFN production. Protein kinase R (PKR) detects the viral dsRNA and activates MAVS. MAVS also activates NF-κB.

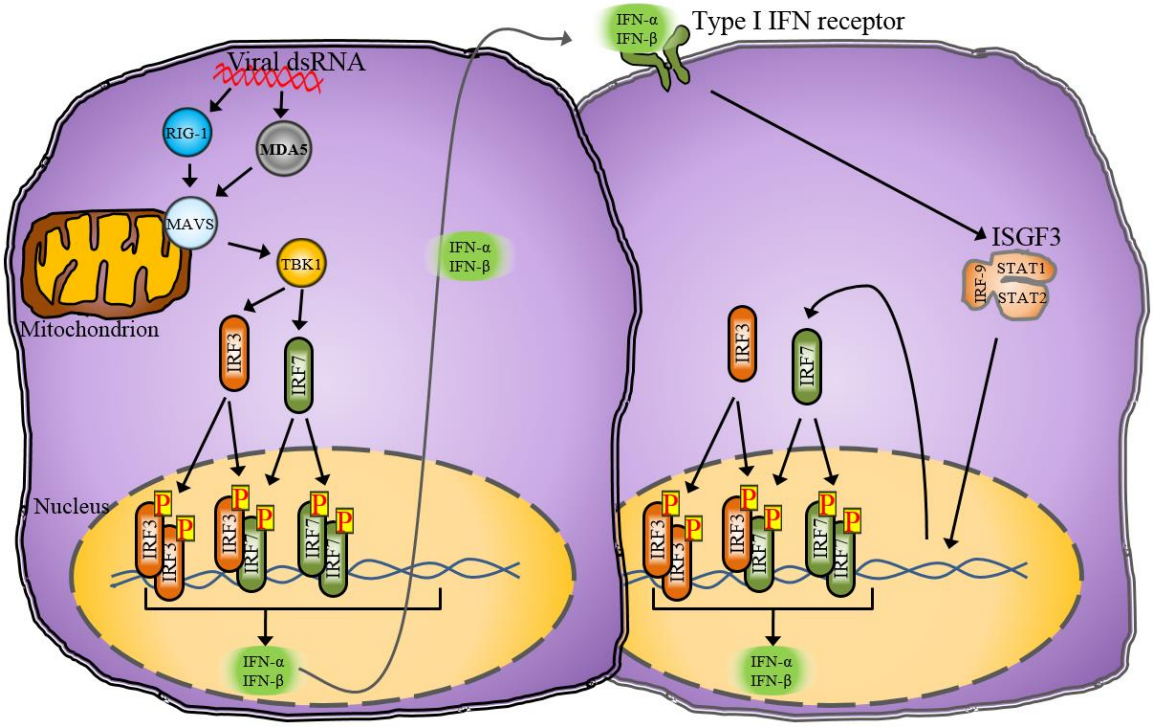

Fig. 1.2. Positive-feedback of type I IFN signaling. Type I IFN binds to its receptor activating a heterotrimeric transcriptional activator, IFN-stimulated gene factor 3 (ISGF3, which consists of IRF-9, and signal transducer and activator of transcription 1 (STAT1) and STAT2). Activated ISGF3 increases the induction of the IRF-7 gene and the production of the type I IFN.

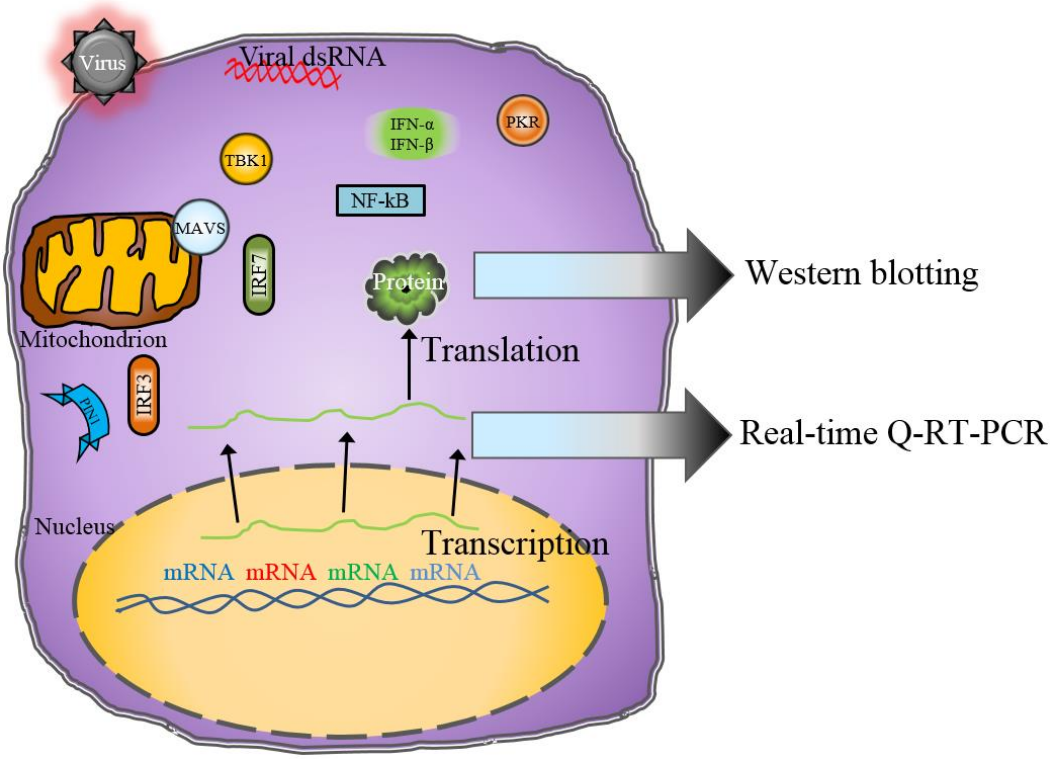

Fig. 1.3. Evaluating cellular signal expression using Real-time Q-RT-PCR or western blotting. Virus infection increases the transcription of numerous adaptor molecules producing the mRNAs of the signals in the nucleus of infected cells. The mRNAs can be detected and evaluated by Real-time Q-RT-PCR. The translation of mRNA in the cellular cytoplasm produces the signal proteins, which can be evaluated by western blotting.

CHAPTER 2:

JOURNAL ARTICLE

Type 2 BVDV N^{pro} suppresses IFN-1 pathway signaling in bovine cells and augments BRSV replication

Published in *Virology* 507:123-134, 2017

Abdulrahman A. Alkheraif, Christina L. Topliff*, Jay Reddy, Chandirasegaran Massilamany, Ruben O. Donis, Gregor Meyers, Kent M. Eskridge, Clayton L. Kelling

* E-mail address: ctopliff2@unl.edu
Tel.: +1 402 472 1480
Fax: +1 402 472 9690

School of Veterinary Medicine and Biomedical Sciences
University of Nebraska – Lincoln
1880 North 42nd Street
Lincoln, NE 68583
United States

ABSTRACT

Bovine viral diarrhea virus (BVDV) infection induces immunosuppression and in conjunction with bovine respiratory syncytial virus (BRSV) contributes to the bovine respiratory disease complex. Bovine turbinate cells were single or co-infected with type 2 BVDV wild-type (BVDV2-wt), its dysfunctional N^{pro} mutant (BVDV2-E), and/or BRSV. BVDV2-E significantly up-regulated PKR, IRF-7, TBK-1, IRF-3, and IFN-β mRNAs based on real-time Q-RT-PCR. BRSV-infected cells expressed significantly up-regulated PKR, IRF-3, IRF-7, and IFN-β mRNAs, whereas BVDV2-wt, but not BVDV2-E, abolished this up-regulation in co-infection. No significant differences were observed in MAVS, NF-κB, and PIN-1 mRNAs. A dual-luciferase reporter assay showed that BVDV2-wt significantly increased NF-κB activity compared to BVDV2-E, while BVDV2-E significantly increased IFN-β activity compared to BVDV2-wt. The BRSV titer and RNA levels significantly increased in cells co-infected with BRSV/BVDV2-wt compared to cells co-infected with BRSV/BVDV2-E or infected with BRSV alone. This data supports the synergistic action of BVDV2-wt and BRSV inhibition of IFN-1.

Keywords

BVDV2 N^{pro}; BRSV; Bovine respiratory disease complex; IFN-1 pathway signaling; mRNA; Viral replication.

1. Introduction

Bovine viral diarrhea virus (BVDV) is a member of the genus *Pestivirus* within the Family *Flaviviridae* (Simmonds *et al.,* 2017). Bovine respiratory syncytial virus (BRSV) is a member of the genus *Pneumovirus* within the Family *Paramyxoviridae* (Bunt *et al.,* 2005). BVDV infections are commonly associated with cattle, but other members of the order *Artiodactyla* may be infected (Løken, 1995; Raizman *et al.,* 2009; Topliff *et al.,* 2009). BVDV infections are endemic in cattle in North America and cause significant economic losses to the cattle industry. Mortality rates associated with infectious disease are significantly higher in feedlot cattle seropositive for BVDV (Booker *et al.,* 2008). BVDV potentiates the severity of other respiratory viral infections, such as BRSV (Brodersen and Kelling, 1998, 1999) or gastrointestinal pathogens, such as rotavirus (Kelling *et al.,* 2002). In calves, concurrent infection with BVDV and BRSV caused more severe respiratory and enteric disease than infection with either virus alone (Brodersen and Kelling, 1998, 1999).

BVDV1 and BVDV2 can be differentiated based on sequence differences of the 5’ untranslated region (UTR) (Pellerin *et al.,* 1994; Pletnev *et al.,* 2011; Ridpath *et al.,* 1994). BVDV isolates can also be separated into one of two biotypes, cytopathic (cp) or noncytopathic (ncp), based on effects in cell culture (Meyers *et al.,* 1996). BVDV is an enveloped virus with a single-stranded, positive-sense RNA genome of approximately 12.5 kb. The genome consists of a single large open reading frame with a UTR on both the 5’ and 3’ ends (Collett *et al.,* 1988a, 1988b). *Pestivirus* (including BVDV) proteins are synthesized from 5’ to 3’ as NH_2–N^{pro}/C/E^{rns}/E1/E2/p7/NS2/NS3/NS4A/NS4B/NS5A/NS5B–COOH (Collett *et al.,* 1991; Tautz *et al.,* 2015).

Interferon (IFN), an inducible cytokine, plays a major role in host innate immune responses and is a bridge between innate and adaptive immunity. Synthesis and secretion of type I IFN α/β (IFN-1) is the first step of the innate immune response to viral infection or double-stranded RNA (dsRNA) exposure of cells (Bautista *et al.,* 2005) and activates cellular factors to degrade viral RNA and shut down viral mRNA synthesis (Castelli *et al.,* 1997). IFN-1 controls certain cellular functions such as inducing dendritic cell differentiation and stimulating the proliferation and class switching of B cells (Litinskiy *et al.,* 2002; Paquette *et al.,* 2002; Tough, 2004). IFN-1 also stimulates the motility, differentiation, and cross-priming of T cells, enhances the cytotoxicity of natural killer cells, and stimulates the production of inflammatory cytokines (Le Bon *et al.,* 2003; Rogge *et al.,* 1998; Sato *et al.,* 2001).

When cells are infected with a RNA virus, the viral dsRNA will be recognized by cytosolic pattern-recognition receptors (PRRs) which will trigger innate immune responses and activate stress responses. Cytosolic PRRs, called RIG-I-like receptors (RLRs), include retinoic-acid-inducible gene I (RIG-I) and melanoma-differentiation-associated gene 5 (MDA5). The interaction of dsRNA and RLRs induces interaction with their adaptor protein on the mitochondrial membrane, mitochondrial antiviral signaling protein (MAVS, also known as IPS-1/VISA/Cardif). MAVS activates TANK-binding kinase 1 (TBK-1) which induces the phosphorylation of interferon regulatory factor 3 (IRF-3) and IRF-7 leading to their homo- or hetero-dimerization and their translocation to the nucleus to activate the transcription of IFN-1 genes. In the nucleus, the phosphorylated IRF-3 interacts with the cis–trans peptidylprolyl isomerase, NIMA-interacting 1 (PIN-1), which facilitates proteasome-dependent degradation of IRF-3 in the

cytoplasm. MAVS contributes in the NF-κB-activation pathway, which induces pro-inflammatory cytokine genes (Honda and Taniguchi, 2006). Double-stranded RNA-dependent protein kinase (PKR) can detect the viral dsRNA and initiates the antiviral stress granule (avSG) formation in the cytoplasm which will trigger innate immunity (Onomoto *et al.,* 2012; Yoneyaman *et al.,* 2015).

BVDV N^{pro} is a nonstructural protein with autoprotease activity involved in viral evasion of the innate immune response. Ruggli *et al.,* 2003 demonstrated that classical swine fever virus (CSFV), a *Pestivirus* species closely related to BVDV, with a functional N^{pro} prevented IFN-1 production from infected cells while the N^{pro}-deleted CSFV mutant did not (Ruggli *et al.,* 2003). BVDV N^{pro} prevents the production of IFN-1 by suppressing levels of IRF-3 to avoid host antiviral responses (Hilton *et al.,* 2006; Horscroft *et al.,* 2005). The ability of type 1 BVDV N^{pro} to suppress the production of IFN was abolished by substituting glutamic acid with leucine at amino acid position 22 or histidine with valine at position 49 of the N^{pro} protein (Gil *et al.,* 2006a).

This study describes the influence of type 2 BVDV-mediated IFN-1 antagonism on the enhancement of BRSV replication during co-infection. BVDV2 with a modified N^{pro} (BVDV2-enhanced green fluorescent protein (EGFP) coding sequence, BVDV2-E) to render it dysfunctional in interferon inhibition (Gil *et al.,* 2006a), BVDV2 wild-type (BVDV2-wt), and BRSV were used to characterize the effects of BVDV2 N^{pro} on IFN-1 production and its pathway signaling and on BRSV replication *in vitro*. Results showed that BRSV replication was enhanced when co-infected with BVDV2-wt having a functional N^{pro}, while BVDV2-E with a dysfunctional N^{pro} induced IRF-3 pathway

signaling and higher levels of IFN-1 than BVDV2-wt and did not enhance the replication of BRSV during co-infection.

2. Materials and Methods

2.1. Cells and viruses

Bovine turbinate (BT, National Veterinary Services Laboratory, United States Department of Agriculture, Ames, IA) and Madin–Darby bovine kidney (MDBK, CCL-22, American Type Culture Collection, Manassas, VA) cells were grown in Dulbecco's Modified Eagle's Medium (DMEM, Invitrogen, Carlsbad, CA, USA) supplemented with 10% (v/v) equine serum (Hyclone, Logan, UT, USA). NCL1-ISRE-Luc-Hygro cells, a modified bovine uterine cell line constitutively expressing an IFN response element gene coupled with firefly luciferase, were maintained in DMEM supplemented with 10% (v/v) equine serum and 300 µg/ml hygromycin (Cellgro, Manassas, VA, USA). Bovine cell lines were free of adventitious BVDV and BRSV.

Ncp BVDV2 isolates used in the study were ncp NY93-wt (BVDV2-wt) (Animal, Plant, and Health Inspection Service, Center for Veterinary Biologics, Ames, IA) and NY93/c N-N^{pro} 18 EGFP (BVDV2-E) derived from the infectious clone, NY93/c (Meyer *et al.*, 2002). BVDV2-E was constructed by mutating NY93/c between N^{pro} codons 18 and 19 creating a *Nae*I restriction site. The EGFP coding region from pEGFP-N1 (Clontech, Mountain View, CA, USA) was PCR amplified and ligated into the *Nae*I site. The field isolate, BRSV 236-652 (BRSV), was used in this study (Brodersen and Kelling, 1998).

2.2. Viral stocks

Monolayers of MDBK cells at 90% confluency were mock-infected or infected with each individual BVDV isolate in 162 cm^2 tissue culture flasks and incubated at 37 °C in a humidified incubator with 5% (v/v) CO_2 for four days. Following a single freeze-thaw cycle, aliquots of mock- and BVDV-infected MDBK cell lysates were stored at –80 ºC. Monolayers of BT cells at 90% confluency were infected with BRSV in 162 cm^2 tissue culture flasks and incubated at 33 °C in a humidified incubator with 5% (v/v) CO_2 for eight to ten days until the cells demonstrated 50% cytopathic effect. Following a single freeze-thaw cycle, aliquots of BRSV-infected BT cell lysates were stored at –80 ºC.

2.3. dsRNA stock

Polyriboinosinic polyribocytidylic acid (poly I:C, Amersham Biosciences, Piscataway, NJ, USA) was reconstituted in PBS to a stock concentration of 2 mg/ml, passed through a 21 gauge needle to shear the RNA, and stored in aliquots at –80 °C.

2.4. Virus preparation for IFN-1 assay

Virus preparation for the IFN-1 assay has been previously described (Gil *et al.,* 2006a). Briefly, 75 cm^2 tissue culture flasks of MDBK cells at 90% confluency were inoculated with BVDV2-wt or BVDV2-E and incubated at 37 °C in a humidified incubator with 5% (v/v) CO_2 for 4 days, then frozen at –80 °C. Flasks were thawed, cell lysates harvested and centrifuged at 2,000×g for 30 minutes at 4 °C. The clarified supernatant was then transferred to ultracentrifuge tubes and centrifuged at 100,000×g for

2 h at 4 °C. The resulting viral pellet was re-suspended in 500 µl DMEM and stored in aliquots at –80 °C.

2.5. IFN-1 reporter gene assay

MDBK (4×10^5) or BT cells (3×10^5) were seeded onto 6-well plates and grown to 90% confluency. Cells were then infected with each pelleted virus isolate at a multiplicity of infection (m.o.i.) of 0.5, stimulated with poly I:C (100 µg/ml), or treated with media as uninfected (UI) control. Plates were incubated at 37 °C in a humidified incubator with 5% (v/v) CO_2 for 24 h, and then frozen at –80 °C. The plates were thawed and the cell lysate clarified by centrifugation at 2000×g for 30 minutes at 4 °C. The pH of the clarified supernatant was adjusted to pH 2 with 2 M HCl. After incubation at 4 °C for 24 h, the pH of the supernatant was adjusted to pH 7 using 2 M NaOH. Each experimental sample (0.5 ml) was added to one well of a 12-well plate seeded with NCL1-ISRE-Luc-Hygro cells (Gil *et al.*, 2006a) prepared 12 h earlier by adding 1.5×10^5 cells per well and incubating at 37 ºC in a humidified incubator with 5% CO_2. After addition of the experimental sample, the NCL1-ISRE-Luc-Hygro cells were incubated at 37 ºC in a humidified incubator with 5% (v/v) CO_2 for 8 h, followed by cell lysis in 100 µl of reporter lysis buffer (Promega, Madison, WI, USA) (Gil *et al.*, 2006a). Each NCL1-ISRE-Luc-Hygro cell lysate was analyzed using the firefly luciferase assay system (Promega) according to the manufacturer's instructions, with sample luminescence measured by a FLUOStar luminometer (BMG Labtech, Offenburg, Germany). A standard curve using a dilution series of an IFN-1 standard was prepared and sample luminescence (relative light units, RLU) expressed as units of IFN-1.

2.6. IFN-1 inhibition assay

MDBK cells (4×10^5) were seeded onto 6-well plates and grown to 90% confluency. Cells were then infected with BVDV2-wt or BVDV2-E at a m.o.i. of 1.2, stimulated with poly I:C (100 µg/ml), or treated with media as UI control. Plates were incubated at 37 °C for 48 h, at which time the media was replaced with fresh media containing poly I:C at a concentration of 50 µg/ml (Baigent *et al.,* 2002; Gil *et al.,* 2006a). Following incubation at 37 °C for 20 h, cells were harvested by a freeze-thaw cycle at –80 °C and pH adjusted to pH 2 for 24 h at 4 °C to inactivate virus. The pH of the cell lysates was then adjusted to pH 7 and added to reporter cell plates containing NCL1-ISRE-Luc-Hygro cells and assayed as described previously (Gil *et al.,* 2006a).

2.7. BRSV growth kinetics in single and co-infected cells

BT cells (3×10^5) were seeded onto individual wells of 6-well plates and incubated at 37 °C in a humidified incubator with 5% (v/v) CO_2 until 90% confluent. Duplicate wells of cells were then infected with BRSV alone or co-infected with BRSV/BVDV2-wt or BRSV/BVDV2-E, at a m.o.i. of 0.6 and incubated at 37 °C in a humidified incubator with 5% (v/v) CO_2 for 1.5 h with rocking. Following adsorption, cells were washed with DMEM and incubated in fresh media supplemented with 5% (v/v) equine serum. Cells were monitored by microscopic examination and frozen at –80 °C 2, 6, 12, and 24 h post-infection (HPI), and 2, 3, 5, 7, and 9 days post-infection (DPI). Cell lysates were thawed on ice and virus titers determined and viral RNA was extracted.

2.8. Virus titration

Serial ten-fold dilutions (10^{-1} to 10^{-8}) of virus in DMEM from each time point were assayed as previously described (Brodersen and Kelling, 1998). Briefly, 50 µl of each dilution was added to two replicates of 4 wells/dilution of a 96-well tissue culture plate. A 100 µl suspension of BT cells (1×10^4 cells per well) in DMEM supplemented with 3% (v/v) equine serum, 75 µg/ml Gentamicin (Sigma, St. Louis, MO, USA), and 0.375 µg/ml Fungizone (Invitrogen) was added to each well of a 96-well tissue culture plate. After incubating for 7 days at 33 °C in a humidified incubator with 5% (v/v) CO_2, cells were fixed in 20% (v/v) acetone in PBS for 15 minutes at room temperature and plates allowed to dry overnight. An enzyme-linked immunosorbent assay (ELISA) (Brodersen and Kelling, 1998) was performed using the monoclonal antibody 8G12 specific for BRSV F protein (Klucas and Anderson, 1988) as the primary antibody and biotinylated horse anti-mouse immunoglobulin (Vector Laboratories, Burlingame, CA) as the secondary antibody. Antibody binding was detected using streptavidin horseradish peroxidase (HRP) conjugate (Zymed, San Francisco, CA) and 3-amino-9-ethyl-carbazole (AEC). Virus titration from each time point was determined using the Reed–Muench method.

2.9. BRSV RNA extraction and Real-time Q-RT-PCR

Viral RNA was extracted from 140 µl BT cell lysate infected with BRSV alone or co-infected with BRSV/BVDV2-wt or BRSV/BVDV2-E from each of the nine time points 2, 6, 12, and 24 HPI, and 2, 3, 5, 7, and 9 DPI using the QIAamp® Viral RNA Mini kit (Qiagen, Valencia, CA, USA) according to the manufacturer's directions. Extracted RNA was stored in AVE buffer at –80 °C until used. Real-time Quantitative-

RT-PCR (Q-RT-PCR) was performed in single wells of a 96-well plate (Bio-Rad, Hercules, CA, USA) in a 25 µl reaction volume using components of a commercial RT-PCR kit (QuantiTect Probe RT-PCR kit, Qiagen). Primers and probes were purchased from Integrated DNA Technologies, Inc. (Coralville, IA, USA). The primers and probe for BRSV amplification, based on conserved regions of the N gene were: forward primer: 5'-GCAATGCTGCAGGACTAGGTATAAT-3'; reverse primer: 5'-ACACTGTAATTG-ATGACCCCATTCT-3'; and probe: 5'-/5HEX/-ACCAAGACTTGTATGATGCTGCC-AAAGCA-/31ABkFQ/-3' (Boxus *et al.,* 2005). The 25 µl Q-RT-PCR reaction mixture contained: 12.5 µl QuantiTect Probe RT-PCR Mix (2X), 1 µl of 10 µM (BRSV) forward primer, 1 µl of 10 µM (BRSV) reverse primer, 1 µl of 5 µM (BRSV) fluorogenic probe, 4.25 µl of RNase-Free Water, 0.25 µl of QuantiTect RT Mix, and 5 µl of viral RNA sample. Both reverse transcription and PCR were carried out in the same well of a 96-well plate using iCycler iQ™ Thermal Cycler (Real-Time PCR Detection System, Bio-Rad). Thermocycling parameters for BRSV amplification consisted of 50 °C for 30 minutes, 95 °C for 15 minutes, followed by 45 cycles of 94 °C for 15 seconds and 59 °C for 60 seconds . Fluorescence was measured following each cycle and displayed graphically. The iCycler iQ software (Bio-Rad) determined a quantification cycle (Cq) (also known as cycle threshold, Ct) value, which identified the first cycle at which the fluorescence was detected above the baseline for that sample or standard.

The standard curve, Cq value vs. starting BRSV RNA amounts extracted from serial BRSV dilutions, was used to determine the initial starting quantity of unknown BRSV RNA from each time point based on the Cq values for the known BRSV standards.

2.10. Determination of two reference genes

EXPRESS One-Step SYBR® GreenER™ Kit (Invitrogen) with a prime PCR Custom 96-well plate with 19 genes (Cow B96 reference plate, 20X, Bio-Rad) was used to determine the appropriate reference genes for BT cells. RNA samples were extracted from BRSV-infected BT cells at 1 or 5 DPI. Glyceraldehyde 3-phosphate dehydrogenase (GAPDH) and bovine ribosomal protein S18 (RPS18) were chosen as endogenous controls to normalize all gene expression results. This experiment was repeated two times generating similar results.

2.11. Cellular gene mRNA extraction and Real-time Q-RT-PCR

BT cells in 75 cm^2 flasks were infected with BVDV2-wt, BVDV2-E, BRSV, BRSV and BVDV2-wt, or BRSV and BVDV2-E at a m.o.i. of 0.05, stimulated with poly I:C (100 µg/ml), or treated with media as UI control. Cells were harvested at 2 HPI, 1, 2, 3, 5, 7, or 9 DPI by removing the media and lysing cells with RLT buffer (Qiagen). Cell lysates were stored at –80 °C. Total RNA was extracted using the RNeasy plus Mini kit (Qiagen) according to the manufacturer's directions. This kit includes gDNA Eliminator Mini Spin Columns specially designed to effectively remove genomic DNA (gDNA) contamination. RNA was eluted and then diluted to 20 µg/µl in RNase-free water and stored in 0.5-ml tube aliquots at –80 °C until used. The cellular gene mRNA levels were quantified using Q-RT-PCR in single wells of a 96-well plate (Bio-Rad) in a 20 µl reaction volume using the EXPRESS One-Step SuperScript qRT-PCR kit (Invitrogen). The cellular genes (MAVS, PKR, TBK-1, NF-κB, IRF-3, IRF-7, IFN-β, and PIN-1) were detected using commercially available primer and probe sets specific for bovine genes (TaqMan Gene Expression Assays, Applied Biosystems, Foster City, CA, USA). The 20

µl Q-RT-PCR reaction mixture contained: 10 µl EXPRESS SuperScript qRNA SuperMix Universal, 1.6 µl of RNase-Free Water, 0.4 µl of ROX Reference Dye (25 µM), 2 µl of SuperScript® Reverse Transcriptase (RT), 1 µl of TaqMan Gene Expression Assays, and 5 µl (100 ng) of the total RNA sample. Both reverse transcription and PCR were carried out in the same well of a 96-well plate using C1000 Touch™ Thermal Cycler (Bio-Rad). Thermocycling parameters for all gene amplifications consisted of 50 °C for 15 minutes, 95 °C for 2 minutes, followed by 40 cycles of 95 °C for 15 seconds and 60 °C for 60 seconds . Fluorescence was measured following each cycle and displayed graphically. The CFX Manager™ Software (Bio-Rad) determined a Cq value, which identified the first cycle at which the fluorescence was detected above the baseline for that sample. The results were normalized against two reference genes, GAPDH and RPS18, and represented as fold change expressed relative to UI at the 2 HPI time point using the ΔΔCq method (Hellemans *et al.*, 2007). Briefly, the ΔCq value was calculated by normalizing each sample to the average of GAPDH and RPS18 using the equation ΔCq = Cq (target gene) – Cq ((GAPDH + RPS18) /2). Then, ΔΔCq was calculated by subtracting the ΔCq of the control (UI at 2 HPI) sample from the ΔCq of each experimental and control sample using the equation ΔΔCq =ΔCq (a normalized sample) – ΔCq (the control sample). Lastly, the relative values to the control sample were calculated by using the formula $2^{-(\Delta\Delta Cq)}$, where the control sample $=2^{-(0)} =2^{0} =1$. The experiment was replicated independently three times resulting in a randomized complete block design and the averages are represented. Three PCR wells were used for a common sample (inter-run calibration) in every plate to normalize among the runs in multiple plates. Two PCR wells were used without RT, using RNase-Free Water to ensure that

there was no gDNA contamination. The common total RNA sample was extracted from BT cells incubated for 5 days using the same kit and stored in aliquots at –80 °C until used.

2.12. IFN-β and NF-kB activities using a Dual-luciferase reporter assay

BT cells (1.5×10^4) were seeded into seven individual wells of seven 96-well plates and incubated at 37 °C in a humidified incubator with 5% (v/v) CO_2 for 16 h and then transfected with pGL4.32 [luc2P/NF-κB-RE/Hygro] Vector (Promega) or IFN-β plasmid (Beura *et al.*, 2010; a kind gift provided by Dr. Fernando Osorio) (firefly) and control (pRL Renilla Luciferase Reporter) Vector (Promega) using ViaFect™ Transfection Reagent (Promega). The transfection cocktails prepared consisted of pGL4.32 (50 ng) with pRL-TK (2.5 ng) (20:1) or IFN-β plasmid (100 ng) with pRL-TK (2.5 ng) (40:1). After 24 HPI, cells were infected with BVDV2-wt, BVDV2-E, BRSV, BRSV and BVDV2-wt, or BRSV and BVDV2-E at a m.o.i. of 0.05, stimulated with poly I:C (100 µg/ml), or treated with media as UI control. Cells were harvested at 2 HPI, 1, 2, 3, 5, 7, or 9 DPI by removing the media and lysing cells with 1X PLB (Promega). Using the Dual-Luciferase® Reporter Assay System (Promega), lysates were evaluated for NF-kB or IFN-β activity. Luciferase activities were measured by using a 20/20n luminometer (Turner Biosystems, CA, USA) and expressed as relative luciferase units (RLU). Ratios were obtained by dividing the RLU for firefly luciferase activity (NF-kB or IFN-β) by RLU for Renilla luciferase activity (internal control) in each sample. Then, all ratios were divided by a UI ratio to represent the results as relative fold increases or decreases. The experiment was repeated three times and the graphs represent the averages.

2.13. Statistical analysis

Data were analyzed using the SAS statistical software program (SAS Institute Inc., Cary, NC, USA). Statistical significance was evaluated using analysis of variance (ANOVA) for a randomized complete block experimental design, and mean comparisons and contrasts were used to separate treatments. Bio-Rad CFX Manager 3.1 was used to analyze the gene mRNA results. The mRNA results that were upregulated at least 2-fold were identified. A P-value less than 0.05 was considered statistically significant.

3. Results

3.1. Influence of type 2 BVDV N^{pro} on the IFN-1 response of MDBK cells

The influence of ncp BVDV2-wt and BVDV2-E (Fig. 2.1A) on the IFN-1 response in MDBK cells was evaluated using the NCL1-ISRE-Luc-Hygro reporter cell line. BVDV2-wt isolate with a functional N^{pro} was a poor inducer of IFN-1 response *in vitro*, while BVDV2-E, a mutant with a dysfunctional N^{pro} fused with EGFP, induced a significant IFN-1 response. Cells infected with BVDV2-E synthesized a significantly ($P < 0.0001$) greater level of IFN-1 compared to the UI control cells and to the BVDV2-wt-infected cells; however, cells infected with BVDV2-wt synthesized an equivalent level of IFN-1 compared to the UI control cells (Fig. 2.1B). The levels of IFN-1 synthesized by cells infected with BVDV2-E were 22 times greater than the UI control cells and BVDV2-wt-infected cells. MDBK cells exposed to poly I:C (positive control) synthesized significantly greater levels of IFN-1 compared to viral infected or UI control cells.

BVDV2-E-infected MDBK cells produced significantly greater amounts of IFN-1 than cells infected with BVDV2-wt, while BVDV2-wt strongly inhibited IFN-1 production in cells stimulated with poly I:C. MDBK cells infected with BVDV2-wt and stimulated 48 HPI with poly I:C for 20 h synthesized low levels of IFN-1 compared to BVDV2-E-infected or UI control cells. Cells infected with BVDV2-E synthesized a significantly greater level (P=0.023; 3.6 times) of IFN-1 than cells infected with the BVDV2-wt isolate (Fig. 2.1C). MDBK cells exposed to poly I:C twice (positive control) and UI control cells exposed to poly I:C once synthesized significantly ($P < 0.0002$) greater levels of IFN-1 compared to viral infected cells stimulated once with poly I:C.

3.2. IFN-1 response of BT cells to BRSV, BVDV2 or BRSV/BVDV2 infections

BT cells were used to characterize the IFN-1 response to BRSV, BVDV2 or BRSV/BVDV2 infections. IFN-1 inhibition was significantly greater in cells co-infected with BRSV/BVDV2-wt than in cells co-infected with BRSV/BVDV2-E or BRSV-infected cells (Fig. 2.2A). BT cells infected with BVDV2-E had IFN-1 levels 2.6 times greater (P=0.0013) than cells infected with BVDV2-wt. Cells co-infected with BRSV/BVDV2-E had IFN-1 levels 2.2 times greater than cells co-infected with BRSV/BVDV2-wt (P=0.0012). Cells infected with BRSV alone had IFN-1 levels 2.7 times greater than BVDV2-wt-infected cells (P=0.0013). UI control cells synthesized twice the amount of IFN-1 compared to cells infected with the BVDV2-wt isolate. BT cells exposed to poly I:C synthesized a significantly ($P < 0.0001$) greater amount of IFN-1 compared to UI control cells or cells infected with either BVDV2 virus alone or co-infected with BRSV/BVDV2.

3.3. BRSV titers and RNA levels in BRSV and BRSV/BVDV2 co-infected BT cells

BT cells infected with BRSV/BVDV2-wt, BRSV/BVDV2-E, or BRSV alone were assayed for BRSV infectivity at 2, 6, 12 and 24 HPI, and 2, 3, 5, 7 and 9 DPI. The BRSV titer was significantly (P=0.0228) greater in BT cells infected with BRSV/BVDV2-wt compared to other infections at 5 DPI (Fig. 2.2B). Increased BRSV replication did not occur in cells co-infected with BRSV/BVDV2-E compared to cells infected with BRSV alone.

BRSV RNA levels in cells co-infected with BRSV/BVDV2-wt were 2.5, 2.8, and 2.9 copy number logs significantly (P=0.0008) greater than in cells infected with BRSV alone or co-infected with BRSV/BVDV2-E at 5, 7, and 9 DPI, respectively (Fig. 2.2B). There was no significant difference in BRSV RNA levels between cells infected with BRSV or co-infected with BRSV/BVDV2-E.

3.4. BVDV2-E induces the mRNA expression of PKR and TBK-1

Using real-time Q-RT-PCR, BT cells infected with BVDV2-E, a mutant with a dysfunctional N^{pro}, significantly ($P < 0.0001$) increased PKR mRNA production compared to BVDV2-wt-infected, BRSV-infected, or UI cells. BVDV2-E-infected cells produced 2.2, 2.7, 9.8, 3.8, 3.1, 3.8, and 3.5 times greater levels of PKR mRNA compared to BVDV2-wt-infected cells at 2 HPI, 1, 2, 3, 5, 7, and 9 DPI, respectively (Fig. 2.3A). BT cells infected with BVDV2-wt and BRSV had similar levels of PKR mRNA at all time points evaluated and were increased after 2 DPI compared to UI cells. Cells co-infected with BRSV/BVDV2-E significantly ($P < 0.0001$) increased the PKR mRNA production compared to cells co-infected with BRSV/BVDV2-wt or UI cells. Cells co-infected with BRSV/BVDV2-E produced 2.0, 2.7, 7.2, 3.6, 6.0, 6.8, and 9.2

times greater levels of PKR mRNA compared to cells co-infected with BRSV/BVDV2-wt at 2 HPI, 1, 2, 3, 5, 7, and 9 DPI, respectively (Fig. 2.3B). After 3 DPI, co-infection of cells with BRSV and BVDV2-wt decreased levels of the PKR mRNA compared to single infections with BVDV2-wt or BRSV. At 5, 7, and 9 DPI, BRSV reduced the PKR mRNA levels in cells co-infected with BVDV2-E compared to BVDV2-E-infected cells alone (Fig. 2.3A and 2.3B).

TBK-1 mRNA production started to increase in BT cells infected with BVDV2-E 2 DPI and became significantly ($P < 0.01$) greater than levels in BVDV2-wt-infected, BRSV-infected, or UI cells at 5, 7, and 9 DPI. BVDV2-E-infected cells produced 2.0, 2.5, and 2.2 times greater levels of TBK-1 mRNA compared to BVDV2-wt-infected cells at 5, 7, and 9 DPI, respectively (Fig. 2.4A). No significant differences were observed in TBK-1 mRNA levels between BVDV2-wt-infected, BRSV-infected or UI cells. Cells co-infected with BRSV/BVDV2-E had increased TBK-1 mRNA production two DPI and significantly ($P < 0.01$) greater TBK-1 mRNA levels 5, 7, and 9 DPI compared to cells co-infected with BRSV/BVDV2-wt or UI cells. Cells co-infected with BRSV/BVDV2-E produced 2.3, 2.1, and 2.3 times greater levels of TBK-1 mRNA compared to cells co-infected with BRSV/BVDV2-wt at 5, 7, and 9 DPI, respectively (Fig. 2.4B). Cells co-infected with BRSV/BVDV2-wt had TBK-1 mRNA levels similar to UI cells. At 7 and 9 DPI, BRSV reduced the TBK-1 mRNA levels in cells co-infected with BVDV2-E compared to BVDV2-E-infected cells alone (Fig. 2.4A and 2.4B).

3.5. BVDV2-E induces the mRNA expression of IRF-3 and IRF-7

Using real-time Q-RT-PCR, BT cells infected with ncp BVDV2-E, a mutant with a dysfunctional N^{pro}, significantly ($P < 0.0001$) increased the IRF-3 mRNA production

compared to BVDV2-wt-infected, BRSV-infected, or UI cells. BVDV2-E-infected cells produced 3.1, 3.3, 3.5, 4.6, and 4.0 times greater levels of IRF-3 mRNA compared to BVDV2-wt-infected cells at 2, 3, 5, 7, and 9 DPI, respectively (Fig. 2.5A). BRSV modestly induced IRF-3 mRNA after 3 DPI. No significant differences were detected in the levels of IRF-3 mRNA between cells infected with ncp BVDV2-wt compared to UI cells at all time points evaluated (Fig. 2.5A). Cells co-infected with BRSV/BVDV2-E significantly ($P < 0.0001$) increased the IRF-3 mRNA production compared to cells co-infected with BRSV/BVDV2-wt or UI cells. Cells co-infected with BRSV/BVDV2-E produced 2.9, 3.3, 4.5, 4.2, and 4.4 times greater levels of IRF-3 mRNA compared to cells co-infected with BRSV/BVDV2-wt at 2, 3, 5, 7, and 9 DPI, respectively. Cells co-infected with BRSV/BVDV2-wt had IRF-3 mRNA levels equivalent to UI cells (Fig. 2.5B). At 7 and 9 DPI, BRSV reduced the IRF-3 mRNA levels in cells co-infected with BVDV2-E compared to BVDV2-E-infected cells (Fig. 2.5A and 2.5B).

BT cells infected with BVDV2-E had significantly ($P < 0.0001$) increased IRF-7 mRNA production compared to BVDV2-wt-infected, BRSV-infected, or UI cells. BVDV2-E-infected cells produced 5.9, 5.9, 13.8, 3.9, 2.6, 3.2, and 4.0 times greater levels of IRF-7 mRNA compared to BVDV2-wt-infected cells at 2 HPI, 1, 2, 3, 5, 7, and 9 DPI, respectively. Compared to UI cells, BT cells infected with BVDV2-wt or BRSV produced greater levels of IRF-7 mRNA after 2 DPI. BVDV2-wt and BRSV induced similar levels of IRF-7 mRNA (Fig. 2.6A). Cells co-infected with BRSV/BVDV2-E had significantly ($P < 0.0001$) increased IRF-7 mRNA production compared to cells co-infected with BRSV/BVDV2-wt or UI cells. Cells co-infected with BRSV/BVDV2-E produced 3.5, 5.4, 9.0, 3.9, 5.9, 7.7, and 13.0 times greater levels of IRF-7 mRNA

compared to cells co-infected with BRSV/BVDV2-wt at 2 HPI, 1, 2, 3, 5, 7, and 9 DPI, respectively (Fig. 2.6B). Co-infection of cells with BRSV/BVDV2-wt had decreased levels of IRF-7 mRNA compared to single infections with BVDV2-wt or BRSV. At 7 and 9 DPI, BRSV reduced the IRF-7 mRNA levels in cells co-infected with BVDV2-E compared to BVDV2-E-infected cells (Fig. 2.6A and 2.6B).

3.6. BVDV2-E induces the mRNA expression of IFN-β

BT cells infected with BVDV2-E had significantly ($P < 0.01$) increased IFN-β mRNA production compared to BVDV2-wt-infected or UI cells. BVDV2-E-infected cells produced 3.0, 5.7, 8.5, 7.0, and 3.4 times greater levels of IFN-β mRNA compared to BVDV2-wt-infected cells at 2, 3, 5, 7, and 9 DPI, respectively. There was no significant difference in IFN-β mRNA levels between ncp BVDV2-wt and UI cells (Fig. 2.7A). Cells co-infected with BRSV/BVDV2-E had significantly ($P < 0.01$) increased IFN-β mRNA production compared to cells co-infected with BRSV/BVDV2-wt or UI cells. Cells co-infected with BRSV/BVDV2-E produced 2.8, 5.2, 7.5, 3.1, and 2.2 times greater levels of IFN-β mRNA compared to cells co-infected with BRSV/BVDV2-wt at 2, 3, 5, 7, and 9 DPI, respectively. In BRSV-infected cells, IFN-β mRNA production began increasing at 5 DPI and became significant ($P < 0.01$) at 7 and 9 DPI compared to BVDV2-wt-infected cells or UI cells. In co-infected cells, BVDV2-wt abolished the increased effect of BRSV and decreased the IFN-β mRNA to levels equivalent to those found in UI cells (Fig. 2.7B). BRSV did not reduce the IFN-β mRNA levels in cells co-infected with BRSV/BVDV2-E or BRSV/BVDV2-wt compared to BVDV2-E- or BVDV2-wt-infected cells, respectively. Within 2 HPI, cells stimulated with poly I:C produced 49 times greater level of IFN-β mRNA compared to UI cells and viral infected

cells; however, there were no significant differences between cells stimulated with poly I:C and UI cells at any other time point evaluated (Fig. 2.7A and 2.7B).

3.7. IFN-β and NF-κB luciferase activities in infected BT cells

Using a dual-luciferase reporter assay, IFN-β luciferase activity in BT cells infected with BVDV2-E was 2.6, 2.6, and 2.3 times significantly ($P < 0.05$) greater than in cells infected with BVDV2-wt at 1, 2, and 5 DPI, respectively. The IFN-β luciferase activity in cells co-infected with BRSV/BVDV2-E was 2.5, 2.2, and 1.9 times significantly ($P < 0.05$) greater than in cells co-infected with BRSV/BVDV2-wt at 1, 2, and 5 DPI, respectively (Fig. 2.7C). No significant differences between treatment groups were observed at 3 DPI, as well as at 2 HPI, 7, and 9 DPI (Fig. 3.11). There were no significant differences in the IFN-β luciferase activity among cells infected with BRSV, BVDV2-wt, or co-infected with BRSV/BVDV2-wt at any time point evaluated.

BVDV2-wt in BT cells co-infected with BRSV significantly ($P < 0.05$) increased NF-κB luciferase activity within 3 DPI compared to BRSV-infected or UI cells (Fig. 2.8). The NF-κB luciferase activity in cells infected with BVDV2-wt was 9.7, 12.7, and 6.9 times significantly ($P < 0.05$) greater than cells infected with BVDV2-E at 5, 7, and 9 DPI, respectively. The NF-κB luciferase activity in cells co-infected with BRSV/BVDV2-wt was 8.5 times significantly ($P < 0.05$) greater than cells co-infected with BRSV/BVDV2-E at both 5 and 7 DPI and 11.7 and 11.8 times greater than cells infected with BRSV alone at 5 and 7 DPI, respectively (Fig. 2.8). No significant differences between treatment groups were detected at 2 HPI, 1 DPI, and 2 DPI (Fig. 3.12).

4. Discussion

Our findings of ncp BVDV2 inhibition of IFN-1 pathway signaling and the enhancement of BRSV replication demonstrates the important role of BVDV2 in single and co-infected cells. The importance of the BVDV2 N^{pro} protein suggests a similar importance of the intact BVDV2 N^{pro} in animals infected with BRDC. *In vitro,* ncp BVDV1 N^{pro} mediates inhibition of IFN-1 production in host cells (Gil *et al.,* 2006a; Hilton *et al.,* 2006; Schweizer *et al.,* 2006). In the present study, the BVDV2-wt isolate with a functional N^{pro} was a poor inducer of IFN-1, while BVDV2-E, a mutant with a dysfunctional N^{pro} fused with EGFP, induced a significant IFN-1 response in both MDBK and BT cells. These results are consistent with a previous report of a mutant type 1 BVDV strain NADL with modified N^{pro} fused with EGFP, which showed reduced antagonism of IFN-1 synthesis. It was determined that the IFN-1 response was dependent on N^{pro} expression and independent of viral replication efficiency (Gil *et al.,* 2006a). The increased production of IFN-1 by cells infected with BVDV2-E may have reduced viral replication to significantly lower levels, which suggests that the antagonism of IFN-1 production enhances BVDV2 replication. These results are similar to a study where recombinant IFN-1 inhibited CSFV replication in different cell lines (Xia *et al.,* 2005). BVDV2-wt strongly inhibited IFN-1 production in MDBK cells stimulated 48 HPI with poly I:C, while BVDV2-E-infected cells produced significantly greater amounts of IFN-1 than cells infected with BVDV2-wt. These results demonstrate the role of an intact functional BVDV2 N^{pro} in the antagonism of IFN-1 production in host cells and suggest that BVDV2-E is able to replicate effectively in the presence of IFN-1 but at lower levels.

In this study, IFN-1 inhibition was significantly greater in BT cells co-infected with BRSV and BVDV2-wt than in cells co-infected with BRSV and BVDV2-E or in cells infected with BRSV alone. The N^{pro} product of BVDV interferes with the transcription and synthesis of IFN-1 by promoting the degradation of IRF-3 by proteosomal degradation (Hilton *et al.,* 2006; Seago *et al.,* 2007). It was reported that the insertion of EGFP within the amino end of N^{pro} interferes with the protein's ability to promote IRF-3 degradation. The structural integrity of the BVDV N^{pro} amino terminus was important for IFN-1 suppression rather than the enzymatic activity of the protein (Gil *et al.,* 2006a). In this study, results showed that cells co-infected with BRSV/BVDV2-wt exhibit greater IFN-1 inhibition than cells infected with BRSV alone. Inhibition of the IFN-1 response of cells with BVDV2-wt infection enhanced BRSV replication. The decrease in IFN-1 inhibition observed in cells co-infected with BRSV/BVDV2-E confirms the role of N^{pro} on IFN-1 inhibition.

The BRSV titer and RNA levels significantly increased in BT cells co-infected with BRSV/BVDV2-wt compared to cells co-infected with BRSV/BVDV2-E or infected with BRSV alone. This increased BRSV replication was attributed to the synergistic action of BVDV2-wt and BRSV inhibition of IFN-1. These results are consistent with a previous study where the IFN-1 pathway signaling was inhibited by using a TBK-1 inhibitor, which decreased the IFN-β mRNA expression and increased the viral mRNA expression of dengue virus serotype 2 (DENV2), a member of the family *Flaviviridae* (Zhang *et al.,* 2013). The nonstructural BRSV proteins, NS1 and NS2, together inhibit the phosphorylation and transcriptional activity of IRF-3 resisting IFN-1 production (Bossert and Conzelmann, 2002; Bossert *et al.,* 2003). In addition, the N^{pro} protein of BVDV

inhibits the production of IFN-1 by targeting the IRF-3 for proteosomal degradation, resulting in the inhibition of IFN-1 transcription (Seago *et al.*, 2007). Increases in BRSV titer and RNA levels did not occur in cells co-infected with BRSV/BVDV2-E compared to cells infected with BRSV alone, which is attributed to the diminished ability of BVDV2-E to inhibit IFN-1. Similarly, *in vivo*, enhanced respiratory and digestive tract diseases have been reported with BRSV/BVDV co-infections compared to infection with either virus alone (Brodersen and Kelling, 1998, 1999). Brodersen and Kelling (1998; 1999) showed that calves concurrently infected with BRSV and BVDV had more severe clinical signs of disease and extensive lung lesions, and shed virus in greater concentration for longer duration compared to calves infected with either virus alone (Brodersen and Kelling, 1998, 1999). BVDV2-wt, unlike BVDV2-E, enhances BRSV replication because of the intact BVDV2 N^{pro} role in the antagonism of IFN production.

Using a real-time Q-RT-PCR assay, we observed decreased effects of the BVDV2 N^{pro} protein on IFN-1 pathway signaling during single and co-infection with BRSV. Compared to intact BVDV2 N^{pro}, the dysfunctional N^{pro} had greatly increased mRNA levels of PKR, TBK-1, IRF-3, IRF-7, and IFN-β, while no significant differences in MAVS and NF-κB mRNA, as well as the mRNA of the protein that facilitates the IRF-3 degradation, PIN-1, were observed.

MAVS (IFN-β-promoter stimulator 1, IPS-1) is essential for IFN-1 production in viral infections through IRF-3 and NF-κB pathways. In the current study, BRSV, BVDV2-wt, and BVDV2-E did not affect MAVS mRNA expression. These results are consistent with a previous study reporting that MAVS was largely intact when HEC-1B

cells were infected with poliovirus, a virus that significantly reduced the IFN-β mRNA levels (Kotla and Gustin, 2015). The importance of MAVS in the IFN-1 pathway was reported in mammalian (feline) cells. During Sendai virus infection, inhibiting MAVS by using siRNA inhibited the IFN-β promoter activation. In contrast, MAVS over-expression activated IRF-3 and NF-κB pathway signaling and induced IFN-β production (Wu *et al.,* 2016). Our results showed no significant differences in MAVS mRNA among the different treatment groups at all time points compared to UI cells (Fig. 3.6A and 3.6B), while the IFN-β mRNA levels and the IFN-1 production were significantly reduced in cells infected BVDV2-wt. These results indicate that the intact BVDV2 N^{pro} antagonism of IFN-1 production does not appear to be mediated by MAVS mRNA expression inhibition.

The IFN-induced double-stranded RNA-dependent protein kinase (PKR) is activated in response to dsRNA and a wide range of activators and cell stresses. Phosphorylated (activated) PKR can activate NF-κB, phosphorylate eIF2α, and induce apoptosis (García *et al.,* 2006). In this study, BVDV2-wt increased PKR mRNA after two DPI, which is consistent with an *in vivo* study where both types of ncp BVDV, type 1 and 2, increased PKR mRNA at 5 DPI in spleen and tracheo-bronchial lymph nodes of infected beef calves (Palomares *et al.,* 2013). Although BVDV2-wt increased PKR mRNA, BVDV2-E increased PKR mRNA more rapidly and to greater levels suggesting an important role of ncp BVDV2 N^{pro} protein in PKR inhibition. In contrast, it was determined that unlike cp BVDV, ncp BVDV1 inhibited the PKR signaling pathway resulting in enhanced protein synthesis and cell survival (Gil *et al.,* 2006b). CSFV activates PKR which phosphorylates the eIF2α leading to apoptosis (Hsu *et al.,* 2014).

Our study showed that BRSV and BVDV2-wt increased PKR mRNA to similar levels, while co-infection with BRSV and BVDV2-wt did not increase the PKR mRNA, which was attributed to the synergistic action of these two viruses. Minimal difference in BRSV cytopathic effects was observed between cells infected with BRSV and cells co-infected with BRSV and BVDV2-wt. Although the PKR mRNA levels in cells co-infected with BRSV and BVDV2-E were increased compared to cells infected with BRSV alone, the BRSV cytopathic effects were decreased in co-infected cells (data not shown). These results suggest that PKR is not essential for the cytopathic effects of BRSV. PKR detects viral dsRNA and initiates the antiviral stress granule (avSG) formation in the cytoplasm which triggers innate immunity. Removal of PKR diminished IFN production and enhanced viral replication (Onomoto *et al.,* 2012). Secreted IFN-1 binds to IFN-1 receptor on the neighboring cells triggering a variety of genes, including PKR, which can be induced by the IFN treatment (García *et al.,* 2007). The increased PKR mRNA levels caused by BVDV2-E compared to BVDV2-wt may, in part, relate to the increased IFN-1 production (feedback effect). The rapid increase in PKR mRNA observed within 2 HPI following BVDV2-E infection demonstrates an inhibitory role of intact N^{pro} in PKR mRNA expression.

TANK-binding kinase 1 (TBK-1, also known as NF-κB-activating kinase (NAK) or T2K) regulates the IRF-3 and NF-κB pathways. Activated TBK-1 phosphorylates the transcription factors IRF-3 and IRF-7 (Zhao, 2013). The NS3 protein of hepatitis C virus, a member of the BVDV family (*Flaviviridae*), binds to TBK-1 and inhibits the interaction between TBK-1 and IRF-3 leading to cellular antiviral response inhibition (Otsuka *et al.,* 2005). In our study, TBK-1 mRNA levels were increased by BVDV2-E

while they were not changed in infections with BVDV2-wt and/or BRSV compared to UI cells. The lack of TBK-1 up-regulation in BVDV2-wt-infected cells was associated with the inhibition of the IRF-3/7 pathway signaling and decreased IFN-1 production, which may be associated with lack of IRF-3/7 phosphorylation. Whereas, BVDV2-E up-regulated the TBK-1 and increased the IFN-1 production, which suggests a central role of BVDV2 N^{pro} on TBK-1 regulation in the IRF-3/7 signaling pathway. Similar results were reported when HepG2 cells were treated with a TBK-1 inhibitor (BX795) and stimulated with poly I:C, which decreased the IFN-β mRNA expression and increased the DENV2 viral mRNA expression (Zhang *et al.*, 2013). Preventing the IRF-3/7 activation by inhibiting the TBK-1 mRNA expression suggests another role of intact N^{pro} in the antagonism of IFN-1 production and immunosuppression associated with BVDV infection.

The transcription factor, nuclear factor-κB (NF-κB), induces the expression of immune and inflammatory genes and IFN-1 production. To determine whether BRSV and/or BVDV2 can inhibit inflammatory reactions via inhibition of the NF-κB signaling pathway, we utilized a dual-luciferase reporter assay system. While there were no significant differences in the expression of NF-κB mRNA (Fig. 3.7A and 3.7B) among different infections at different time points, BVDV2-wt, unlike BVDV2-E, significantly increased NF-κB luciferase activity. Similar to our results, cp BVDV type 1 was able to induce the production of cytokines and modulate transcriptional factors, including IRF-7, in MDBK cells through activating NF-κB. The expression of the negative regulator of the immune response A20 (TNFAIP3), a target ubiquitin-editing enzyme of NF-κB, is mediated by the NF-κB pathway. Using the pharmacological inhibitor of NF-κB

signaling pathway (BAY-117085) blocked the BVDV type 1 activities (Fredericksen *et al.*, 2015, 2016). The significantly increased BVDV2-wt activation of NF-κB suggests that the intact N^{pro} antagonizes the IFN-1 production through a NF-κB-independent pathway. In cells infected with cp BVDV NADL, the N^{pro} does not affect the NF-κB activation of gene expression (Chen *et al.*, 2007). However, our results indicate that only the dysfunctional BVDV2 N^{pro} did not affect the NF-κB activity suggesting a positive role of intact ncp BVDV2 N^{pro} in the NF-κB activation. The increase in NF-κB activity and the decrease in IFN-1 production in cells infected with BVDV2-wt suggest that the IRF3/7 pathway is the main pathway of IFN-1 production that is reduced by intact BVDV2 N^{pro} in single and co-infection with BRSV. It has been reported that respiratory syncytial virus (RSV) is a potent activator of NF-κB (Jamaluddin *et al.*, 1998). This is in contrast to our results that showed that BRSV did not increase NF-κB luciferase activity. Our results of NF-κB activity and mRNA expression suggest a limited role of NF-κB pathway in IFN-1 production in BVDV2- and BRSV-infected BT cells.

The mammalian interferon-regulatory factor (IRF) family includes nine members named from one to nine. They have different roles in the gene regulatory networks in the immune system. IRF-3 and IRF-7 are closely related to each other and are important cellular transcription factors targeting the IFN-1 gene and increasing the IFN-1 production in infected cells. IRF-3 and IRF-7 monomers are activated into phosphorylated dimers and translocated to the nucleus of virus-infected cells (Taniguchi *et al.*, 2001). Our results showed that BVDV2-wt and BRSV similarly increased the IRF-7 mRNA levels. However, only BRSV induced the IRF-3 mRNA after 5 DPI, which may explain the increased IFN-1 production by BRSV compared to BVDV2-wt. BVDV-1

induced the IRF-7 production through activating NF-κB (Fredericksen *et al.,* 2015). In our study, BVDV2-wt increased the mRNA levels of IRF-7 within 3 DPI and enhanced the NF-κB activity within 3 DPI, while the TBK-1 mRNA levels were not increased by BVDV2-wt-infection. These results suggest that BVDV2-wt increased the IRF-7 mRNA levels through NF-κB pathway. Compared to single infection, co-infection of cells with BRSV and BVDV-wt had reduced IRF-3 and IRF-7 mRNA levels indicating the role of BRSV and BVDV-wt in IRF-3 and IRF-7 inhibition and the synergistic interaction of these viruses. It has been reported that NS1 and NS2 proteins of BRSV mediate the inhibition of IRF-3 activation and IFN induction in infected MDBK cells (Bossert *et al.,* 2003). In our study, the dysfunctional N^{pro} of BVDV2-E greatly induced IRF-3 mRNA levels within 2 DPI and IRF-7 mRNA levels within 2 HPI indicating the role of intact BVDV2 N^{pro} in the antagonism of IFN-1 production. These results are consistent with studies previously reported showing that the N^{pro} protein of *Pestivirus* directly interacts with the monomer and dimer forms of IRF-3 preventing the IFN production (Gottipati *et al.,* 2016). BVDV N^{pro} interacts with IRF-3 before the virus-induced phosphorylation of IRF-3 leading to polyubiquitination and proteasomal degradation of IRF-3 (Chen *et al.,* 2007). Both cp and ncp BVDV inhibit the full function of IRF-3 but do not increase or decrease the nuclear uptake of IRF-7 (Baigent *et al.,* 2004). Our results demonstrate the role of intact BVDV2 N^{pro} in the inhibition of the IRF-3 and IRF-7 mRNA expression in order to antagonize the IFN production and increase the BRSV replication.

We found that BVDV2-wt did not change the IFN-β mRNA levels compared to UI cells and no significant change in IFN-β luciferase activity was detected, which indicated the role of intact N^{pro} in the antagonism of IFN-1. Similar to our results, other

studies have shown that the BVDV N^{pro} prevents IFN-β mRNA production in infected cells (Chen *et al.*, 2007; Hilton *et al.*, 2006). We found that BVDV2-E greatly increased the IFN-β mRNA levels as well as the IFN-β luciferase activity. Our results are consistent with a study where cp BVDV with mutant N^{pro} did not suppress the IFN production (Gil *et al.*, 2006a). BRSV induced IFN-β mRNA after 5 DPI, which may explain the increased IFN-1 production in BRSV-infected cells. This BRSV-mediated increased IFN-β mRNA was abolished by BVDV-wt indicating the major role of intact BVDV2 N^{pro} in immunosuppression. BRSV had no negative effect on the IFN-β mRNA levels when co-infected with BVDV2-wt or BVDV2-E. These results demonstrate the importance and strength of IFN-1 antagonism by BVDV2-wt, which will increase the replication of BRSV.

The peptidylprolyl isomerase (cis–trans peptidylprolyl isomerase, NIMA-interacting 1, PIN-1) interacts with the phosphorylated IRF-3 in the nucleus to facilitate the IRF-3 degradation and terminate the action of IRF-3 (Saitoh *et al.*, 2006). In our study, there were no significant effects of BVDV2-wt, BVDV2-E, and/or BRSV on the PIN-1 mRNA levels in different treatment groups (Fig. 3.8A and 3.8B), which is consistent with a study by Chen *et al.*, 2007, which suggested that BVDV N^{pro} induces IRF-3 degradation via a PIN-1-independent mechanism (Chen *et al.*, 2007). While the intact BVDV2 N^{pro} decreases IFN-β mRNA levels and the IFN-1 production, it has no impact on the PIN-1 mRNA levels. These results suggest that PIN-1 has no role in IFN antagonism during BVDV2 and/or BRSV infections.

Infection with BVDV2-E having a dysfunctional N^{pro} induced greater levels of IFN-1 than BVDV2-wt, confirming the role of the intact type 2 BVDV N^{pro} in the antagonism of IFN-1 in BVDV2-infected cells. BVDV2-E induced mRNA expression of the IRF-3 pathway signals indicating the important inhibition of the IRF-3 pathway by intact BVDV2 N^{pro}. *In vitro*, BVDV-wt, unlike BVDV2-E, decreased mRNA expression of the IRF-3 pathway signal in cells co-infected with BRSV/BVDV2-wt and enhanced BRSV replication. This enhancement of BRSV replication *in vitro* correlates with the *in vivo* increased pathogenicity of BRSV in calves co-infected with BVDV (Brodersen and Kelling, 1998). *In vitro*, infection of cells with ncp BVDV having a functional N^{pro} interferes with IFN-1 production, yet *in vivo* BVDV induces a sustained IFN production in postnatal animals (Charleston *et al.,* 2002). These findings may contribute to the understanding of the immunosuppressive effects of BVDV and the mechanism(s) involved in the increased pathogenicity of BRSV and other viral infections during co-infection with ncp BVDV, which may lead to a better understanding of the BRDC. Understanding the role of BVDV and up-regulating the host's immune response by use of a mutant BVDV while maintaining antigenicity should add to the development of a safer and more effective BVDV vaccine.

Acknowledgment

This work was supported by the University of Nebraska Agricultural Research Division (grant NEB 39-152) from funds provided through Animal Health, U.S. Department of Agriculture and from funds provided through Qassim University, Buraydah, Al-Qassim, Saudi Arabia. We thank Dr. Fernando Osorio for providing the

IFN-β plasmid. We are grateful to Dr. Matthew Wiebe, Dr. Samodha Fernando, and Dr. Jean-Jack Riethoven for their helpful discussions.

References

Baigent, S.J., Goodbourn, S., McCauley, J.W., 2004. Differential activation of interferon regulatory factors-3 and -7 by non-cytopathogenic and cytopathogenic bovine viral diarrhoea virus. Vet. Immunol. Immunopathol. 100(3-4):135-44.

Baigent, S.J., Zhang, G., Fray, M.D., Flick-Smith, H., Goodbourn, S., McCauley, J.W., 2002. Inhibition of beta interferon transcription by noncytopathogenic bovine viral diarrhea virus is through an interferon regulatory factor 3-dependent mechanism. J. Virol. 76, 8979-8988.

Bautista, E.M., Ferman, G.S., Gregg, D., Brum, M.C., Grubman, M.J., Golde, W.T., 2005. Constitutive expression of alpha interferon by skin dendritic cells confers resistance to infection by foot-and-mouth disease virus. J. Virol. 79, 4838-4847.

Beura, L.K., Sarkar, S.N., Kwon, B., Subramaniam, S., Jones, C., Pattnaik, A.K., Osorio, F.A., 2010. Porcine reproductive and respiratory syndrome virus nonstructural protein 1beta modulates host innate immune response by antagonizing IRF3 activation. J. Virol. 84(3):1574-84. doi: 10.1128/JVI.01326-09.

Booker, C.W., Abutarbush, S.M., Morley, P.S., Guichon, P.T., Wildman, B.K., Jim, G.K., Schunicht, O.C., Pittman, T.J., Perrett, T., & authors, 2008. The effect of bovine viral diarrhea virus infections on health and performance of feedlot cattle. Can. Vet. J. 49, 253-260.

Bossert, B., Conzelmann, K.K., 2002. Respiratory syncytial virus (RSV) nonstructural (NS) proteins as host range determinants: a chimeric bovine RSV with NS genes from human RSV is attenuated in interferon-competent bovine cells. J. Virol. 76, 4287-4293.

Bossert, B., Marozin, S., Conzelmann, K.K., 2003. Nonstructural proteins NS1 and NS2 of bovine respiratory syncytial virus block activation of interferon regulatory factor 3. J. Virol. 77, 8661-8668.

Boxus, M., Letellier, C., Kerkhofs, P., 2005. Real Time RT-PCR for the detection and quantitation of bovine respiratory syncytial virus. J. Virol. Methods 125, 125-130.

Brodersen, B.W., Kelling, C.L., 1998. Effect of concurrent experimentally induced bovine respiratory syncytial virus and bovine viral diarrhea virus infection on respiratory tract and enteric diseases in calves. Am. J. Vet. Res. 59, 1423-1430.

Brodersen, B.W., Kelling, C.L., 1999. Alteration of leukocyte populations in calves concurrently infected with bovine respiratory syncytial virus and bovine viral diarrhea virus. Viral. Immunol. 12, 323-334.

Bunt, A.A., Milne, R.G., Sayaya, T., Verbeek, M., Vetten, H.J., Walsh, J.A., 2005. Paramyxoviridae. In Virus Taxonomy. Eighth report of the International Committee on Taxonomy of Viruses. pp. 655-671. Edited by C.M., Fauquet, M.A., Mayo, J., Maniloff, U., Desselberger, L.A., Ball, London, UK: Elsevier/Academic Press.

Castelli, J.C., Hassel, B.A., Wood, K.A., Li, X.L., Amemiya, K., Dalakas, M.C., Torrence, P.F., Youle, R.J., 1997. A study of the interferon antiviral mechanism: apoptosis activation by the 2-5A system. J. Exp. Med. 186, 967-972.

Charleston, B., Brackenbury, L.S., Carr, B.V., Fray, M.D., Hope, J.C., Howard, C.J., Morrison, W.I., 2002. Alpha/beta and gamma interferons are induced by infection with noncytopathic bovine viral diarrhea virus in vivo. J. Virol. 76, 923-927.

Chen, Z., Rijnbrand, R., Jangra, R.K., Devaraj, S.G., Qu, L., Ma, Y., Lemon, S.M., Li, K., 2007. Ubiquitination and Proteasomal Degradation of Interferon Regulatory Factor-3 induced by Npro from a Cytopathic Bovine Viral Diarrhea Virus. Virology 366(2), 277–292.

Collett, M.S., Larson, R., Belzer, S.K., Retzel, E., 1988a. Proteins encoded by bovine viral diarrhea virus: the genomic organization of a pestivirus. Virology. 165(1):200-8.

Collett, M.S., Larson, R., Gold, C., Strick, D., Anderson, D.K., Purchio, A.F., 1988b. Molecular cloning and nucleotide sequence of the pestivirus bovine viral diarrhea virus. Virology. 165(1):191-9.

Collett, M.S., Wiskerchen, M., Welniak, E., Belzer, S.K., 1991. Bovine viral diarrhea virus genomic organization. Arch. Virol. Suppl. 3, 19-27.

Fredericksen, F., Carrasco, G., Villalba, M., Olavarría, V.H., 2015. Cytopathic BVDV-1 strain induces immune marker production in bovine cells through the NF-κB signaling pathway. Mol. Immunol. 68(2 Pt A):213-22. doi: 10.1016/j.molimm.2015.08.010.

Fredericksen, F., Villalba, M., Olavarría, V.H., 2016. Characterization of bovine A20 gene: Expression mediated by NF-κB pathway in MDBK cells infected with bovine viral diarrhea virus-1. Gene. 581(2):117-29. doi: 10.1016/j.gene.2016.01.030.

García, M.A., Gil, J., Ventoso, I., Guerra, S., Domingo, E., Rivas, C., Esteban, M., 2006. Impact of Protein Kinase PKR in Cell Biology: from Antiviral to Antiproliferative Action. Microbiology and Molecular Biology Reviews, 70(4), 1032–1060.

García, M.A., Meurs, E.F., Esteban, M., 2007. The dsRNA protein kinase PKR: virus and cell control. Biochimie. 89(6-7):799-811. Review.

Gil, L.H., Ansari, I.H., Vassilev, V., Liang, D., Lai, V.C., Zhong, W., Hong, Z., Dubovi, E.J., Donis, R.O., 2006a. The amino-terminal domain of bovine viral diarrhea virus Npro protein is necessary for alpha/beta interferon antagonism. J. Virol. 80, 900-911.

Gil, L.H., van Olphen, A.L., Mittal, S.K., Donis, R.O., 2006b. Modulation of PKR activity in cells infected by bovine viral diarrhea virus. Virus Res. 116(1-2):69-77.

Gottipati, K., Holthauzen, L.M., Ruggli, N., Choi, K.H., 2016. Pestivirus Npro Directly Interacts with Interferon Regulatory Factor 3 Monomer and Dimer. J. Virol. 90(17):7740-7. doi: 10.1128/JVI.00318-16.

Hellemans, J., Mortier, G., De Paepe, A., Speleman, F., Vandesompele, J., 2007. qBase relative quantification framework and software for management and automated analysis of real-time quantitative PCR data. Genome Biol. 8(2):R19.

Hilton, L., Moganeradj, K., Zhang, G., Chen, Y.H., Randall, R.E., McCauley, J.W., Goodbourn, S., 2006. The Npro product of bovine viral diarrhea virus inhibits DNA binding by interferon regulatory factor 3 and targets it for proteasomal degradation. J. Virol. 80(23):11723-32.

Honda, K., Taniguchi, T., 2006. IRFs: master regulators of signalling by Toll-like receptors and cytosolic pattern-recognition receptors. Nat. Rev. Immunol. 6(9):644-58. Review.

Horscroft, N., Bellows, D., Ansari, I., Lai, V.C., Dempsey, S., Liang, D., Donis, R., Zhong, W., Hong, Z., 2005. Establishment of a subgenomic replicon for bovine viral diarrhea virus in Huh-7 cells and modulation of interferon-regulated factor 3-mediated antiviral response. J. Virol. 79, 2788-2796.

Hsu, W.L., Chen, C.L., Huang, S.W., Wu, C.C., Chen, I.H., Nadar, M., Su, Y.P., Tsai, C.H., 2014. The untranslated regions of classic swine fever virus RNA trigger apoptosis. PLoS One. 9(2):e88863. doi: 10.1371/journal.pone.0088863.

Jamaluddin, M., Casola, A., Garofalo, R.P., Han, Y., Elliott, T., Ogra, P.L., Brasier, A.R., 1998. The major component of IkappaBalpha proteolysis occurs independently of the proteasome pathway in respiratory syncytial virus-infected pulmonary epithelial cells. J. Virol. 72(6):4849-57.

Kelling, C.L., Steffen, D.J., Cooper, V.L., Higuchi, D.S., Eskridge, K.M., 2002. Effect of infection with bovine viral diarrhea virus alone, bovine rotavirus alone, or concurrent infection with both on enteric disease in gnotobiotic neonatal calves. Am. J. Vet. Res. 63, 1179-1186.

Klucas, C.A., Anderson, G.A., 1988. Bovine respiratory syncytial virus-specific monoclonal antibodies. Vet. Immunol. Immunopathol. 18, 307-315.

Kotla, S., Gustin, K.E., 2015. Proteolysis of MDA5 and IPS-1 is not required for inhibition of the type I IFN response by poliovirus. Virol. J. 12:158. doi: 10.1186/s12985-015-0393-2.

Le Bon, A., Etchart, N., Rossmann, C., Ashton, M., Hou, S., Gewert, D., Borrow, P., Tough, D.F., 2003. Cross-priming of CD8+ T cells stimulated by virus-induced type I interferon. Nat. Immunol. 4, 1009-1015.

Litinskiy, M.B., Nardelli, B., Hilbert, D.M., He, B., Schaffer, A., Casali, P., Cerutti, A., 2002. DCs induce CD40-independent immunoglobulin class switching through BLyS and APRIL. Nat. Immunol. 3, 822-829.

Løken, T., 1995. Ruminant pestivirus infections in animals other than cattle and sheep. Vet. Clin. N Am. Food Anim. Pract. 11, 597-614.

Meyer, C., Von Freyburg, M., Elbers, K., Meyers, G., 2002. Recovery of virulent and RNase-negative attenuated type 2 bovine viral diarrhea viruses from infectious cDNA clones. J. Virol. 76, 8494-8503.

Meyers, G., Tautz, N., Becher, P., Thiel, H.J., Kümmerer, B.M., 1996. Recovery of cytopathogenic and noncytopathogenic bovine viral diarrhea viruses from cDNA constructs. J. Virol. 70(12):8606-13.

Onomoto, K., Jogi, M., Yoo, J.S., Narita, R., Morimoto, S., Takemura, A., Sambhara, S., Kawaguchi, A., Osari, S., Nagata, K., et al., 2012. Critical role of an antiviral stress granule containing RIG-I and PKR in viral detection and innate immunity. PLoS ONE, 7:e43031.

Otsuka, M., Kato, N., Moriyama, M., Taniguchi, H., Wang, Y., Dharel, N., Kawabe, T., Omata, M., 2005. Interaction between the HCV NS3 protein and the host TBK1 protein leads to inhibition of cellular antiviral responses. Hepatology. 41(5):1004-12.

Palomares, R.A., Walz, H.G., Brock, K.V., 2013. Expression of type I interferon-induced antiviral state and pro-apoptosis markers during experimental infection with low or high virulence bovine viral diarrhea virus in beef calves. Virus Res. 173(2):260-9. doi: 10.1016/j.virusres.2013.02.010.

Paquette, R.L., Hsu, N., Said, J., Mohammed, M., Rao, N.P., Shih, G., Schiller, G., Sawyers, C., Glaspy, J.A., 2002. Interferon-alpha induces dendritic cell differentiation of CML mononuclear cells in vitro and in vivo. Leukemia 16, 1484-1489.

Pellerin, C., van den Hurk, J., Lecomte, J., Tijssen, P., 1994. Identification of a new group of bovine viral diarrhea virus strains associated with severe outbreaks and high mortalities. Virology. 203(2):260-8.

Pletnev, A., Gould, E., Heinz, F.X., Meyers, G., Thiel, H.J., Bukh, J., Stiasny, K., Collett, M.S., Bechner, P., & authors, 2011. *Flaviviridae*. In Virus Taxonomy: Classification and Nomenclature of Viruses: Ninth Report of the International Committee on Taxonomy of Viruses. pp. 1003-1020. Edited by A.M.Q. King, M.J. Adams, E.B., Carstens, E.J., Lefkowitz. Oxford, UK: Elsevier.

Raizman, E.A., Pogranichniy, R., Lévy, M., Negron, M., Langohr, I., Van Alstine, W., 2009. Experimental infection of white-tailed deer fawns (Odocoileus virginianus) with bovine viral diarrhea virus type-1 isolated from free-ranging white-tailed deer. J. Wildl. Dis. 45, 653-660.

Ridpath, J.F., Bolin, S.R., Dubovi, E.J., 1994. Segregation of bovine viral diarrhea virus into genotypes. Virology 205, 66-74.

Rogge, L., D'Ambrosio, D., Biffi, M., Penna, G., Minetti, L.J., Presky, D.H., Adorini, L., Sinigaglia, F., 1998. The role of Stat4 in species-specific regulation of Th cell development by type I IFNs. J. Immunol. 161, 6567-6574.

Ruggli, N., Tratschin, J.D., Schweizer, M., McCullough, K.C., Hofmann, M.A., Summerfield, A., 2003. Classical swine fever virus interferes with cellular antiviral defense: evidence for a novel function of N(pro). J. Virol. 77, 7645-7654.

Saitoh, T., Tun-Kyi, A., Ryo, A., Yamamoto, M., Finn, G., Fujita, T., Akira, S., Yamamoto, N., Lu, K.P., Yamaoka, S., 2006. Negative regulation of interferon-regulatory factor 3-dependent innate antiviral response by the prolyl isomerase Pin1. Nat. Immunol. 7(6):598-605.

Sato, K., Hida, S., Takayanagi, H., Yokochi, T., Kayagaki, N., Takeda, K., Yagita, H., Okumura, K., Tanaka, N., & authors, 2001. Antiviral response by natural killer cells through TRAIL gene induction by IFN-alpha/beta. Eur. J. Immunol. 31, 3138-3146.

Schweizer, M., Mätzener, P., Pfaffen, G., Stalder, H., Peterhans, E., 2006. "Self" and "nonself" manipulation of interferon defense during persistent infection: bovine viral diarrhea virus resists alpha/beta interferon without blocking antiviral activity against unrelated viruses replicating in its host cells. J. Virol. 80, 6926-6935.

Seago, J., Hilton, L., Reid, E., Doceul, V., Jeyatheesan, J., Moganeradj, K., McCauley, J., Charleston, B., Goodbourn, S., 2007. The Npro product of classical swine fever virus and bovine viral diarrhea virus uses a conserved mechanism to target interferon regulatory factor-3. J. Gen. Virol. 88, 3002-3006.

Simmonds, P., Becher, B., Bukh, J., Gould, E.A., Meyers, G., Monath, T., Muerhoff, S., Pletnev, A., Rico-Hesse, R., Smith, D.B., Stapleton, J.T., and ICTV Report Consortium, 2017. ICTV Virus Taxonomy Profiles: *Flaviviridae*, Journal of General Virology (In Press).

Taniguchi, T., Ogasawara, K., Takaoka, A., Tanaka, N., 2001. IRF family of transcription factors as regulators of host defense. Annu. Rev. Immunol. 19:623-55. Review.

Tautz, N., Tews, B.A., Meyers, G., 2015. The Molecular Biology of Pestiviruses. Adv Virus Res. 2015;93:47-160. doi: 10.1016/bs.aivir. 03.002. Review.

Topliff, C.L., Smith, D.R., Clowser, S.L., Steffen, D.J., Henningson, J.N., Brodersen, B.W., Bedenice, D., Callan, R.J., Reggiardo, C., & authors, 2009. Prevalence of bovine viral diarrhea virus infections in alpacas in the United States. J. Am. Vet. Med. Assoc. 234, 519-529.

Tough, D.F., 2004. Type I interferon as a link between innate and adaptive immunity through dendritic cell stimulation. Leuk. Lymphoma. 45, 257-264.

Wu, H., Zhang, X., Liu, C., Liu, D., Liu, J., Wang, G., Tian, J., Qu, L., 2016. Molecular cloning and functional characterization of feline MAVS. Immunol. Res. 64(1):82-92. doi: 10.1007/s12026-015-8682-9.

Xia, C., Dan, W., Wen-Xue, W., Jian-Qing, W., Li, W., Tian-Yao, Y., Qin, W., Yi-Bao, N., 2005. Cloning and expression of interferon-alpha/gamma from a domestic porcine breed and its effect on classical swine fever virus. Vet. Immunol. Immunopathol. 104, 81-89.

Yoneyama, M., Onomoto, K., Jogi, M., Akaboshi, T., Fujita, T., 2015. Viral RNA detection by RIG-I-like receptors. Curr. Opin. Immunol. 32:48-53. doi: 10.1016/j.coi.2014.12.012. Review.

Zhang, P., Wu, S., Li, L., Liang, Z., Li, Y., Feng, L., Huang, X., 2013. Adjuvant PIKA protects hepatoma cells from dengue virus infection by promoting a TBK-1-dependent innate immune response. Arch. Virol. 158(4):829-38. doi: 10.1007/s00705-012-1556-8.

Zhao, W., 2013. Negative regulation of TBK1-mediated antiviral immunity. FEBS Lett. 587(6):542-8. doi: 10.1016/j.febslet.2013.01.052. Review.

Figure legends

Fig. 2.1. Genomic organization of BVDV2 isolates and IFN production. (A) Genomic organization and encoded proteins of BVDV2 NY93/c (BVDV2-wt) and BVDV2 NY93/c N-N^{Pro} 18 EGFP (BVDV2-E) isolates. The coding sequence of the EGFP was inserted into the BVDV2 NY93 genome between amino acids 18 and 19 of the N^{pro} protein forming BVDV2-E. (B) MDBK cells infected with BVDV2-E synthesized significantly greater levels of IFN-1 compared to UI control cells or cells infected with BVDV2-wt. MDBK cells were infected with each BVDV2 isolate and cell lysates harvested 24 HPI, clarified by centrifugation, and pH adjusted to inactivate virus. Experimental samples were added to NCL1-Luc-ISRE-Hygro reporter cells and incubated for 8 h followed by cell lysis. Luciferase activity of the cell lysates was measured. (C) MDBK cells infected with BVDV2-E synthesized significantly greater levels of IFN-1 than cells infected with BVDV2-wt. MDBK cells were treated with poly I:C, mock-infected with media (UI) or infected with each of the BVDV2 isolates. The media and inoculum were replaced with fresh poly I:C in all plates at 48 HPI and incubated for an additional 20 h. Cells were then treated as in (B). (*) Groups are statistically different from the other groups at $P < 0.05$. Error bars represent standard error of the means (SEM).

Fig. 2.2. BVDV2 N^{pro} decreases IFN-1 production and increases BRSV replication in co-infected BT cells. (A) IFN-1 inhibition was significantly greater in BT cells co-infected with BRSV/BVDV2-wt than in cells co-infected with BRSV/BVDV2-E or in cells infected with BRSV alone. IFN-1 inhibition was significantly greater in BT cells infected with BVDV2-wt compared to BVDV2-E. BT cells were infected with BRSV, BVDV2-wt, BRSV/BVDV2-wt, BVDV2-E or BRSV/BVDV2-E and after 48 h, media

was replaced with fresh media and incubation continued for 20 h. Cells were then treated as in Fig. 2.1B. (B) BRSV titers and RNA levels. The BRSV titer was significantly greater at 5 DPI in cells co-infected with BRSV/BVDV2-wt compared to cells infected with BRSV alone or co-infected with BRSV/BVDV2-E. BVDV2-wt, but not BVDV2-E, enhanced BRSV replication in BRSV co-infected BT cells. BT cells were infected with BRSV alone, BRSV/BVDV2-wt or BRSV/BVDV2-E. Cell lysates were harvested at 2, 6, 12, and 24 HPI, and 2, 3, 5, 7, and 9 DPI. BRSV growth kinetics were determined using an enzyme-linked immunosorbent assay. BRSV RNA levels were quantified using Q-RT-PCR. (*) Groups are statistically different from the other groups at $P < 0.05$. Error bars represent SEM.

Fig. 2.3. BVDV2-E greatly induces PKR mRNA expression. BT cells were infected with BVDV2-wt, BVDV2-E, BRSV, or co-infected with BRSV/BVDV2-wt or BRSV/BVDV2-E at a m.o.i. of 0.05, or stimulated with poly I:C: (A) single infections and (B) co-infections. Cells were harvested at 2 HPI, 1, 2, 3, 5, 7, or 9 DPI. Total RNA was extracted and PKR mRNA levels quantified using real-time Q-RT-PCR and normalized against two reference genes, GAPDH and RPS18. Results are represented as fold change expressed relative to UI control at 2 HPI. (*) Groups are statistically different from the other groups at $P < 0.05$. Error bars represent SEM.

Fig. 2.4. ncp BVDV2 N^{pro} is essential for TBK-1 inhibition. BT cells were infected, (A) single infections and (B) co-infections, and cells harvested and RNAs extracted as in Fig. 2.3. The TBK-1 mRNA levels were quantified using Q-RT-PCR and normalized. Results are represented as in Fig. 2.3. (*) Groups are statistically different from the other groups at $P < 0.05$. Error bars represent SEM.

Fig. 2.5. ncp BVDV2 N^{pro} reduces IRF-3 mRNA expression. BT cells were infected, (A) single infections and (B) co-infections, and cells harvested and RNAs extracted as in Fig. 2.3. The IRF-3 mRNA levels were quantified using Q-RT-PCR and normalized. Results are represented as in Fig. 2.3. (*) Groups are statistically different from the other groups at $P < 0.05$. Error bars represent SEM.

Fig. 2.6. ncp BVDV2 N^{pro} reduces IRF-7 mRNA expression. BT cells were infected, (A) single infections and (B) co-infections, and cells harvested and RNAs extracted as in Fig. 2.3. The IRF-7 mRNA levels were quantified using Q-RT-PCR and normalized. Results are represented as in Fig. 2.3. (*) Groups are statistically different from the other groups at $P < 0.05$. Error bars represent SEM.

Fig. 2.7. ncp BVDV2 N^{pro} is essential for IFN-β inhibition. BT cells were infected, (A) single infections and (B) co-infections, and cells harvested and RNAs extracted as in Fig. 2.3. The IFN-β mRNA levels were quantified using Q-RT-PCR and normalized. Results are represented as in Fig. 2.3. (C) IFN-β luciferase activity. BT cells were transfected with IFN-β (firefly) and control (pRL Renilla Luciferase Reporter) vectors. After 24 h, cells were infected with BVDV2-wt, BVDV2-E, BRSV, or co-infected with BRSV/BVDV2-wt or BRSV/BVDV2-E, or stimulated with poly I:C. Cells were harvested at 2 HPI, 1, 2, 3, 5, 7, or 9 DPI. The IFN-β was analyzed using a dual-luciferase reporter assay system. Results are represented as relative fold change expressions. No significant differences were detected at 2 HPI, 7 DPI, and 9 DPI (Fig. 3.11). (*) Groups are statistically different from the other groups at $P < 0.05$. Error bars represent SEM.

Fig. 2.8. NF-κB luciferase activity. BT cells were treated as in Fig. 2.7C using pGL4.32 [luc2P/NF-κB-RE/Hygro] (firefly) and control (pRL Renilla Luciferase Reporter) vectors. Results are represented as in Fig. 2.7C. No significant differences were detected at 2 HPI, 1 DPI, and 2 DPI (Fig. 3.12). (*) Groups are statistically different from the other groups at $P < 0.05$. Error bars represent SEM.

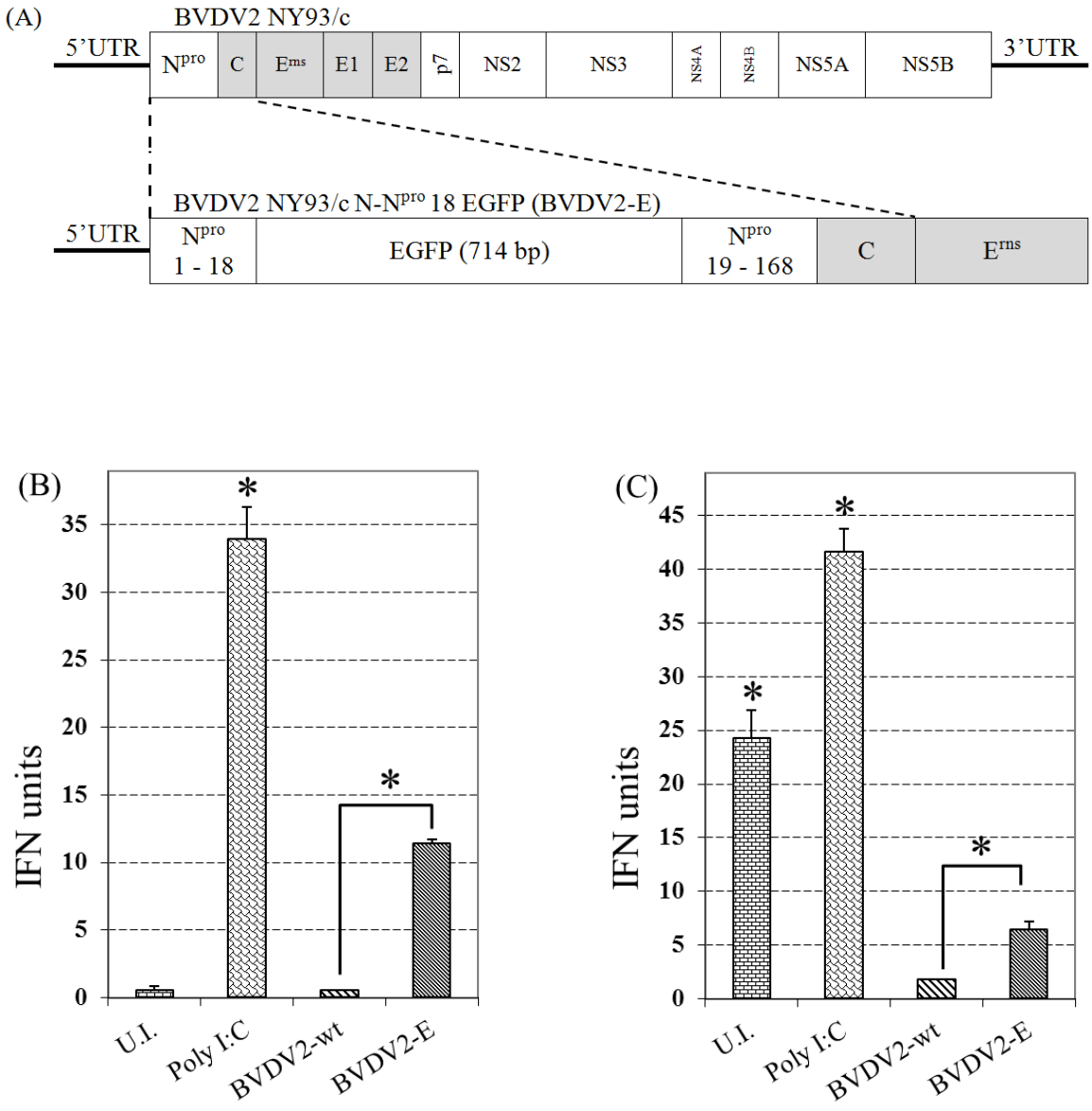

Fig. 2.1. Genomic organization of BVDV2 isolates and IFN production.

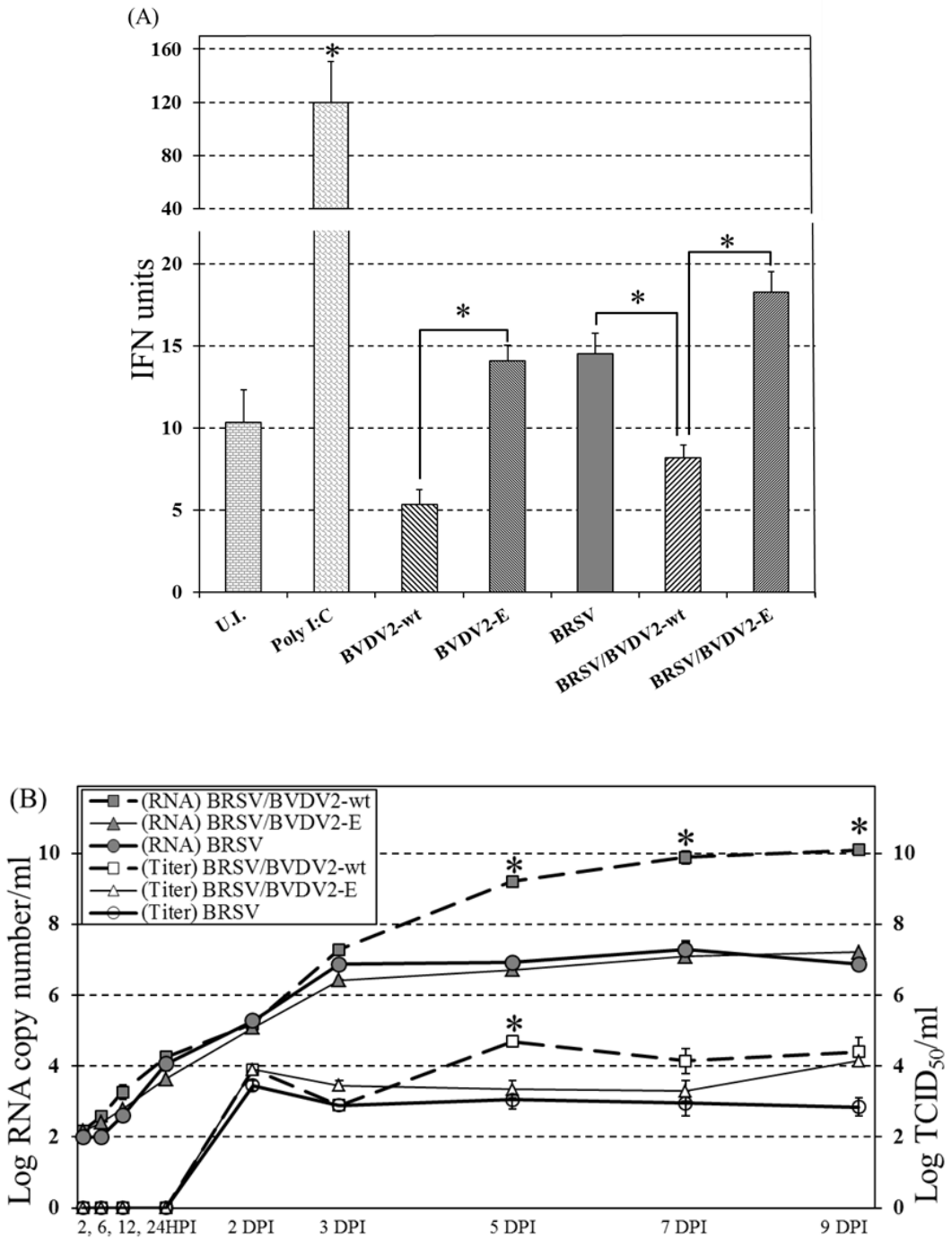

Fig. 2.2. BVDV2 N^{pro} decreases IFN-1 production and increases BRSV replication in co-infected BT cells.

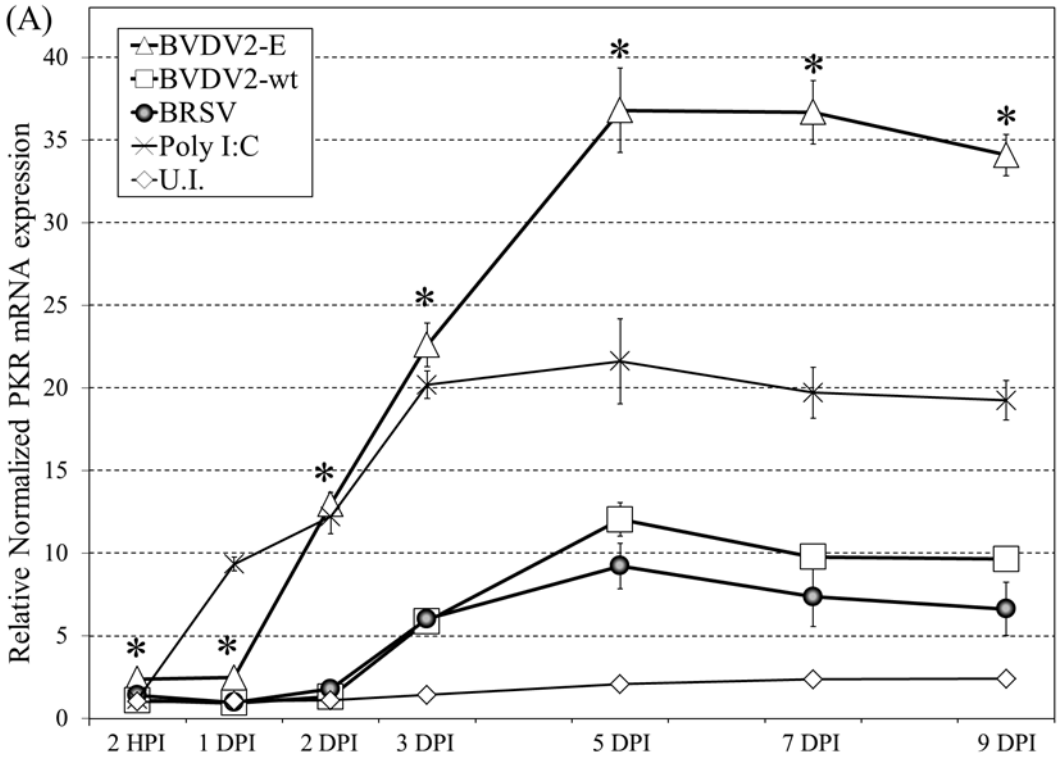

Fig. 2.3 (A). PKR mRNA expression in infected BT cells.

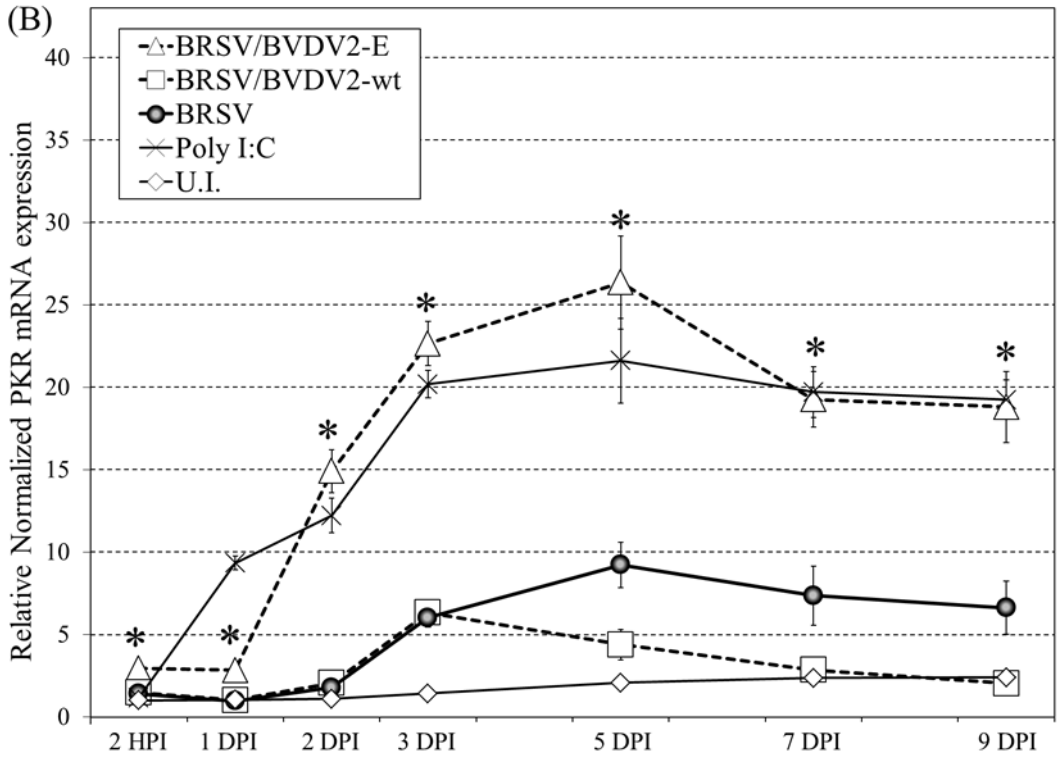

Fig. 2.3 (B). PKR mRNA expression in co-infected BT cells.

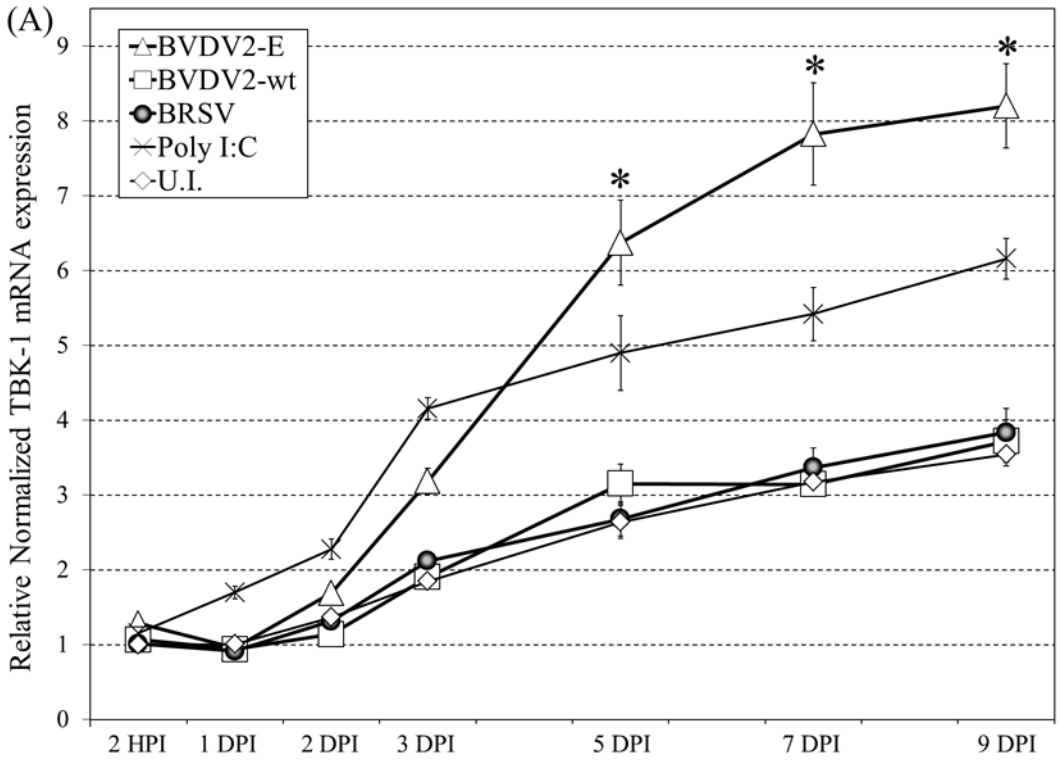

Fig. 2.4 (A). TBK-1 mRNA expression in infected BT cells.

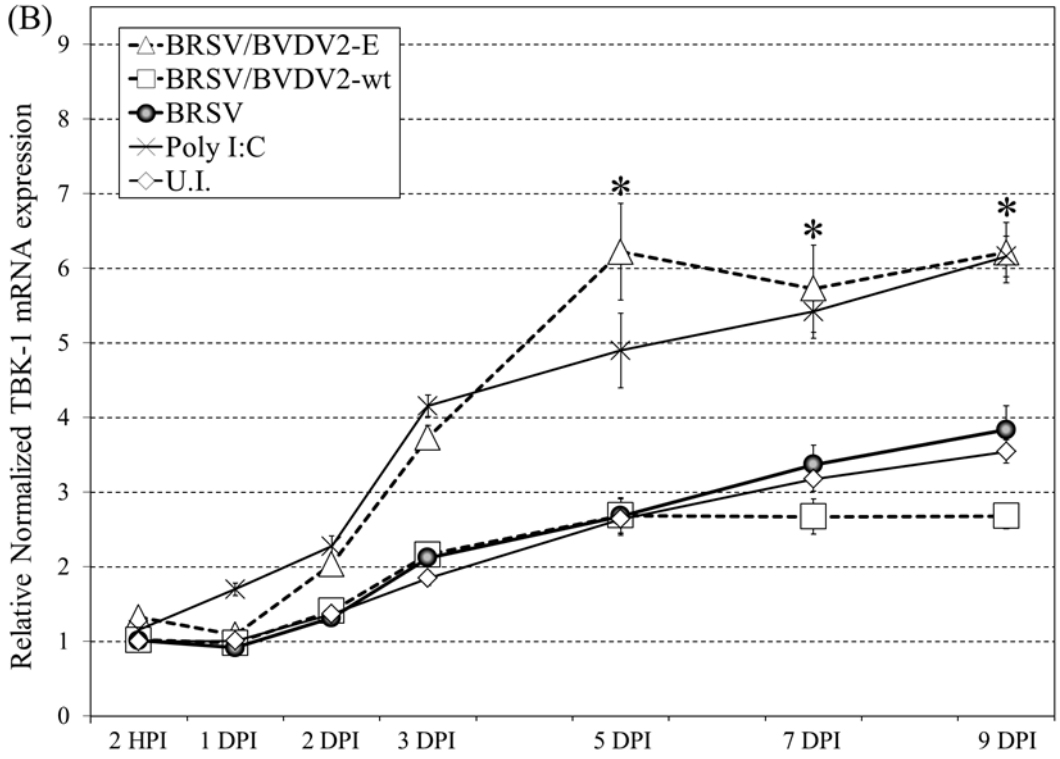

Fig. 2.4 (B). TBK-1 mRNA expression in co-infected BT cells.

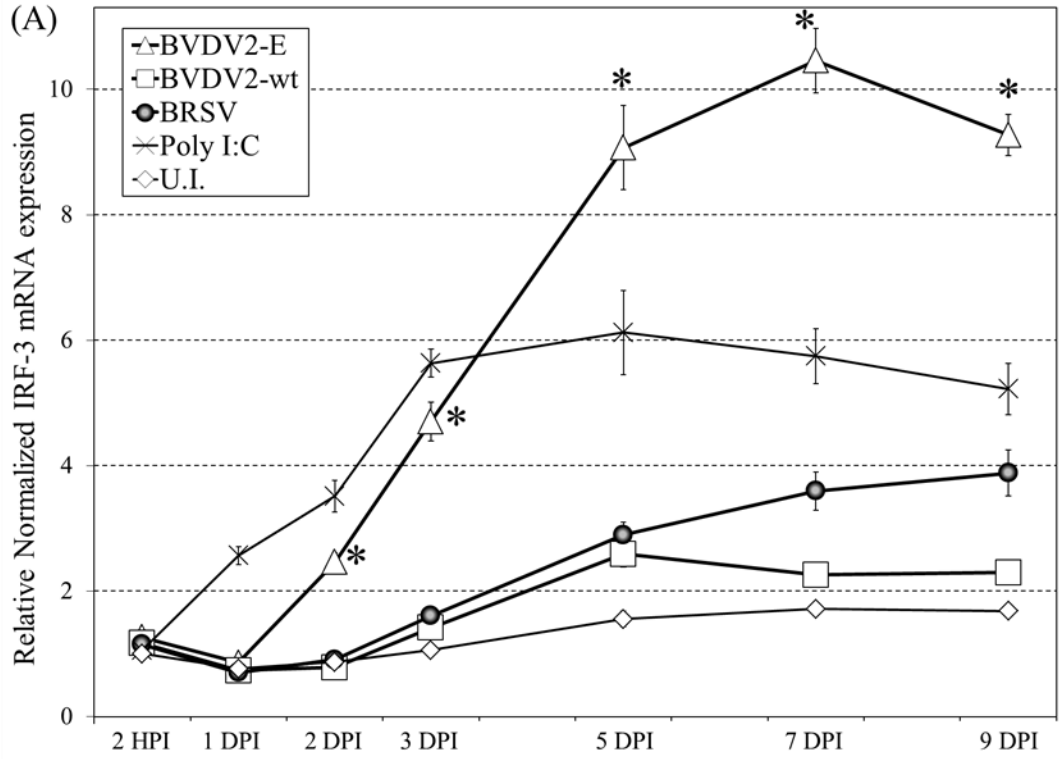

Fig. 2.5 (A). IRF-3 mRNA expression in infected BT cells.

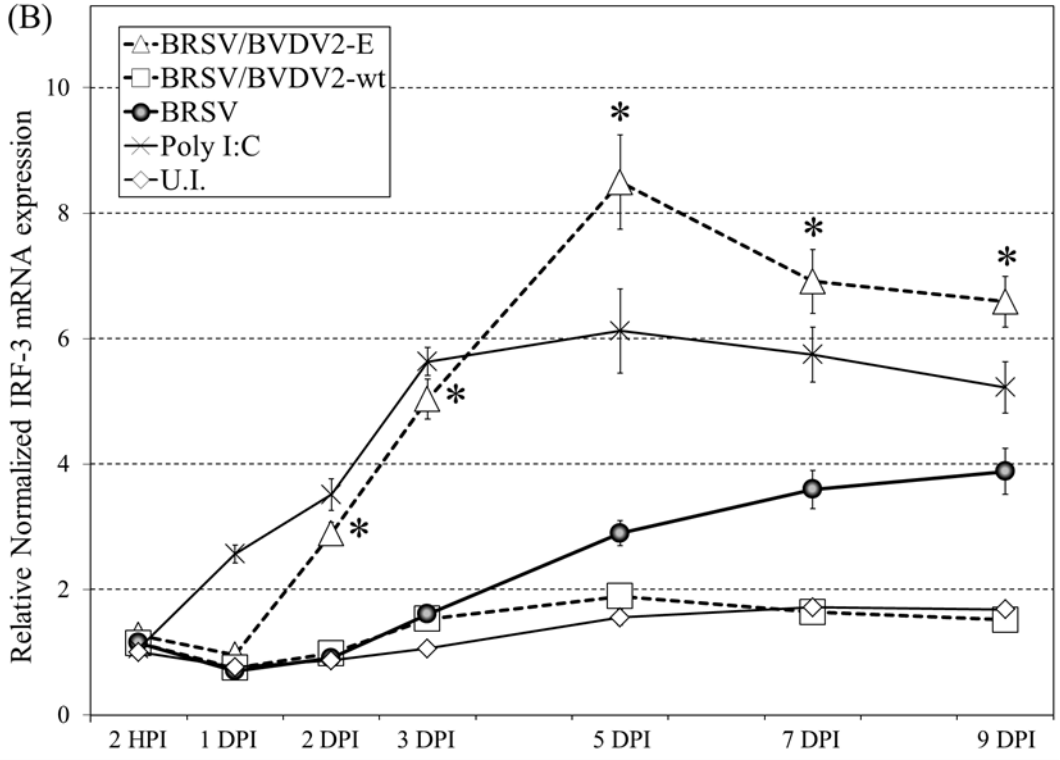

Fig. 2.5 (B). IRF-3 mRNA expression in co-infected BT cells.

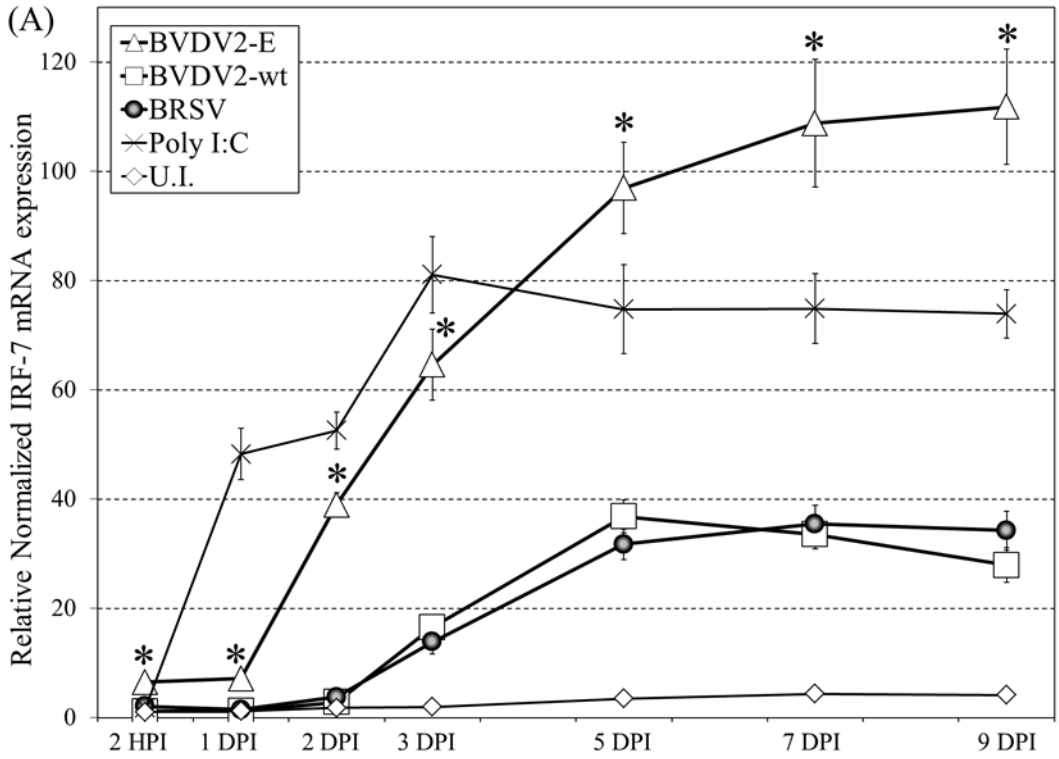

Fig. 2.6 (A). IRF-7 mRNA expression in infected BT cells.

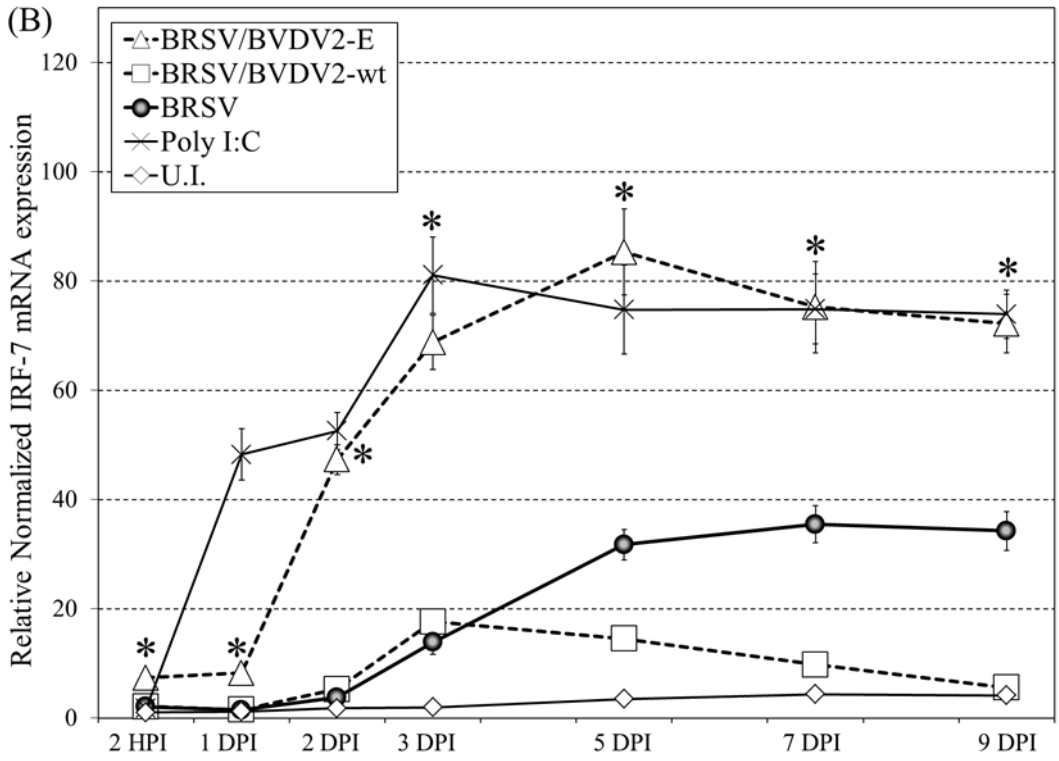

Fig. 2.6 (B). IRF-7 mRNA expression in co-infected BT cells.

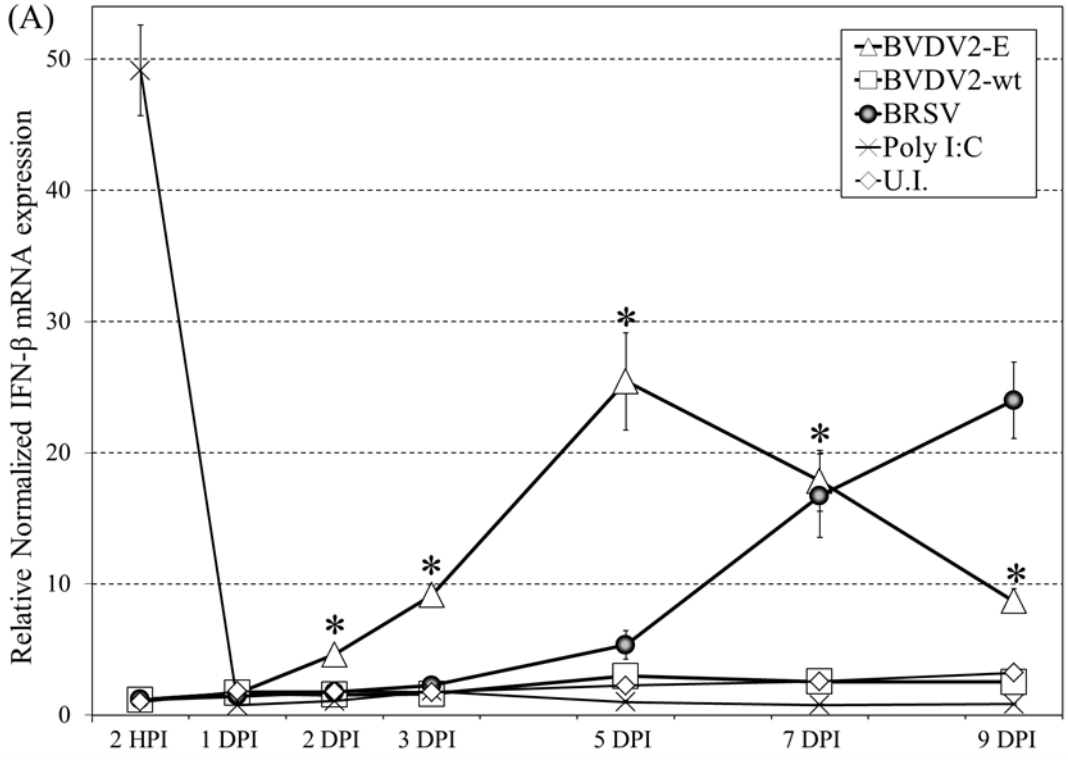

Fig. 2.7 (A). IFN-β mRNA expression in infected BT cells.

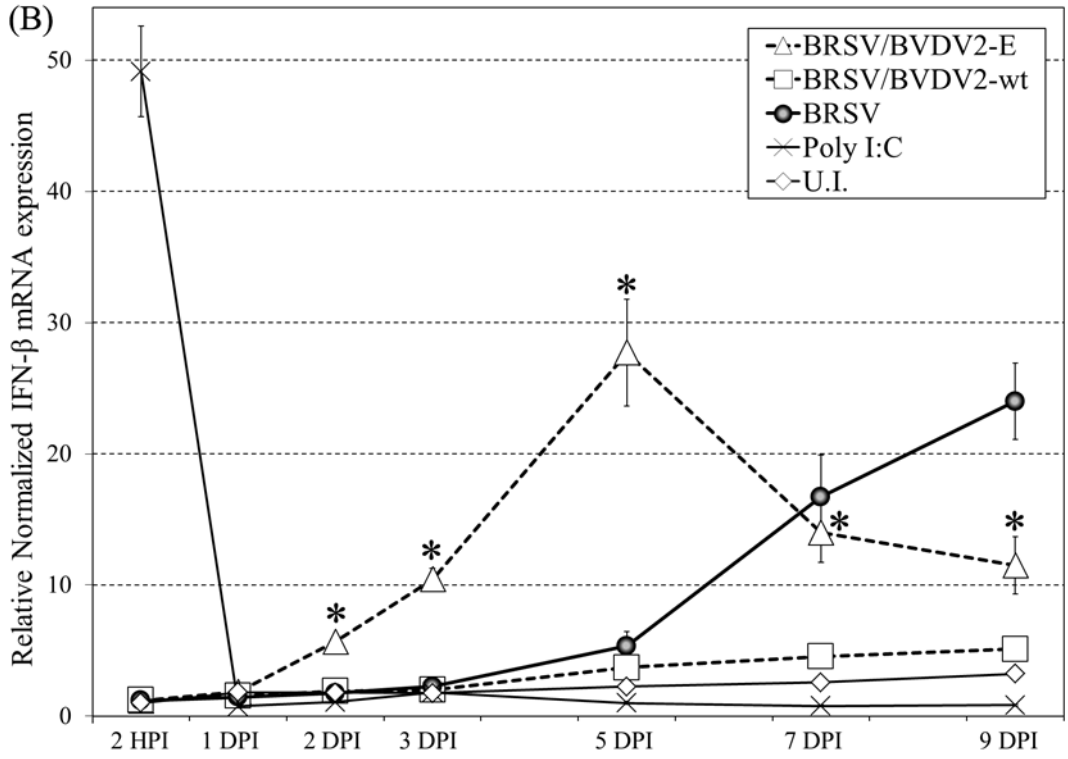

Fig. 2.7 (B). IFN-β mRNA expression in co-infected BT cells.

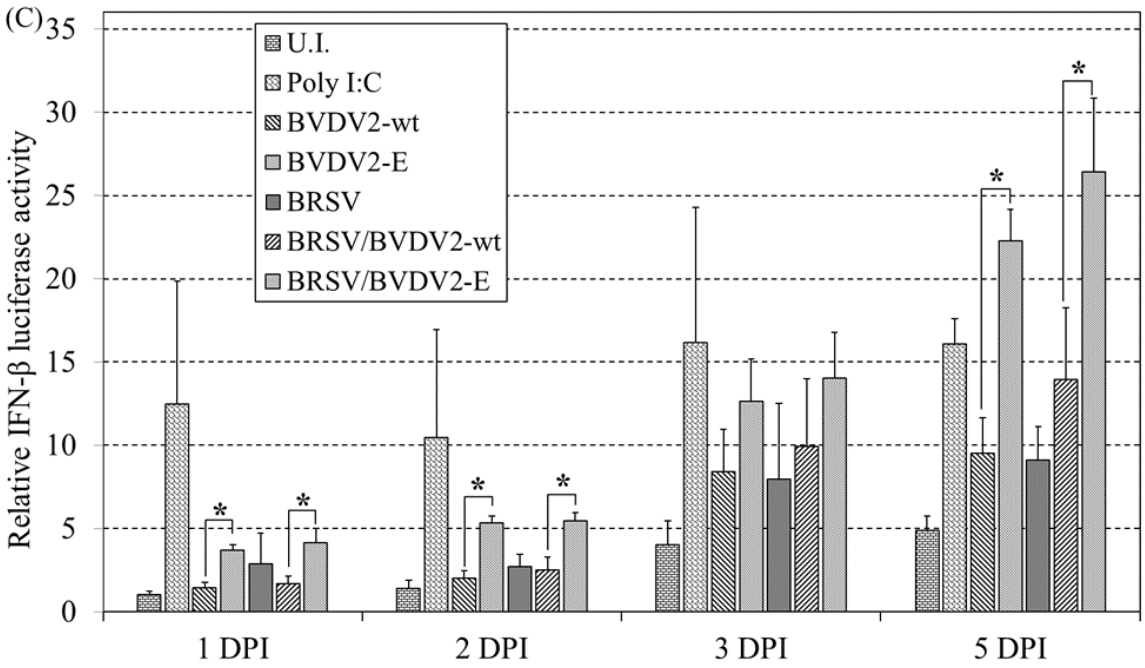

Fig. 2.7 (C). IFN-β luciferase activity. Results are represented as fold change expressed relative to UI at the 1 DPI time point. (Look at the extended graph: Fig. 3.11).

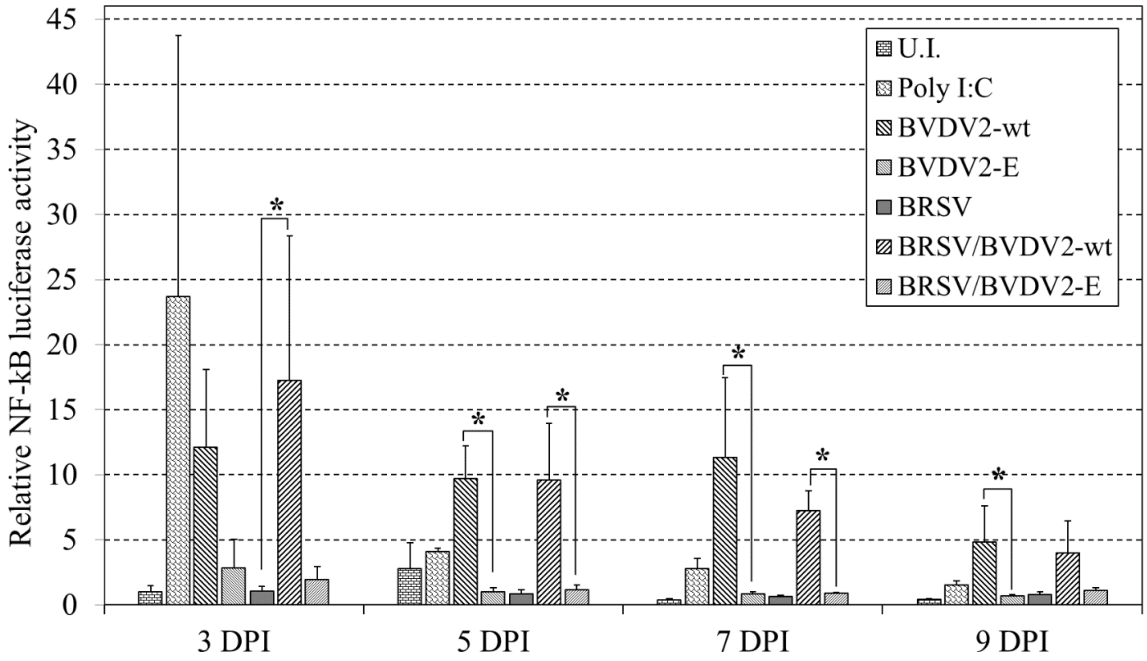

Fig. 2.8. NF-κB luciferase activity. Results are represented as fold change expressed relative to UI at the 3 DPI time point. (Look at the extended graph: Fig. 3.12).

CHAPTER 3:

SUPPLEMENTARY DATA

Introduction

In this research, we used real-time Q-RT-PCR to evaluate the mRNA levels of cell signals in BT cells infected with BRSV, BVDV2-wt, or BVDV2-E, or co-infected with BRSV/BVDV2-wt or BRSV/BVDV2-E. Type I IFN production levels were evaluated and dual-luciferase reporter assays were used for some signals. The main findings of this study are published in *Virology* (Alkheraif *et al.*, 2017). In this section, chapter 3, we are presenting some work that was critical for the real-time Q-RT-PCR assays and its normalization, as well as some other work that was used to convert the results of IFN response assays from luminescence reading (relative light units, RLU) to IFN units. Here also, we are providing some results, which were not included or were not shown in our published paper, 2017.

For a gene expression study, it is a very crucial step to specify reliable reference genes. We determined that bovine GAPDH with bovine RPS18 are the most reliable reference genes to be used in our experiments with BT cells. The quantities of total RNA production increased as cell growth increased until they reached 100% confluency, when the production of total RNA started to decrease with time. Even though the dual-luciferase reporter assay results indicated that BVDV2-wt in BT cells co-infected with BRSV significantly increased NF-κB luciferase activity compared to BRSV-infected or UI cells (Fig. 2.8), real-time Q-RT-PCR did not result in significant differences in the

NF-κB mRNA levels. Likewise, real-time Q-RT-PCR did not show significant differences in the mRNA expression of MAVS and PIN-1 among different infected and co-infected BT cells. BVDV2-E with BRSV in co-infected BT cells increased the production of IRF-3 protein at a higher level compared to other infections.

Total RNA Production in Cells

BT cells were infected when the confluency became 90%. There was no change in the confluency within the first two hours (2 H). Cells continued growing for 24 – 30 hours (1 D) until they reached 100% confluency. Total RNA increased as cell growth increased. When the rate of cell growth decreased because of the limitation of space, the production of total RNA decreased. Cells treated with poly I:C produced more total RNA compared to infected or uninfected cells. (Fig. 3.1A, B, C). Also, the amount of total RNA was affected by the age (passage) of cells. With all infections or treatments, cells at passage # 20 (7 day-old) produced more RNA compared to passage # 23 and # 24. Cells at passage # 23 (9 day-old) produced more RNA than cells at passage # 24 (10 day-old). Younger cells produced more total RNA than older cells (Fig. 3.2A, B, C).

RT-PCR and Q-RT-PCR

RT-PCR is a very sensitive method for virus identification and differentiation. Quantitative RT-PCR (Q-RT-PCR) determines the total amount of viral RNA present in a sample (Menzo *et al.*, 1992). RT-PCR is a quick diagnostic method compared to other methods such as virus isolation, plaque assay, or viral titration. The first amplification of extracted cp and ncp BVDV RNA was in 1990 using BVDV infected cell cultures and clinical samples from PI and acutely-infected calves. The amplified nucleic acid was

visualized using agarose gel electrophoresis and stained with ethidium bromide or hybridized with biotinylated probes. RT-PCR is specific and sensitive. RT-PCR can be used with different primer sets to distinguish between viruses and viral strains. It is possible to determine BVDV species in a sample using RT-PCR (Belák and Ballagi-Pordány, 1991; Hertig *et al.*, 1991; Schmitt *et al.*, 1994; Schroeder and Balassu-Chan, 1990; Tajima *et al.*, 1995). Nevertheless, gel-based RT-PCR results can be compromised during nucleic acid amplification by sample contamination.

A single tube, fluorogenic probe-based, real-time quantitative RT-PCR (Q-RT-PCR), TaqMan RT-PCR, was developed to detect RNA of classical swine fever virus (McGoldrick *et al.*, 1999; Ophuis *et al.*, 2006). Q-RT-PCR is a rapid, economical, high volume, sensitive, and specific procedure to detect, quantify, and classify many viruses in samples. Q-RT-PCR has been used to quantify and classify BVDV in serum and tissue homogenate (Bhudevi and Weinstock, 2001; Mahlum *et al.*, 2002). Using BioRad's iCycler iQ, real-time Q-RT-PCR was used to detect and quantify viral RNA of bovine respiratory syncytial virus (BRSV) in cell lysate harvested at different time points post-infection. Real-time Q-RT-PCR was specific, rapid, efficient, and eliminated the post-PCR processing steps compared to quantitative competitive RT-PCR (QC-RT-PCR) (Achenbach *et al.*, 2004). QC-RT-PCR is an appropriate method for diagnosis of diseases and evaluation of the efficiency of vaccines (Boxus *et al.*, 2005). Inter-run calibration is required whenever samples are analyzed in more than one run (Hellemans *et al.*, 2007).

Determination of Q-RT-PCR Reference Genes

For a real-time Q-RT-PCR gene expression study, it is a very important and crucial step to choose reference genes that are stably expressed amongst different treatment groups. Gene expression results need to be normalized against reference genes and the use of a minimum of two validated reference genes is highly recommended. However, across all gene expression studies, approximately 80% of them used only one reference gene. There are an abundance of reference genes, but β-actin (ACTB) and glyceraldehyde 3-phosphate dehydrogenase (GAPDH, also known as G3PDH) are commonly used. Only 15% of studies tested a panel of potential reference genes for the stability of expression before using them as reference genes (Chapman and Waldenström, 2015; Sharan *et al.*, 2015). The stability of reference genes cannot be evaluated by using only one reference gene. Using multiple reference genes produces data with greater reliability and evaluates the stability of these genes (Hellemans *et al.*, 2007). We used a panel of 19 bovine genes, including 14 reference genes, and two total RNA samples from BT cells infected with BRSV collected at one and five DPI. We found two groups of reference genes, one of which included three reference genes, GAPDH, phosphoglycerate kinase 1 (PGK1), and RPS18, which can be used with each other. We evaluated those genes (Fig. 3.3, 3.4, and 3.5) and determined that GAPDH and RPS18 were the most reliable reference genes to use in combination.

The mRNA expression of MAVS, NF-κB, and PIN-1

Real-time Q-RT-PCR results showed no significant differences in the mRNA expression of some cellular signal genes among the different treatment groups at all time

points compared to UI cells. Those signals included MAVS, NF-κB, and PIN-1. BT cells were infected with BVDV2-wt, BVDV2-E, BRSV, or co-infected with BRSV/BVDV2-wt or BRSV/BVDV2-E at a m.o.i. of 0.05, or stimulated with poly I:C. Cells were harvested at 2 HPI, 1, 2, 3, 5, 7, or 9 DPI. Total RNA was extracted and gene mRNA levels quantified using real-time Q-RT-PCR and normalized against two reference genes, GAPDH and RPS18 (Fig. 3.6, 3.7, and 3.8).

Type I IFN Reporter Gene Assay

Reporter gene assays have been developed to measure type I IFN production. The Mx reporter gene assay uses a plasmid containing a human MxA promoter associated with chloramphenical acetyltransferase (CAT) cDNA. This plasmid is transfected into Madin-Darby Bovine Kidney (MDBK) cells. The IFN in test samples will stimulate the Mx promoter which results in CAT synthesis. CAT is measured using a commercial ELISA kit which reflects the amount of IFN in the test sample (Fray *et al.*, 2001). In the luciferase reporter assay, the reporter cell line, NCL1-ISRE-Luc-Hygro, is used. These cells are bovine uterus cells transfected with a plasmid containing an IFN stimulated response element (ISRE) promoter with luciferase reporter gene. Test samples are added to these cells and type I IFN is quantified using a luciferase assay reagent (Gil *et al.*, 2006a). In addition to reporter gene assays, real-time reverse transcriptase polymerase chain reaction (Real-time RT-PCR) has been used to measure the transcription of IFN-related RNA (Yamane *et al.*, 2008).

Type I IFN Reporter Gene Assay Standard Curve

A type I IFN standard curve was prepared using a 1:2 serial dilution of a type I IFN standard to convert relative light units (RLU, sample luminescence reading) to IFN units. We added 67.5 units to the wells of dilution –1, 33.75 units to the wells of dilution –2, until 0.033 units were added to the wells of the –12 dilution. We determined that the best dilutions to use were from –5 to –12 resulting in a straight line with $R^2 = 0.949$, a slope 7994.9, and a constant 2498.9 in the following equation: $Y = 7994.9X + 2498.9$ (Fig. 3.9). This equation was used for all of the type I IFN reporter gene assay results (Fig. 2.1A and 2.1B and Fig. 2.2A).

IRF-3 Protein Production in Cells

Bovine turbinate cells co-infected with BRSV/BVDV2-E produced IRF-3 protein at higher levels than cells infected with BRSV alone or with BVDV2-wt. Cells infected with BRSV/BVDV2-wt produced less IRF-3 protein compared to cells infected with BRSV alone or with BVDV2-E (Fig. 3.10).

Cells co-infected with BRSV/BVDV2-E produced greater levels of IRF-3 mRNA compared to cells co-infected with BRSV/BVDV2-wt. Cells co-infected with BRSV/BVDV2-wt had IRF-3 mRNA levels equivalent to uninfected (UI) cells (Fig. 2.5B). IRF-3 protein is a 48kDa protein. To check the effects of different infections on the IRF-3 protein levels, BT cell were infected with BRSV alone, BRSV/BVDV2-E, and BRSV/BVDV2-wt. Cells were incubated for four days, the protein was isolated, and western blotting was performed. The western blot membrane was incubated with primary, anti-IRF-3 antibody produced in rabbit (AV31992-50UG, SIGMA-ALDRICH,

dilution 1:2000), secondary antibodies, anti-Rabbit IgG, HRP-linked antibody (7074S, Cell Signaling, dilution 1:2400), and β-Actin antibody (4967S, Cell Signaling, dilution 1:1000).

Other Cellular Signal Proteins

Western blotting was performed using antibodies against some other cellular signal proteins and phosphorylated proteins with different concentrations of skim dry milk or bovine serum albumin for blocking. Unfortunately, we were not successful in detecting these proteins. Antibodies included: anti-IRF-7 antibody produced in rabbit (SAB2101180-50UG, SIGMA-ALDRICH, dilution 1:1000), anti-phospho-IRF-3 (pSer386) antibody produced in rabbit (SAB4504651, SIGMA-ALDRICH, dilution 1:500 ~ 1:1000), anti-phospho-IRF-3 (phospho-Ser396) antibody produced in rabbit (orb6225, biorbyt, dilution 1:100 ~ 1:500), and anti-phospho-PKR (pThr451) antibody produced in rabbit (cat. # PA1-26677, Thermo Scientific, dilution 1:1000).

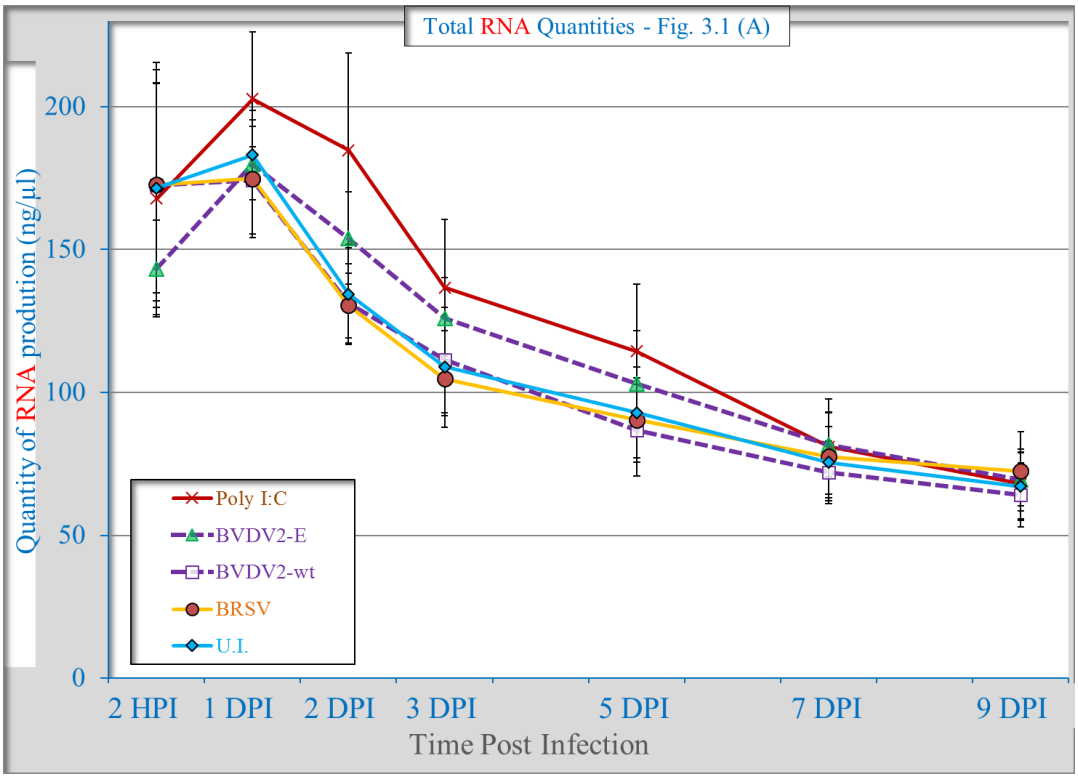

Fig. 3.1 (A). Total RNA production in infected BT cells. BT cells were infected with BVDV2-wt, BVDV2-E, or BRSV at a m.o.i. of 0.05, or stimulated with poly I:C. Cells were harvested at 2 HPI, 1, 2, 3, 5, 7, or 9 DPI. Total RNA was extracted and quantified using a Nanodrop spectrophotometer. The experiment was replicated independently three times resulting in a randomized complete block design and the averages are represented. Error bars represent SEM.

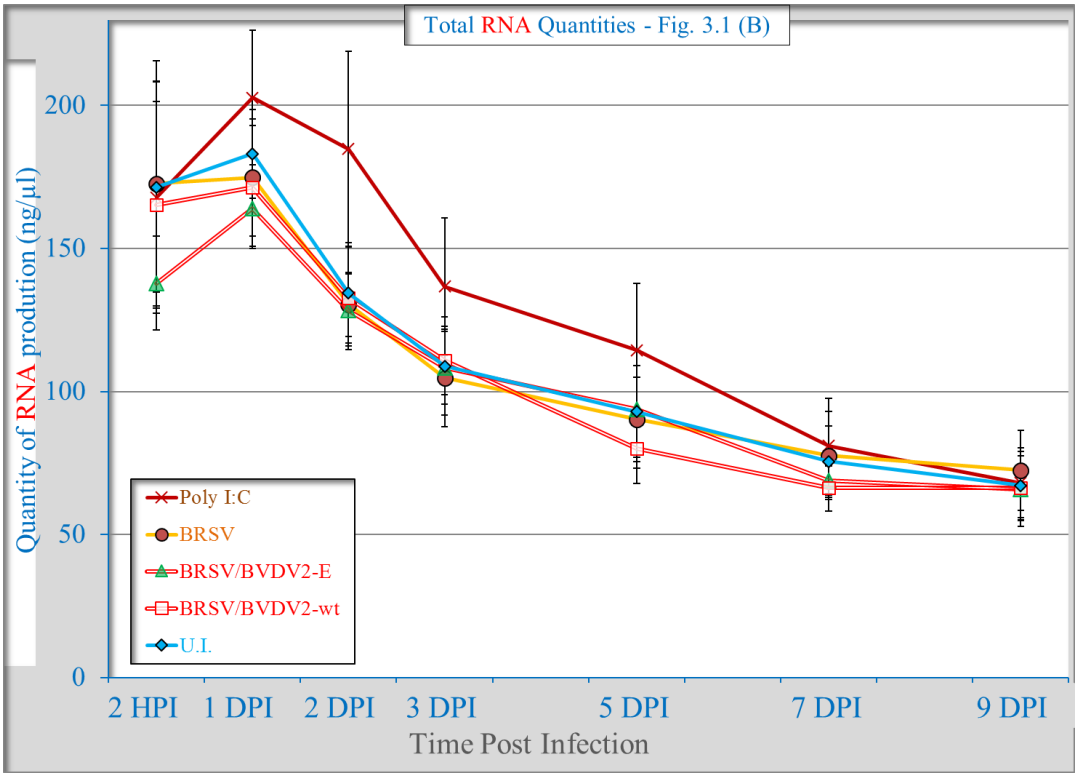

Fig. 3.1 (B). Total RNA production in co-infected BT cells. BT cells were infected with BRSV, co-infected with BRSV/BVDV2-wt or BRSV/BVDV2-E at a m.o.i. of 0.05, or stimulated with poly I:C. Cells were harvested at 2 HPI, 1, 2, 3, 5, 7, or 9 DPI. Total RNA was extracted and quantified using a Nanodrop spectrophotometer. The experiment was replicated independently three times resulting in a randomized complete block design and the averages are represented. Error bars represent SEM.

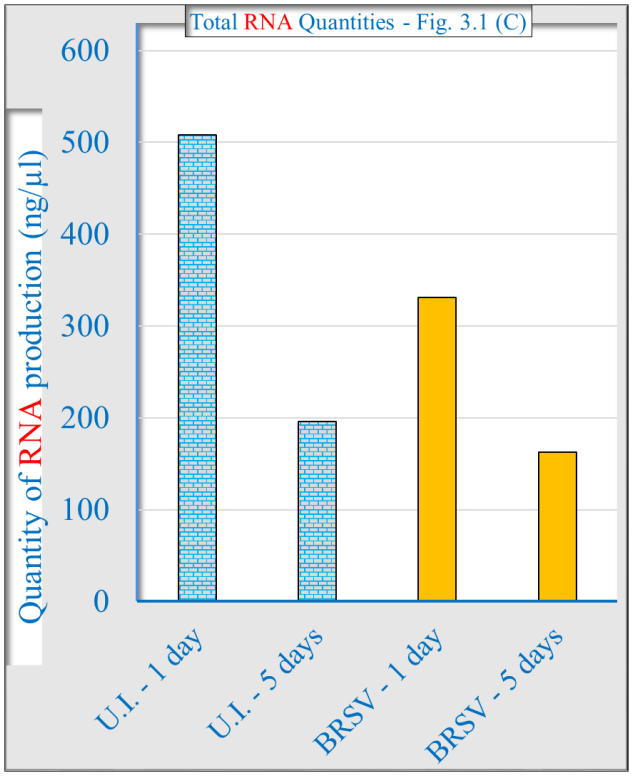

Fig. 3.1 (C). Total RNA production in BT cells. BT cells were infected with BRSV or remained uninfected. Cells were harvested at 1 or 5 DPI. Total RNA was extracted and quantified using a Nanodrop spectrophotometer.

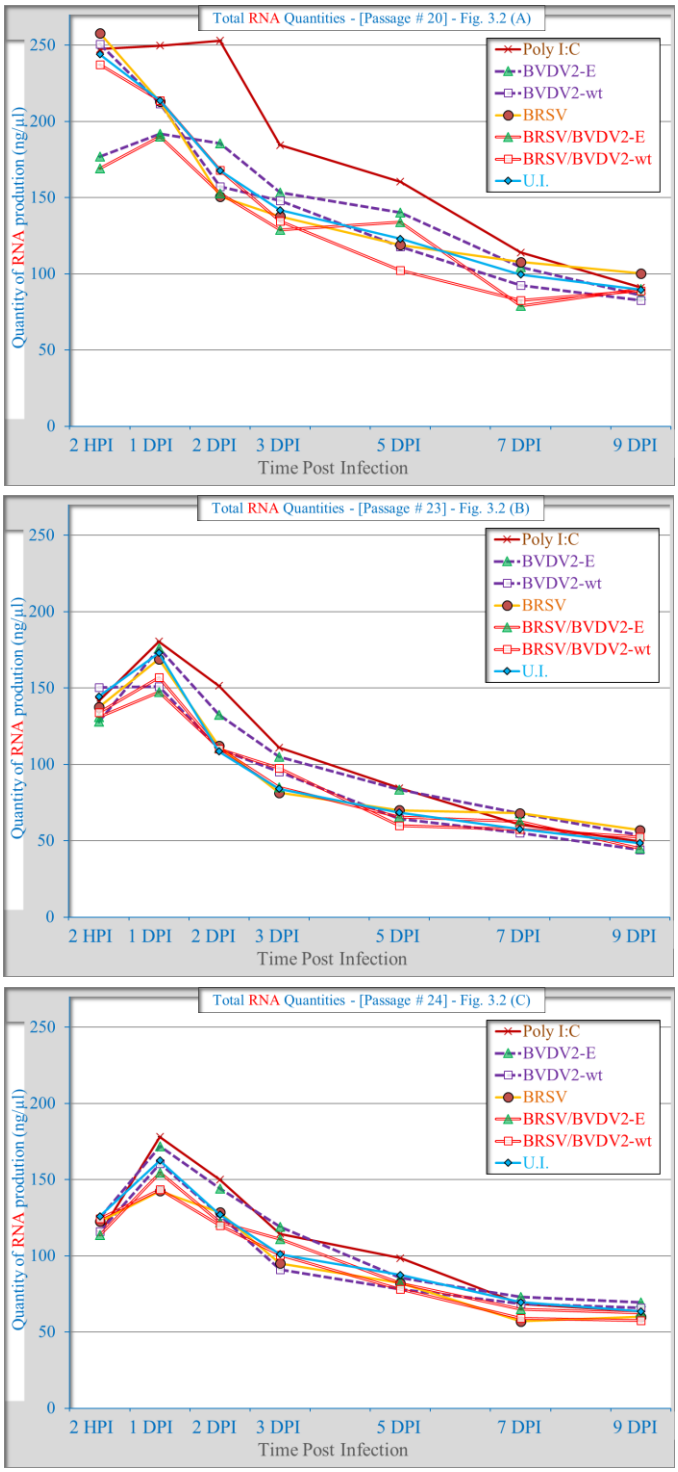

Fig. 3.2. Total RNA production with increasing BT cell passage number. (A) Cell passage # 20, (B) Cell passage # 23, and (C) Cell passage # 24. BT cells were infected and treated, and cells harvested and RNAs extracted as in Fig. 3.1 (A).

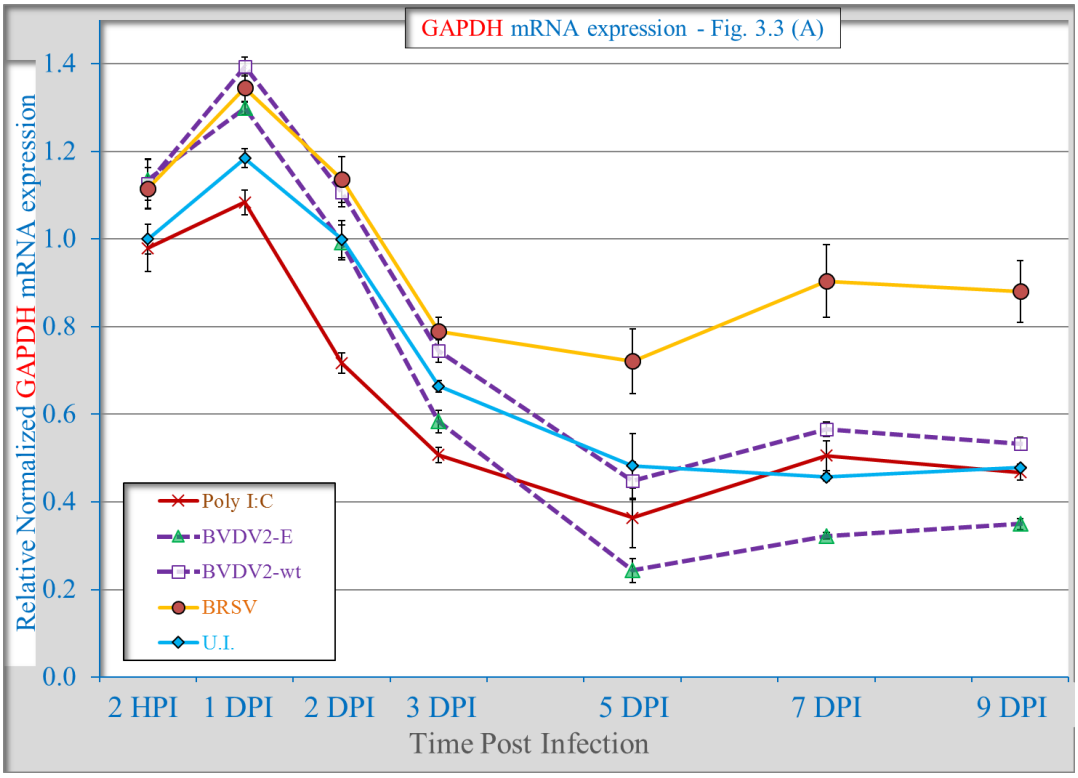

Fig. 3.3 (A). GAPDH mRNA expression in infected BT cells. BT cells were infected with BVDV2-wt, BVDV2-E, or BRSV at a m.o.i. of 0.05, or stimulated with poly I:C. Cells were harvested at 2 HPI, 1, 2, 3, 5, 7, or 9 DPI. Total RNA was extracted and GAPDH mRNA levels quantified using real-time Q-RT-PCR. Results are represented as fold change expressed relative to UI control at 2 HPI. Error bars represent SEM.

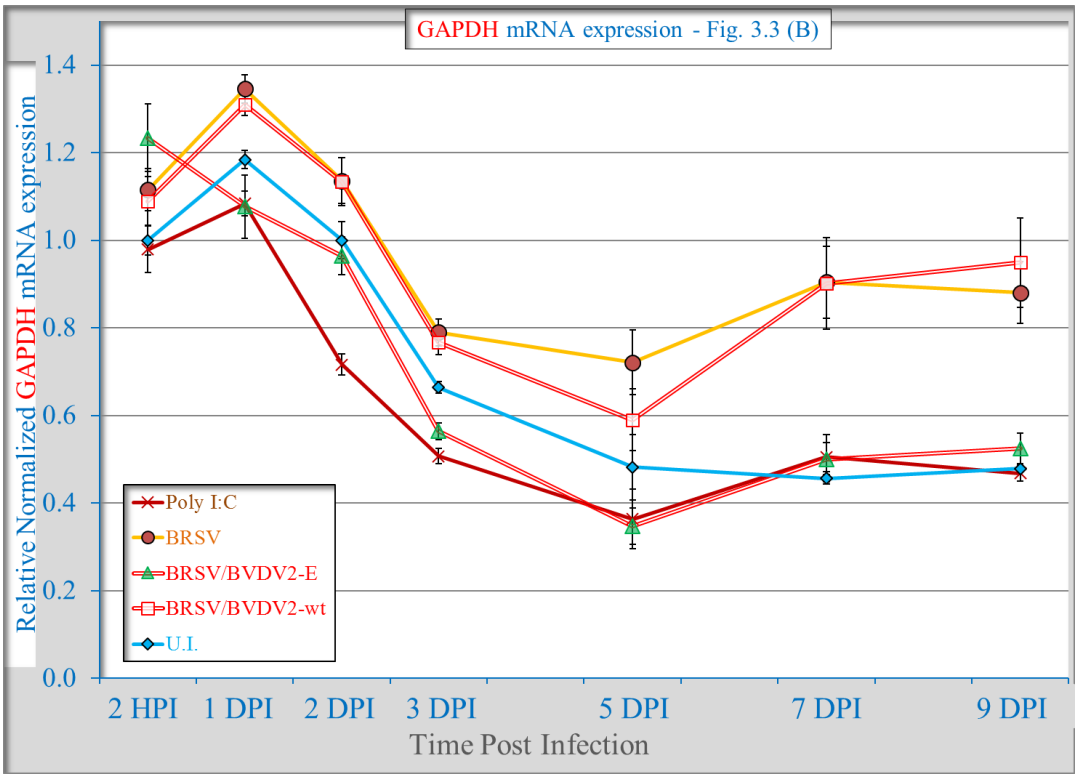

Fig. 3.3 (B). GAPDH mRNA expression in co-infected BT cells. BT cells were infected with BRSV, co-infected with BRSV/BVDV2-wt or BRSV/BVDV2-E at a m.o.i. of 0.05, or stimulated with poly I:C. Cells were harvested at 2 HPI, 1, 2, 3, 5, 7, or 9 DPI. Total RNA was extracted and GAPDH mRNA levels quantified using real-time Q-RT-PCR. Results are represented as fold change expressed relative to UI control at 2 HPI. Error bars represent SEM.

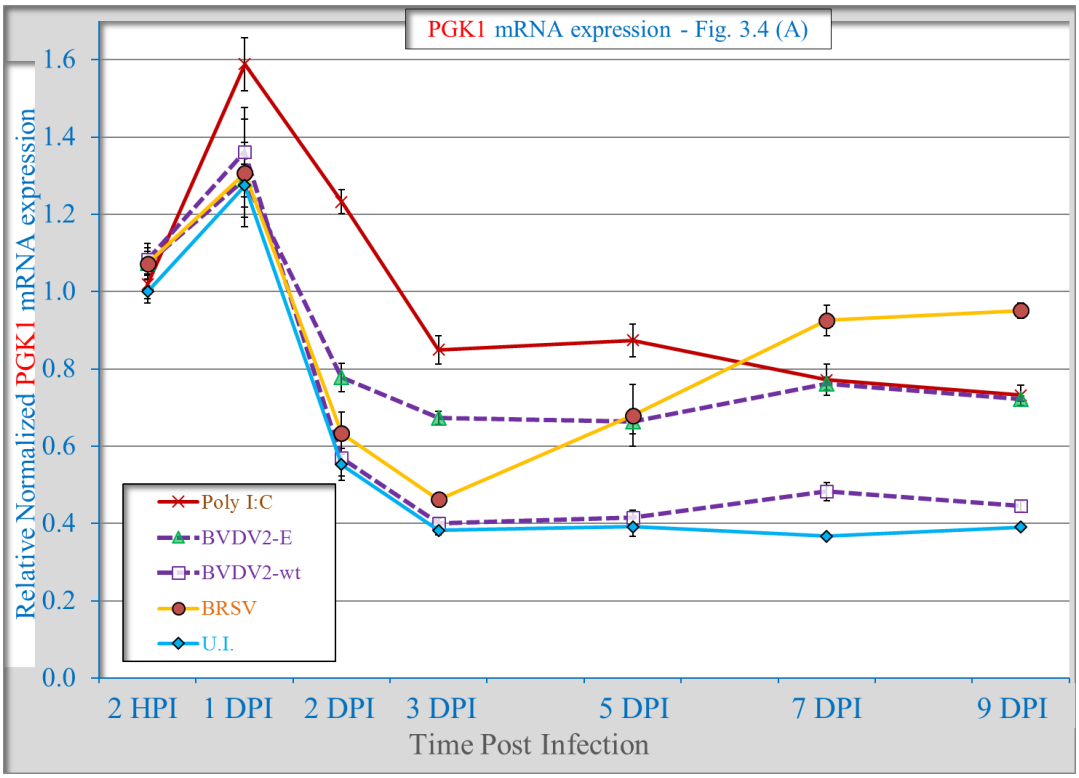

Fig. 3.4 (A). PGK1 mRNA expression in infected BT cells. BT cells were infected with BVDV2-wt, BVDV2-E, or BRSV at a m.o.i. of 0.05, or stimulated with poly I:C. Cells were harvested at 2 HPI, 1, 2, 3, 5, 7, or 9 DPI. Total RNA was extracted and PGK1 mRNA levels quantified using real-time Q-RT-PCR. Results are represented as fold change expressed relative to UI control at 2 HPI. Error bars represent SEM.

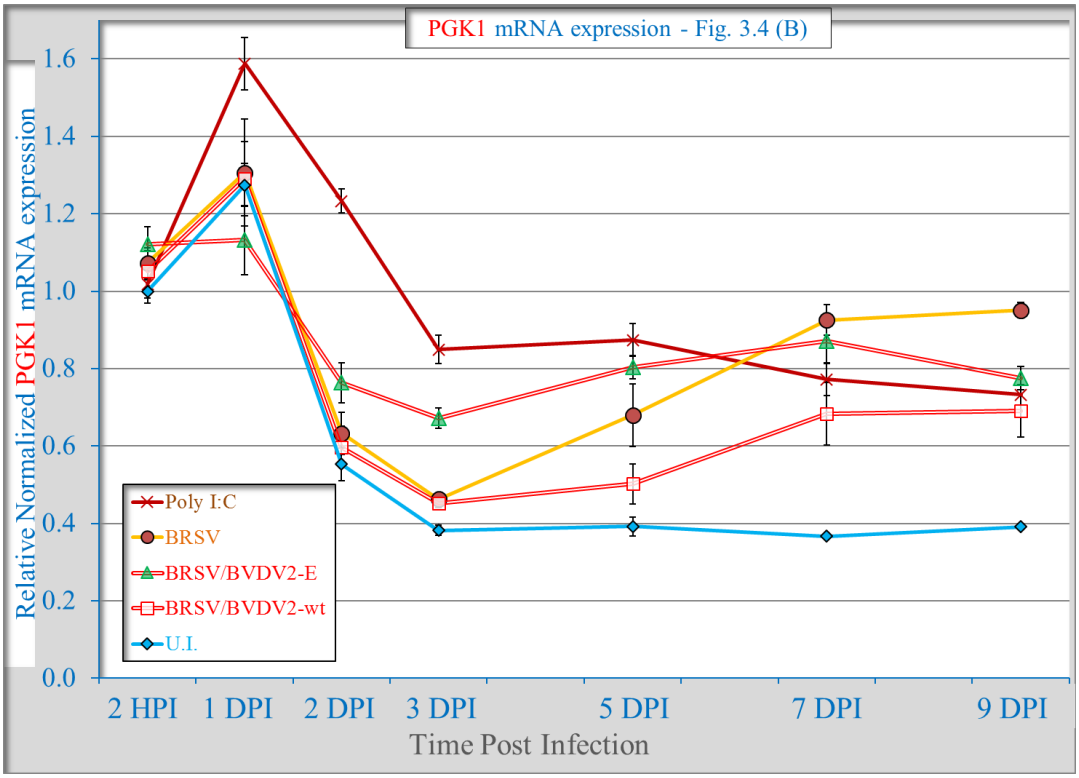

Fig. 3.4 (B). PGK1 mRNA expression in co-infected BT cells. BT cells were infected with BRSV, co-infected with BRSV/BVDV2-wt or BRSV/BVDV2-E at a m.o.i. of 0.05, or stimulated with poly I:C. Cells were harvested at 2 HPI, 1, 2, 3, 5, 7, or 9 DPI. Total RNA was extracted and PGK1 mRNA levels quantified using real-time Q-RT-PCR. Results are represented as fold change expressed relative to UI control at 2 HPI. Error bars represent SEM.

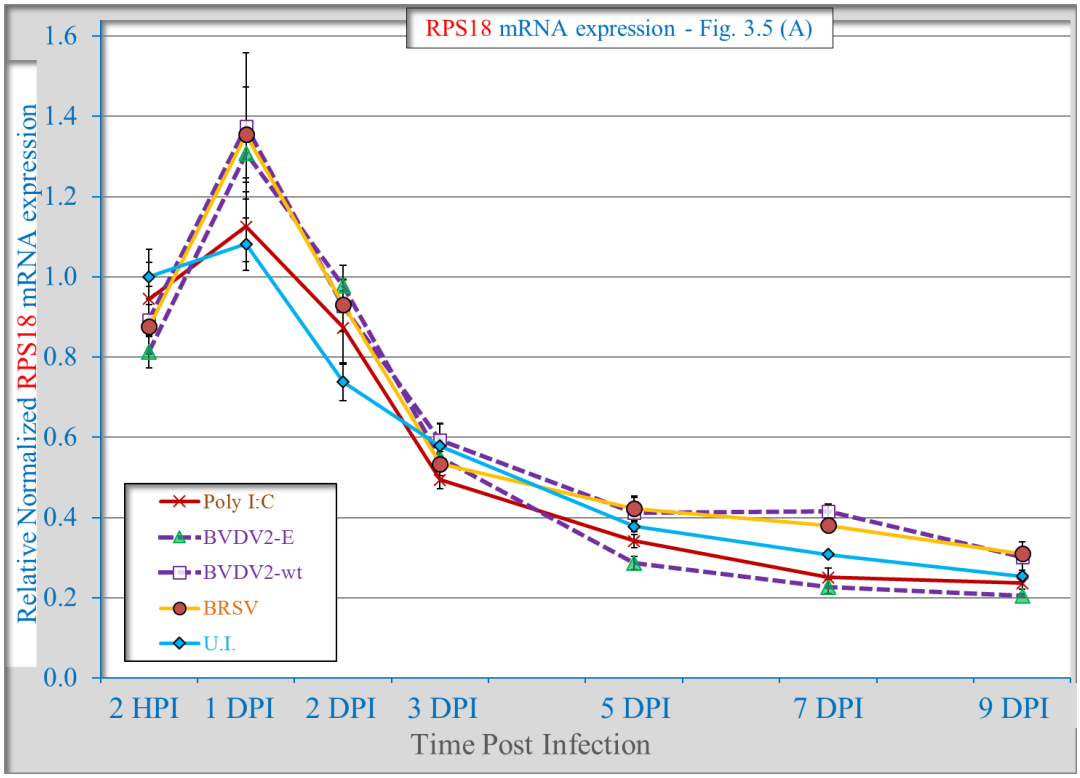

Fig. 3.5 (A). RPS18 mRNA expression in infected BT cells. BT cells were infected with BVDV2-wt, BVDV2-E, or BRSV at a m.o.i. of 0.05, or stimulated with poly I:C. Cells were harvested at 2 HPI, 1, 2, 3, 5, 7, or 9 DPI. Total RNA was extracted and RPS18 mRNA levels quantified using real-time Q-RT-PCR. Results are represented as fold change expressed relative to UI control at 2 HPI. Error bars represent SEM.

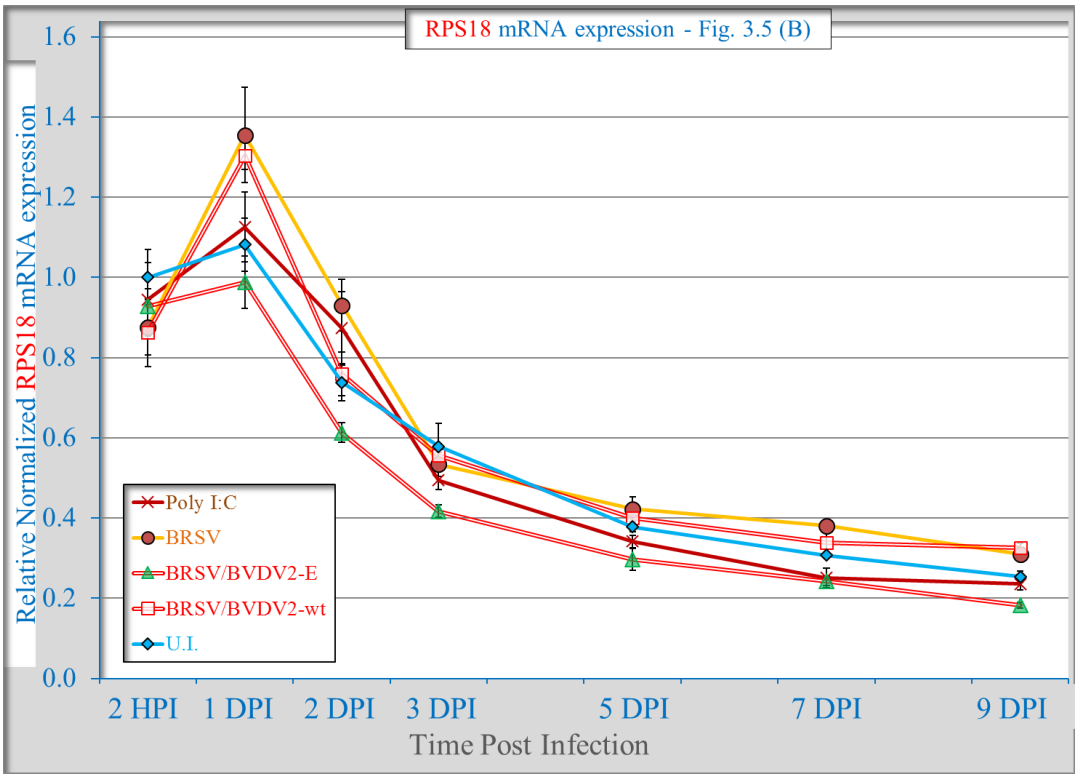

Fig. 3.5 (B). RPS18 mRNA expression in co-infected BT cells. BT cells were infected with BRSV, co-infected with BRSV/BVDV2-wt or BRSV/BVDV2-E at a m.o.i. of 0.05, or stimulated with poly I:C. Cells were harvested at 2 HPI, 1, 2, 3, 5, 7, or 9 DPI. Total RNA was extracted and RPS18 mRNA levels quantified using real-time Q-RT-PCR. Results are represented as fold change expressed relative to UI control at 2 HPI. Error bars represent SEM.

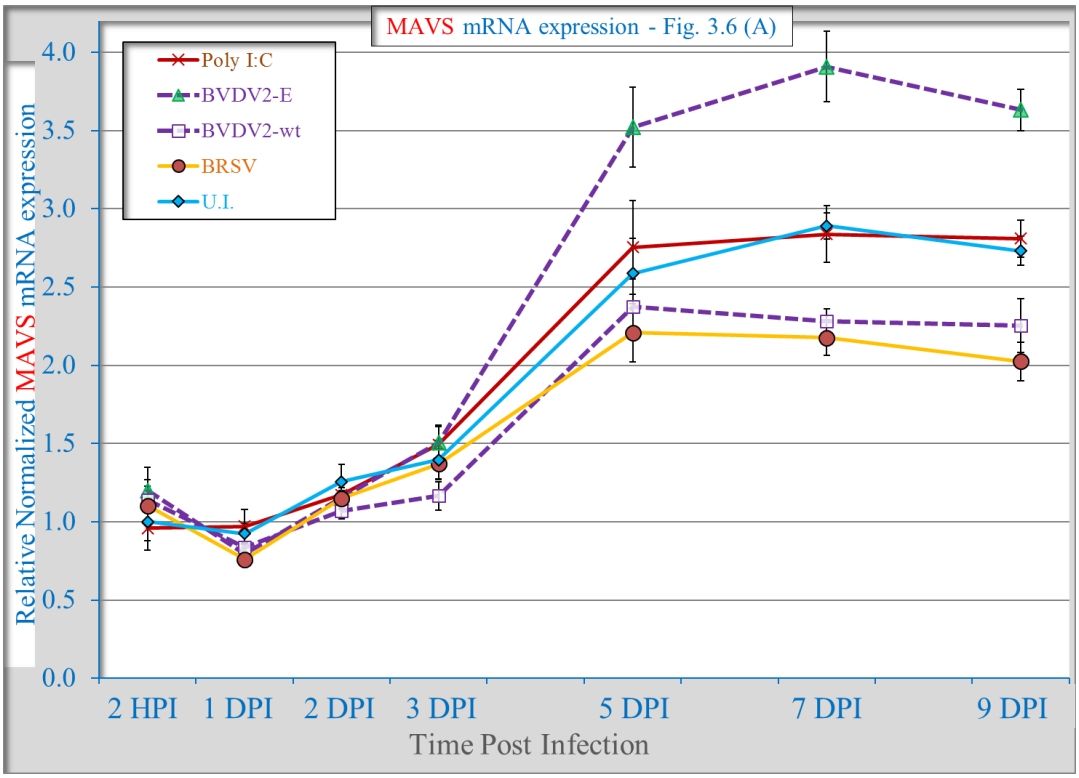

Fig. 3.6 (A). MAVS mRNA expression in infected BT cells. BT cells were infected with BVDV2-wt, BVDV2-E, BRSV at a m.o.i. of 0.05, or stimulated with poly I:C. Cells were harvested at 2 HPI, 1, 2, 3, 5, 7, or 9 DPI. Total RNA was extracted and MAVS mRNA levels quantified using real-time Q-RT-PCR and normalized against two reference genes, GAPDH and RPS18. Results are represented as fold change expressed relative to UI control at 2 HPI. Error bars represent SEM.

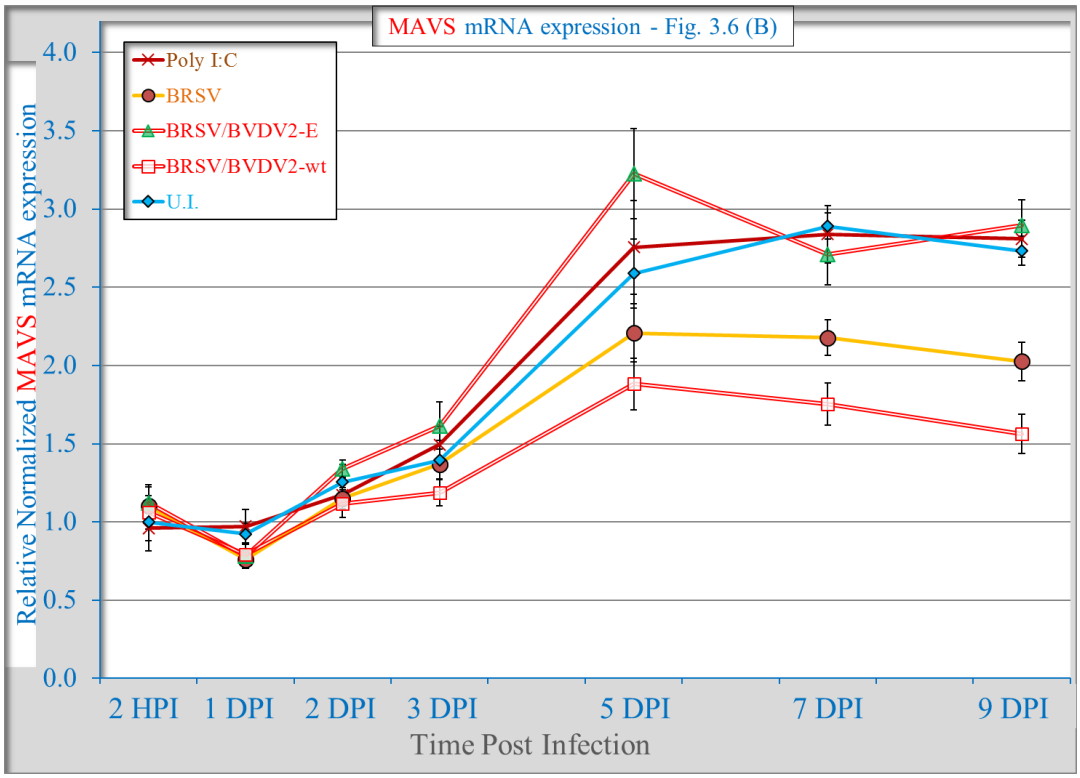

Fig. 3.6 (B). MAVS mRNA expression in co-infected BT cells. BT cells were infected with BRSV, co-infected with BRSV/BVDV2-wt or BRSV/BVDV2-E at a m.o.i. of 0.05, or stimulated with poly I:C. Cells were harvested at 2 HPI, 1, 2, 3, 5, 7, or 9 DPI. Total RNA was extracted and MAVS mRNA levels quantified using real-time Q-RT-PCR and normalized against two reference genes, GAPDH and RPS18. Results are represented as fold change expressed relative to UI control at 2 HPI. Error bars represent SEM.

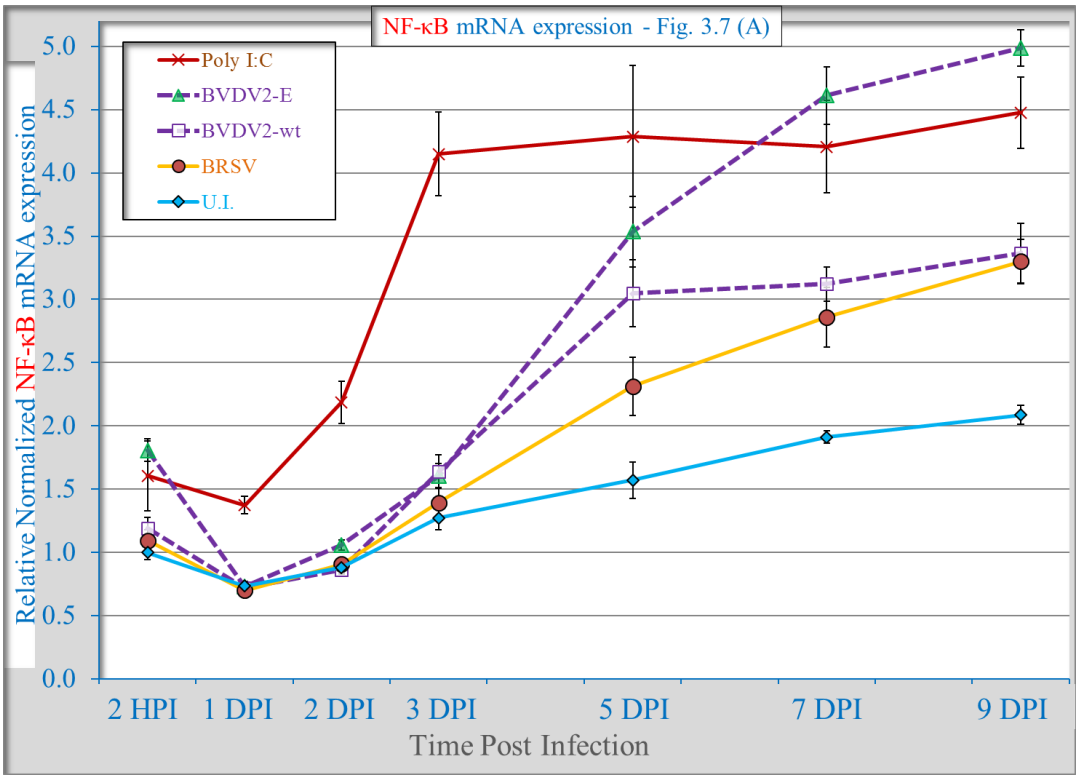

Fig. 3.7 (A). NF-κB mRNA expression in infected BT cells. BT cells were infected with BVDV2-wt, BVDV2-E, BRSV at a m.o.i. of 0.05, or stimulated with poly I:C. Cells were harvested at 2 HPI, 1, 2, 3, 5, 7, or 9 DPI. Total RNA was extracted and NF-κB mRNA levels quantified using real-time Q-RT-PCR and normalized against two reference genes, GAPDH and RPS18. Results are represented as fold change expressed relative to UI control at 2 HPI. Error bars represent SEM.

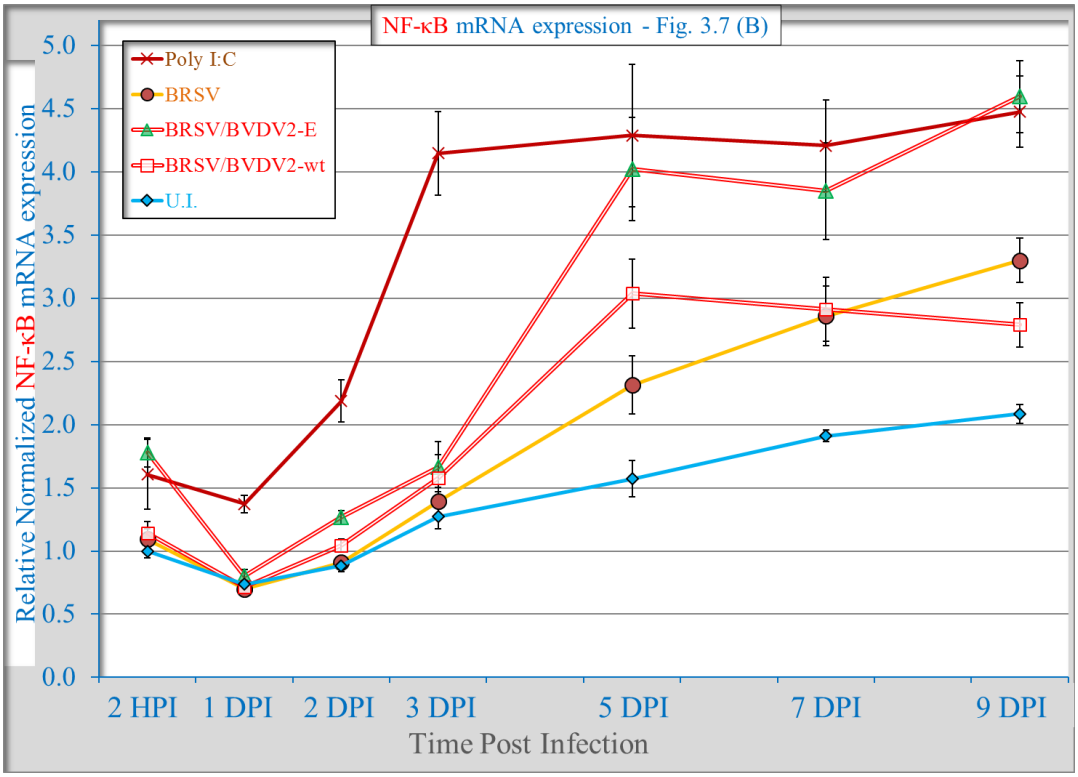

Fig. 3.7 (B). NF-κB mRNA expression in co-infected BT cells. BT cells were infected with BRSV, co-infected with BRSV/BVDV2-wt or BRSV/BVDV2-E at a m.o.i. of 0.05, or stimulated with poly I:C. Cells were harvested at 2 HPI, 1, 2, 3, 5, 7, or 9 DPI. Total RNA was extracted and NF-κB mRNA levels quantified using real-time Q-RT-PCR and normalized against two reference genes, GAPDH and RPS18. Results are represented as fold change expressed relative to UI control at 2 HPI. Error bars represent SEM.

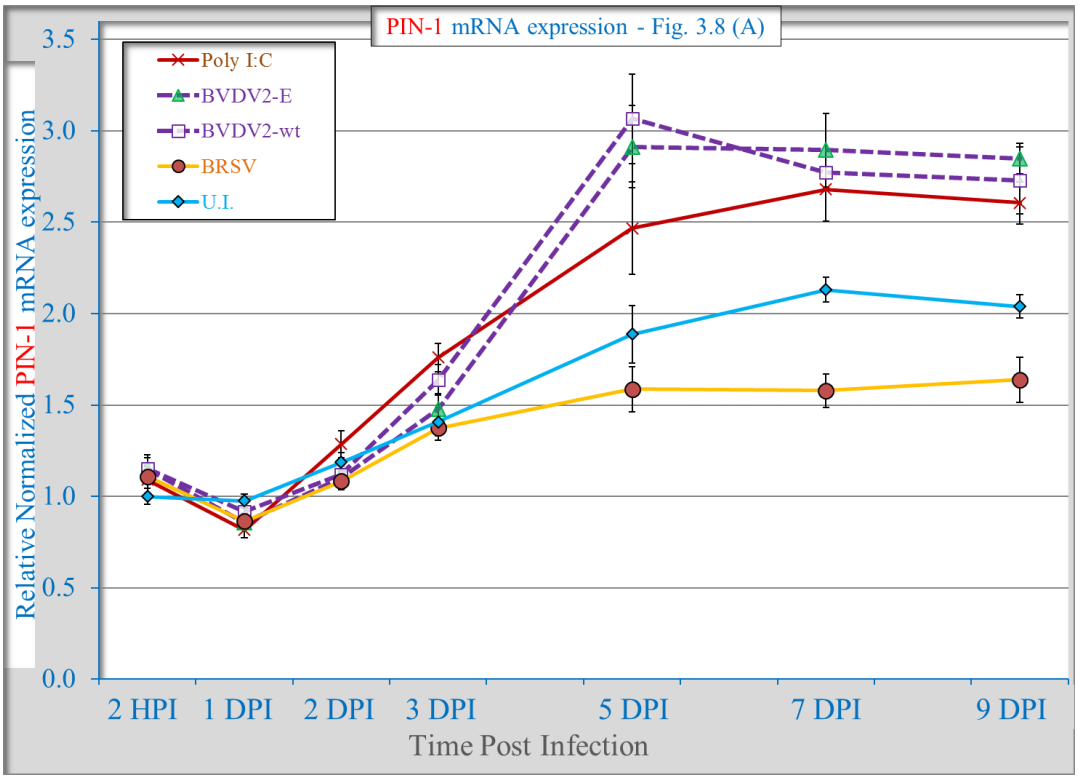

Fig. 3.8 (A). PIN-1 mRNA expression in infected BT cells. BT cells were infected with BVDV2-wt, BVDV2-E, BRSV at a m.o.i. of 0.05, or stimulated with poly I:C. Cells were harvested at 2 HPI, 1, 2, 3, 5, 7, or 9 DPI. Total RNA was extracted and PIN-1 mRNA levels quantified using real-time Q-RT-PCR and normalized against two reference genes, GAPDH and RPS18. Results are represented as fold change expressed relative to UI control at 2 HPI. Error bars represent SEM.

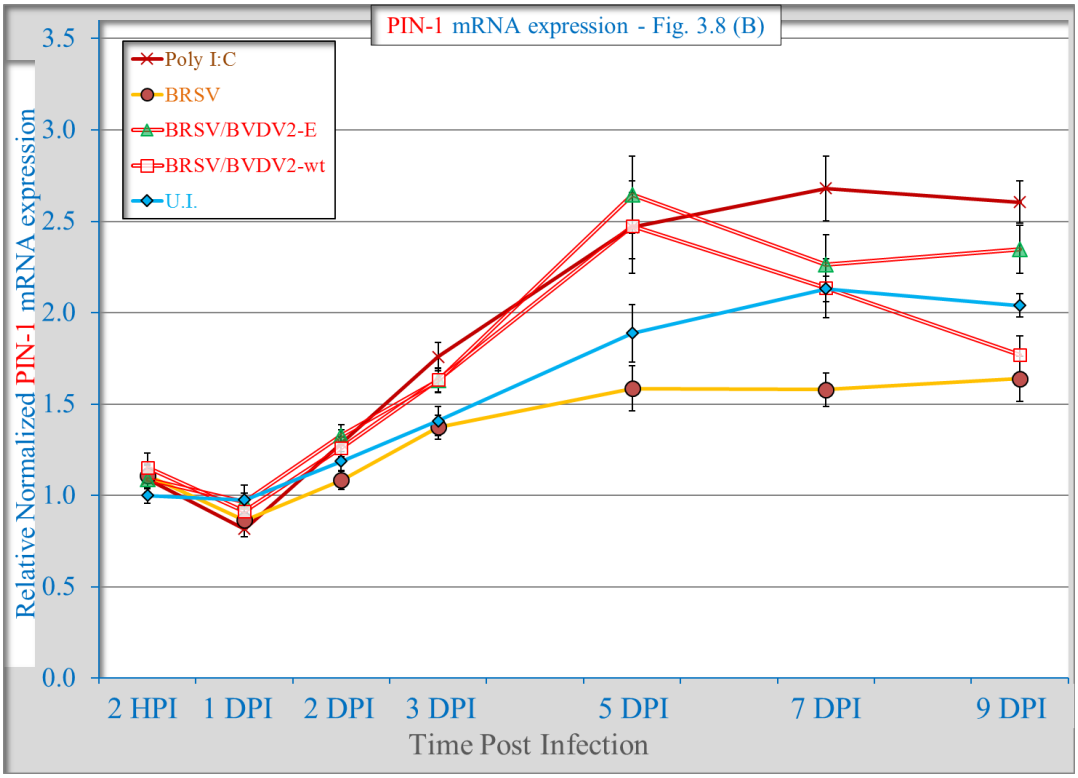

Fig. 3.8 (B). PIN-1 mRNA expression in co-infected BT cells. BT cells were infected with BRSV, co-infected with BRSV/BVDV2-wt or BRSV/BVDV2-E at a m.o.i. of 0.05, or stimulated with poly I:C. Cells were harvested at 2 HPI, 1, 2, 3, 5, 7, or 9 DPI. Total RNA was extracted and PIN-1 mRNA levels quantified using real-time Q-RT-PCR and normalized against two reference genes, GAPDH and RPS18. Results are represented as fold change expressed relative to UI control at 2 HPI. Error bars represent SEM.

X	Y
Units	Reading
4.219	39274
2.109	14658
1.055	8603
0.527	4680
0.264	5578
0.132	4586
0.066	5270
0.033	4534

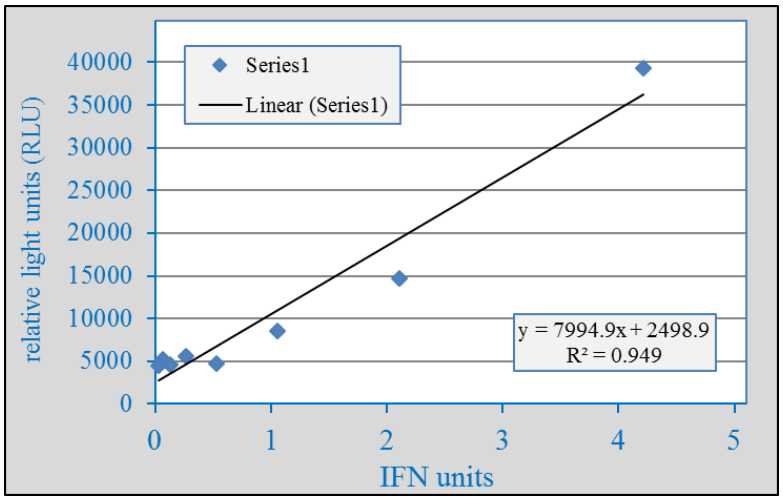

Fig. 3.9. Type I IFN standard curve. NCL1-Luc-ISRE-Hygro reporter cells were treated with 1:2 serial dilution of recombinant human IFN standard using three wells for each dilution. Cells were incubated for 8 hours followed by cell lysis. Luciferase activity of the cell lysates was measured.

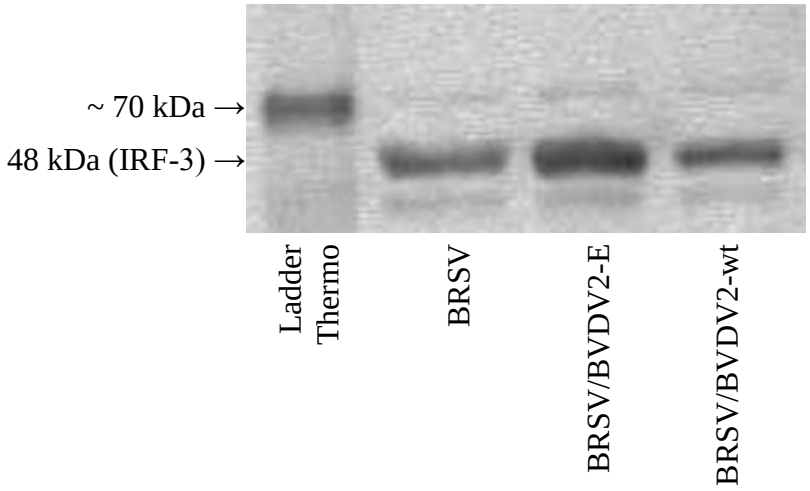

Fig. 3.10. IRF-3 protein production in co-infected BT cells. BT cells co-infected with BRSV/BVDV2-E produced IRF-3 protein at higher levels than cells infected with BRSV alone or with BVDV2-wt. BT cells co-infected with BRSV/BVDV2-wt produced less IRF-3 protein compared to cells infected with BRSV alone or with BVDV2-E. Cells were infected and harvested at 4 DPI. Protein was isolated and quantified and western blotting was performed twice. Spectra^{TM} Multicolor Broad Range Protein Ladder (Cat. # 26634, Thermo Scientific) was used.

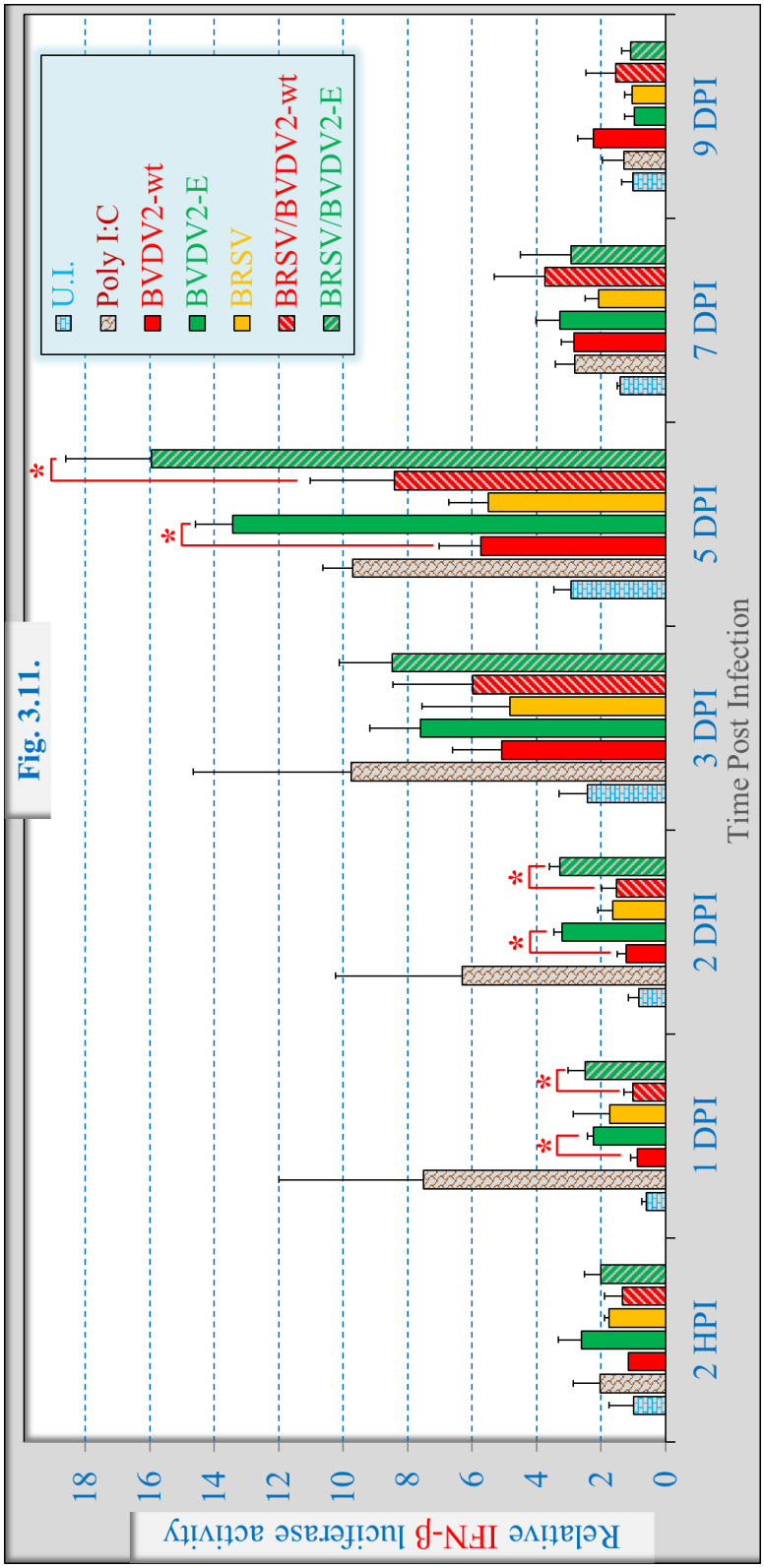

Fig. 3.11. IFN-β luciferase activity. Results are represented as fold change expressed relative to UI at the 2 HPI time point. This Figure is an extended graph for Fig. 2.7 (C).

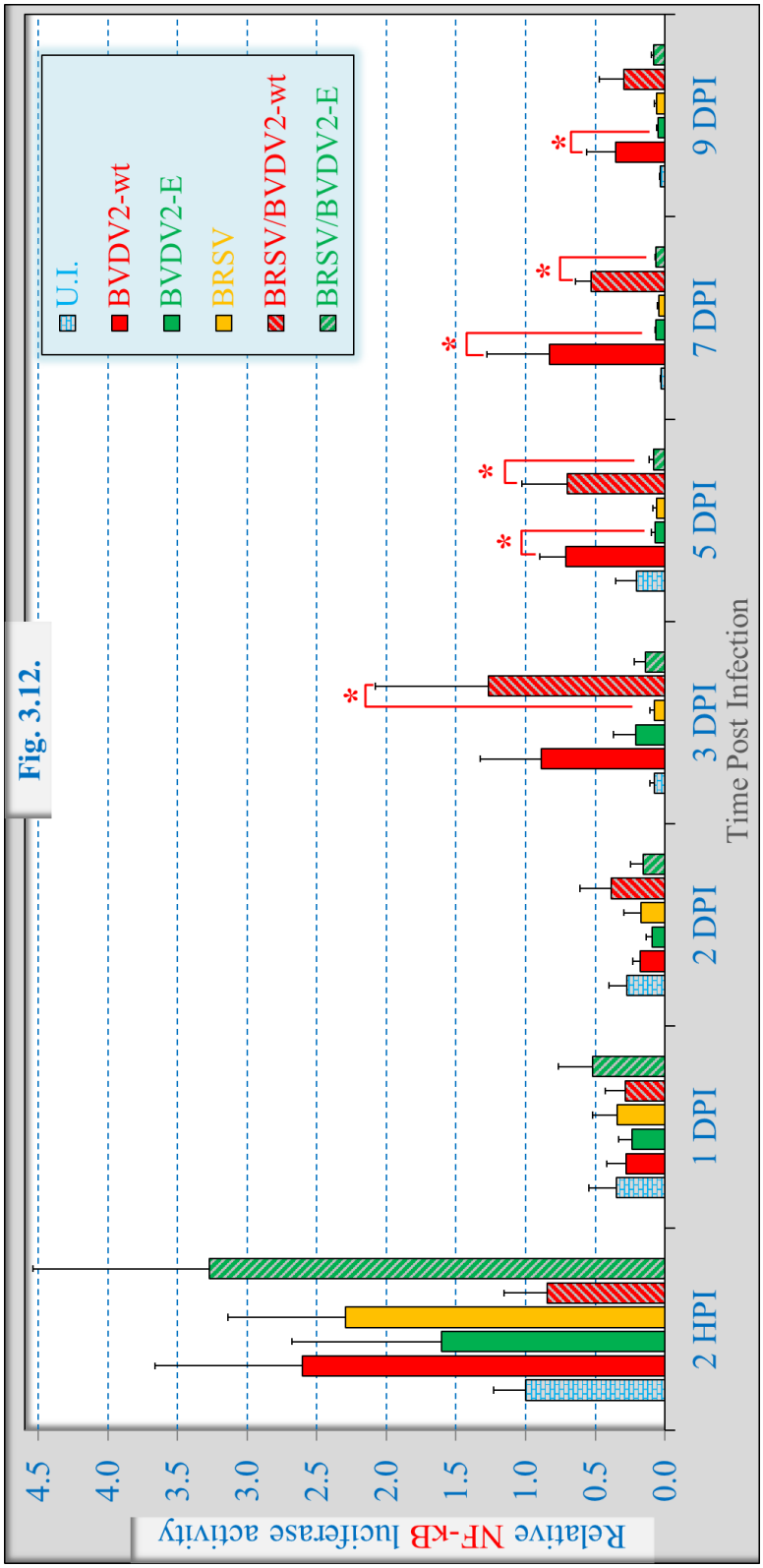

Fig. 3.12. NF-κB luciferase activity. Results are represented as fold change expressed relative to UI at the 2 HPI time point. This Figure is an extended graph for Fig. 2.8. Poly I:C results are not included.

CHAPTER 4:

SUMMARY AND FUTURE DIRECTIONS

The findings of this study confirm the role of the intact BVDV-2 N^{pro} in the antagonism of type I IFN in BVDV2-infected cells. While intact N^{pro} of BVDV prevents the production of type I IFN by suppressing levels of IRF-3 to avoid host antiviral responses, BVDV-1 and BVDV-2 with a dysfunctional N^{pro} fused with EGFP, induced a significant type I IFN response in both MDBK and BT cells and increased the production of IRF-3 protein (Alkheraif *et al.*, 2017; Gil *et al.*, 2006a; Hilton *et al.*, 2006; Horscroft *et al.*, 2005). The importance of the BVDV-2 N^{pro} protein suggests a similar importance of the intact BVDV-2 N^{pro} in animals infected with BRDC. Immunosuppression during BVDV infection in animals may contribute to secondary bacterial and viral infections. Our findings determined that BVDV2-wt, unlike BVDV2-E, decreased type I IFN production and enhanced BRSV replication in BT cells.

Our results showed that, compared to BVDV2-wt, BVDV2-E significantly up-regulated IFN-β mRNA based on real-time Q-RT-PCR and significantly increased IFN-β activity based on a dual-luciferase reporter assay. However, although our finding showed that there were no significant differences in NF-κB mRNA, the dual-luciferase reporter assay showed that BVDV2-wt significantly increased NF-κB activity compared to BVDV2-E. Plasmids encoding bovine IRF-3, IRF-7, PKR, and TBK-1 genes will be used to investigate the activities of these signal proteins in infected or co-infected BT cells. It is expected that BVDV2-E will significantly increase the activities of these signals. Using

western blotting, we found that BT cells co-infected with BRSV/BVDV2-E produced IRF-3 protein at higher levels than cells infected with BRSV alone or with BVDV2-wt. Performing western blotting with the same antibodies and using protein extracted from BT cells infected with BVDV2-wt, BVDV2-E, or BRSV will be a good addition to compare the result of co-infected cells. This western botting can be performed at other different time points.

Although BVDV is commonly associated with cattle, it has also been reported in pigs, deer, and other domesticated animals. In alpaca testicular cells, BVDV infection inhibited type I IFN response and replicated 3 – 4 logs lower compared to bovine cells (Samson *et al.*, 2011). It was reported that the seroprevalence of BVDV was low in alpacas (*Vicugna pacos*) (Cockcroft *et al.*, 2015; Dittmer *et al.*, 2018). However, BVDV can be a primary acute pathogen in alpacas and change leukocyte subset populations, which may result in transient immunosuppression and contribute to secondary infections (Henningson *et al.*, 2013; Topliff *et al.*, 2017). Investigating the effects of BVDV N^{pro} in alpaca cells may provide a better understanding of the BVDV virulence during its infection and mechanisms of enhanced disease from BRSV/BVDV2 co-infection. The mRNA of the cell signals, including MAVS, PKR, TBK-1, IRF-3, IRF-7, IFN, NF-κB and PIN-1, can by characterized in alpaca testicular cells infected with BRSV, BVDV2-wt, or BVDV2-E or co-infected with BRSV/BVDV2-wt or BRSV/BVDV2-E. Evaluating the type I IFN production and BRSV replication in alpaca cells during co-infection with BRSV/BVDV2-wt or BRSV/BVDV2-E will add to the understanding of the role of BVDV N^{pro} during co-infection in alpaca cells. Likewise, similar studies may be evaluated using bison cells.

Inhibiting type I IFN induction cell signals

Using inhibitors of the type I IFN induction cell signals that were induced to greater levels in cells infected with BVDV2-E compared to BVDV2-wt we can determine the significance of these signals in disease pathogenesis during BVDV infections. The pharmacological inhibitor of the NF-κB signaling pathway (BAY-117085) (Fredericksen *et al.*, 2015) can be used to ensure that the increased IRF-7 observed in cells infected with BVDV2-E was independent of the NF-κB signaling pathway. Unlike BRSV and BVDV2-wt, BVDV2-E increased the mRNA of TBK-1. An inhibitor of TBK-1 (BX795) (Zhang *et al.*, 2013) can be used to determine if TBK-1 is essential to the increase of type I IFN and its mRNA expression during BVDV2-E infection. If the TBK-1 inhibitor abolished the IFN increase, this would confirm that the type I IFN was increased through the TBK-1 IRF-3 pathway.

Characterize attenuation and immunogenicity of genetically-modified BVDV

To determine the impact of N^{pro} on attenuation of virulence *in vivo*, the attenuation of virulence of noncytopathic BVDV-2 mutant will be confirmed clinically and pathologically by experimental inoculation of calves. Following BVDV2-wt, BVDV2-E, and BRSV single and/or co-infections, calves will be observed daily and clinical signs (respiration rate, dyspnea, and general condition) will be assigned numerical values based on a scoring system. Calves will be euthanatized nine days post-infection. Systematic necropsy will be performed to collect tissues, and all gross abnormalities will be recorded at necropsy by a pathologist. Postmortem analyses will include determination of the extent of lesions, viral titers, viral RNA levels, and antigen

distribution in lymphoid organs. Virulence will be assessed on the basis of pathologic changes (lymphocytolysis, lymphodepletion), viral titers and BVDV RNA, viral antigen distribution in target cells of lymphoid organs and clinical signs (inappetence and dyspnea) in infected calves compared to control animals. Assessment of induction of host innate and adaptive immune responses to the attenuated BVDV mutant will be achieved by measuring type I INF and antibody responses as well as by assessing protective immunity in challenge-exposed calves (Henningson *et al.,* 2013). We expect to confirm that attenuation of virulence correlates with a dysfunctional N^{pro}.

Overall, it is expected that the proposed research will provide detailed insight into influences on viral function, virulence and immunity. We expect to show that BVDV N^{pro} enhances virulence and modulates innate immune responses to BRSV infection. This understanding will be beneficial for the development of safer and more effective BVDV vaccines.

APPENDIX A:

MATERIALS

Cell Culture Solutions

Dulbecco's Modified Eagle Medium (DMEM)-High Glucose

To prepare 6 liters:

Ultrapure water (UPW, upH_2O)	6 liters
DMEM	80.24 grams
$NaHCO_3$	22.2 grams

Adjust pH to 6.8 ~ 6.9 using 6 M HCl.
Filter sterilize with 0.2 µm Supor® membrane filter into 500-ml bottles.
Use LB plates to test for bacteria and fungi.
Seal lids with parafilm and store at 4 ºC.

Equine Serum

Hyclone, Logan, UT.

Fetal Bovine Serum

Hyclone, Logan, UT.

Calcium and Magnesium-Free Phosphate-Buffered Saline (CMF-PBS)

To prepare 6 liters:

upH_2O	6 liters
NaCl	48 grams
KCl	2.4 grams
$NaHCO_3$	5.25 grams
Glucose (dextrose)	15 grams

Adjust pH to 7.2 using 6 M HCl.
Filter sterilize with 0.2 µm Supor® membrane filter into 500-ml bottles.
Use LB plates to test for bacteria and fungi.
Seal lids with parafilm and store at 4 ºC.

1X Trypsin-EDTA

0.5% Trypsin-EDTA.
To prepare a liter:

CMF-PBS	0.9 liter
10X Trypsin-EDTA	0.1 liter

Add phenol red to adjust color to light pink.
Filter sterilize with 0.2 µm Supor® membrane filter into 100-ml bottles.
Use LB plates to test for bacteria and fungi.
Store at –20 ºC.

Cell Freezing Media

To prepare 101 ml:

Dimethyl sulfoxide (DMSO)	8 ml
Glycerol	8 ml
Equine or fetal bovine serum	15 ml
DMEM	70 ml

Filter sterilize with 0.2 µm Supor® membrane filter.
Store at 4 ºC.

Poly I:C

Polyinosinic-Polycytidylic acid [Poly(I)-Poly(C); Poly (I:C)] sodium salt:
P0913-10MG, ten milligrams lyophilized powder.
Lot# 082M4029V, Amersham Biosciences, Piscataway, NJ, USA.
Store at –20 °C.

Preparing Poly I:C stock (2 mg/ml)
Add 5 ml PBS to the tube that contains the 10 mg Poly I:C powder.
Swirl and pass through a 26-gauge needle several times.
Aliquot 0.5 ml Poly I:C into 2-ml tubes.
Store at –80 °C for up to 3 years.

Preparing 100 µg/ml Poly I:C
To prepare 36 ml of 100 µg/ml Poly I:C.

Poly I:C stock (2 mg/ml):	1.8 ml
2% HS DMEM	34.2 ml

Discard unused portion.

Ampicillin Solution (10 mg/ml)

To prepare 10 ml (Ampicillin, Sodium Salt):
0.1 g (100 mg) Ampicillin + 10 ml upH_2O = 10 ml of 10 mg/ml → 10 µg/µl.
Filter the solution through 0.22 µm filter, using a syringe.
Store Ampicillin at 4 °C for up to one month, or freeze at –20 °C.

Luria-Bertani (LB) Media

To prepare a liter:

upH_2O	1 liter
Bacto tryptone	10 grams
Bacto yeast extract	5 grams
NaCl	10 grams

Adjust pH to 7.0 using 6 M HCl.
Pour into bottles.
Autoclave for 20 minutes.
Store at 4º C.

Luria-Bertani (LB) Plates

To prepare a liter:

upH_2O	1 liter
Bacto tryptone	10 grams
Bacto yeast extract	5 grams
NaCl	10 grams
Adjust pH to 7.0 using 6 M HCl. Then add:	
Bacto agar	15 grams
Autoclave for 20 minutes. Cool to 50 ºC.	
Add antibiotic if needed	

Pour approximately 20 ml into each 90-mm plate.
Leave plates uncovered in the laminar flow hood for 30 minutes to solidify.
Store at 4 ºC.

70% Ethanol for Total RNA Extraction

Prepare:

Absolute ethanol	2.1 ml
Nuclease-free water	0.9 ml

Immunoperoxidase Staining (ELISA) Solutions*

Phosphate Buffered Saline (PBS), 0.01M

To prepare 6 liters:

upH_2O	6 liters
Na_2HPO_4	12 grams
NaH_2PO_4	1.08 grams
NaCl	51 grams

Adjust pH to 7.6 using 6 M HCl.

Fixation Buffer (PBS/20% Acetone)

To prepare a liter:

PBS	0.8 liter
Acetone	0.2 liter

Binding Buffer

To prepare a liter:

PBS	1 liter
NaCl	29.5 grams
Tween 20	0.1 ml

Wash Buffer

To prepare 5 liters:

PBS	5 liters
Tween 20	2.5 ml

Substrate Buffer (Acetate Buffer 0.05M, pH 5.0)

Prepare:

upH_2O	200 ml	**Solution A**
Acetic acid	1.156 ml	

upH_2O	500 ml	**Solution B**
Sodium acetate	6.8 grams	

Mix:

Solution A	148 ml	One liter of substrate buffer
Solution B	352 ml	
upH_2O	500 ml	

Adjust pH to 5.0.

3-Amino-9-Ethyl-Carbozole (AEC) Solution

To prepare a 4 mg/ml stock solution:

N,N-dimethylformamide	100 ml
AEC	400 mg

Using aluminum foil, wrap bottle to protect from light.

* Store all the immunoperoxidase staining solutions at room temperature.

Agarose Gel Electrophoresis Solutions*

0.5X TBE (Working Solution)

To prepare a liter:

5X TBE	100 ml
upH_2O	900 ml

5X TBE Buffer

(Tris base, Boric acid, and EDTA)
To prepare a liter of 5X TBE:

upH_2O	1 liter
Tris base	54 grams
Boric acid	27.5 grams
0.5M EDTA (pH 8.0)	20 ml

Ethidium Bromide

To prepare a 10 mg/ml stock solution:

Sterile upH_2O	10 ml
Ethidium bromide	100 mg

Using aluminum foil, wrap bottle to protect from light.

* Store all the agarose gel electrophoresis solutions at room temperature.

Interferon (IFN) Response Assay Solutions

PBS with 0.1% BSA
To prepare 50 ml of stock solution:

CMF-PBS	50 ml
Bovine serum albumin (BSA)	50 mg

Store at 4 ºC.
(1 mg BSA/ml PBS solution = 0.1% BSA solution)

1X Reporter Lysis Buffer with 1 mg BSA/ml

Prepare a 1.25 mg BSA/ml H_2O stock solution:

Sterile upH_2O	40 ml
Bovine serum albumin (BSA)	50 mg

Store at 4 ºC.
(1.25 mg BSA/ml H_2O solution = 0.125% BSA solution)

To prepare a 1X reporter lysis buffer with 1 mg BSA/ml solution:

1.25 mg BSA/ml upH_2O stock solution	2 ml
5X reporter lysis buffer	0.5 ml

Discard unused buffer after assay.

1X Passive Lysis Buffer

To prepare 5 ml:

Sterile upH_2O	4 ml
5X Passive Lysis Buffer	1 ml

Discard unused buffer after assay.

Western Blotting Solutions

RIPA Buffer

To prepare 250 ml of stock solution:

NaCl	2.1915 grams	
Triton X-100	2.5 ml	1% final
Sodium deoxycholate	1.25 grams	0.5% final
Sodium dodecyl sulfate (SDS)	0.25 grams	0.1% final
Tris base 0.5 M (pH 8)*	25 ml	50mM final
upH_2O	222.5 ml	Up to 250 ml

* To prepare Tris base 0.5 M: add 6.057 grams Tris base to 100 ml upH_2O.
Adjust the pH to 8, using HCl.
Store RIPA buffer at 4 °C.

10% Ammonium Persulfate (10% APS)

Prepare:

Ammonium persulfate, 98%	1 gram
upH_2O	10 ml

Vortex.
Prepare 0.5 ml/tube aliquots in 1.5-ml tubes.
Store at –20 °C.

Bis Tris 3.5X Buffer

Bis tris (C_8 H_{19} N O_5).
To make 1M (molar concentration), add 209.24 grams to one liter upH_2O.
Prepare:

To have:	Molar	Bis tris	upH_2O
	1M	209.24 grams	1 L
1X	0.357M (357mM)	74.73 grams	1 L
1X	0.357M (357mM)	14.95 grams	200 ml
3.5X	1.25M (1250mM)	52.32 grams	200 ml
3.5X	1.25M (1250mM)	13.08 grams	50 ml

Adjust the pH to 6.5 – 6.8, using HCl.
Store at 4 °C for up to 6 months.

1M Sodium Bisulfite Buffer (as Antioxidant)

Sodium bisulfite ($NaHSO_3$).
Prepare:

To have:	Molar	Sodium bisulfite	upH_2O
1X	1M	104.07 grams	Up to 1 L
1X	1M	2.6 grams	Up to 25 ml

Store at 4 °C for up to 2 months.

NuPAGE: MOPS SDS Running Buffer (20X)

Prepare:

	to make 500 ml	to make 250 ml	For 1X Buffer
MOPS	104.6 grams	52.3 grams	50mM final
Tris base	60.6 grams	30.3 grams	50mM final
SDS	10 grams	5 grams	0.1% final
EDTA	3.7224 grams	1.8612 grams	1mM final
upH_2O	Up to 500 ml	Up to 250 ml	

Store at 4 °C for up to 6 months.

To make 1 liter of 1X MOPS SDS Running Buffer

Use 950 ml upH_2O + 50 ml of 20X buffer = 1 L.
Add 5 ml of the antioxidant, 1M Sodium Bisulfite buffer.
The pH of the 1X buffer is 7.7.
Do not use acid or base to adjust the pH.
Store at 4 °C. It may be used for up to 5 times.

NuPAGE: Transfer Buffer (20X)

Prepare:

	to make 150 ml	to make 250 ml	For 1X Buffer
Bicine	12.24 grams	20.4 grams	25mM final
Bis tris	15.7 grams	26.17 grams	25mM final
EDTA	1.117 grams	1.8612 grams	1mM final
upH_2O	Up to 150 ml	Up to 250 ml	

Store at 4 °C for up to 6 months.

To make 1 liter of 1X Transfer Buffer

Use 950 ml upH_2O + 50 ml of 20X buffer = 1 liter.
Add 5 ml of the antioxidant, 1M Sodium Bisulfite buffer.
The pH of the 1X buffer is 7.2.
Do not use acid or base to adjust the pH.
Store at 4 °C. It may be used for up to 5 times.

Western Blotting 8% gel

Prepare:

	8% for 2 Gels	Stacking
Bis tris 3.5X buffer	2. 84 ml	1 ml
30% acrylamide	2. 68 ml	0. 46 ml
upH_2O	4. 48 ml	2. 04 ml
Mix well… then add:		
10% APS	50 µl	40 µl
TEMED	14 µl	20 µl
Use (Pour)	~ 4.5 ml for each	~ 1.5 ml for each

8% gel needs to be prepared and poured immediately at room temperature.
Allow to solidify for 20 – 30 minutes.
Then, prepare and pour the stacking gel.
Insert a 10-well comb.
Allow to solidify for 20 – 30 minutes.

TBS Buffer (10X)

Preparing Tris Buffer Saline (10X)

	to make 1 L	to make 500 ml	For 1X Buffer
NaCl	87.7 grams	43.85 grams	150mM final
Tris base	12.114 grams	6.057 grams	100mM final
upH_2O	Up to 1 L	Up to 500 ml	

Adjust pH to 7.5 with HCl.
Store at 4 °C for up to 3 months.

TBS-T Solution

To prepare Tris Buffer Saline with 0.1% Tween® 20 (TBS-T):

	to make 1 L	to make 500 ml
upH_2O	900 ml	450 ml
TBS (10X)	100 ml	50 ml
Tween® 20	1 ml	0.5 ml

Store at 4 °C for one week only.

Blocking Solution (TBS-T with 5% Milk or BSA)

Using skim dry milk or bovine serum albumin (BSA):

	for two gels	for four gels
TBS-T	10 ml	20 ml
Milk or BSA	0.5 gram	1 gram

APPENDIX B:

METHODS

Cell Culture Methods

The following methods were used with three cell lines:

1. MDBK (Madin-Darby Bovine Kidney) cells:

Cell density is approximately 3.5×10^7 cells in a 100% confluent 75 cm^2 flask, and 3×10^6 cells in a 100% confluent well of 6-well plate.

2. BT (Bovine Turbinate) cells:

Cell density is approximately 4×10^6 cells in a 100% confluent 75 cm^2 flask, and 3×10^5 cells in a 100% confluent well of 6-well plate.

3. NCL1-ISRE-Luc-Hygro (modified bovine uterus) cells:

This reporter cell line has an ISRE (IFN Stimulated Response Element) gene coupled with a luciferase reporter gene and hygromycin antibiotic resistance gene. Use 6 µl of Hygromycin B (50 mg/ml solution) per ml of culture media to maintain selection. Cell density is approximately 6×10^6 cells in a 100% confluent 75 cm^2 flask.

Establishing a Cell Culture from a Frozen Stock

- Mix 27 ml DMEM with 3 ml HS in a 75 cm^2 tissue culture flask.
- Prevent ice crystal formation by thawing cells in cryovial (ampule) rapidly in a 37 ºC water-bath to prevent cell lysis.
- Add cells to tissue culture flask with media.
- Incubate at 37 ºC with 5% CO_2. After 24 hours, change media.

Cell Culture Maintenance

- Discard the old media.
- Rinse cells twice with 10 ml CMF-PBS.
- Add 5 ml 0.05% trypsin-EDTA to cells, swirl, remove all but 1 ml, and allow cells to separate for 3 minutes (8 minutes for MDBK cells).
- Tap flask to dislodge cells.
- Resuspend cells using 10 ml of DMEM/10%HS.
- Add 0.5 – 3 ml of cell suspension to 25 ml 10%HS/DMEM/75-cm^2 flask (35 ml/162-cm^2 flask).
- Incubate at 37 ºC with 5% CO_2.
- Pass cells every week or at least twice a month.

Preparing a Frozen Stock of Cells

- Discard the old media.
- Rinse cells twice with 10 ml CMF-PBS.
- Add 5 ml 0.05% trypsin-EDTA to cells, swirl, remove all but 1 ml, and allow cells to separate for 3 minutes (8 minutes for MDBK cells).

- Tap flask to dislodge cells.
- Resuspend cells in 5 ml freezing media and pipette up and down.
- Aliquot each 1 ml into a 2 ml cryovial.
- Wrap in cotton, place in styrofoam container and freeze at –80 ºC.
- After 24 hours, place cryovials in a box at –80 ºC.

Testing for Bacteria and Fungi

To ensure that there is no contamination in materials, cells, and viruses, spread a 0.2 ml sample onto an LB plate and incubate at 37 ºC for bacteria and another 0.2 ml sample onto another LB plate and incubate at room temperature for fungi, for two weeks.

Virus-Work Methods

Preparation of Virus Stocks

- Use 90% confluent MDBK-cell flasks for BVDV2 isolates. Use 90% confluent BT-cell flasks for BRSV236-652.
- Calculate the virus needed using the following formula:

$$\frac{\text{Cells per flask} \times \#\text{ of flask} \times \%\text{ confluency} \times \text{m.o.i.}}{TCID_{50}}$$

- Add virus inoculum to 2%HS/DMEM to have a final volume of 5 ml for each flask.
- Rinse flask twice with 10 ml DMEM.
- Add 5 ml virus inoculum/flask.
- Incubate at 37 ºC with occasional rocking for 90 minutes.
- Add 20 ml 2%HS/DMEM/75-cm^2 flask (30 ml/162-cm^2 flask).
- Incubate at 37 ºC with 5% CO_2 for 4 days for ncp BVDV2 isolates, and until CPE (Cytopathic Effects) for BRSV 236-652 (8 – 10 days).
- Freeze flasks at –80 ºC for at least 24 hours. Then thaw on ice.
- Pellet the virus if needed (see "Purified Pelleted Virus Stock"), or aliquot 0.5 – 2 ml into 2-ml cryovials, and store at –80 ºC.
- Titer the virus.

Purified Pelleted Virus Stock

- Using the infected flasks from previous protocol "Preparation of virus stocks".
- Thaw flasks on ice and transfer supernatant into 50 ml conical tubes.
- Centrifuge for 30 minutes at 2,000×g (~3,000 rpm) at 4 ºC.
- Transfer supernatant into autoclaved ultracentrifuge tubes, making sure to transfer exactly the same amount into each balanced tube.
- Centrifuge for 2 hours at 25,000 rpm at 4 ºC using Beckman Ultracentrifuge.
- Pour off supernatant carefully and put the tubes up side down on paper towels.
- Re-suspend viral pellet with 0.5 ml DMEM, pipette up and down to mix.
- Use the same 0.5 ml DMEM to re-suspend the second tube.
- Aliquot 100 µl into four and 50 µl into two 2-ml cryovials. Store at –80 ºC.
- Titer the pelleted virus.

Virus Titration

1. Preparation of 96-well flat bottomed plate:

- Use MDBK cells for BVDV isolates, and BT cells for BRSV.
- Rinse flask twice with 10 ml CMF-PBS. Add 5 ml 0.05% trypsin-EDTA, swirl to cover cells and remove all but 1 ml.
- Allow cells to incubate at room temperature for 5 minutes, tap flask to dislodge cells.
- Re-suspend cells using 10 ml of 3%HS/DMEM.
- Seed 2×10^4 MDBK cells/well, or 1×10^4 BT cells/well.
- Incubate at 37 ºC with 5% CO_2 overnight.

2. Preparation of viral ten-fold serial dilution and inoculation of cells in plates:

- Prepare 5 ml tubes with 0.9 ml DMEM (or 0.45 ml DMEM for Pelleted Virus Stock).
- Add 0.1 ml stock virus into tube # –1 (or 50 µl pelleted virus stock), vortex.
- Transfer 0.1 ml (or 50 µl pelleted virus) from tube # –1 to tube # –2, vortex, repeat from tube # –2 to –3… etc. Add 50 µl of dilution –1 into each well of row # 1, and 50 µl of dilution –2 into row # 2, etc.
- Add 50 µl DMEM into each well of N.C. (Negative control) row.
- Incubate at 37 ºC with 5% CO_2 for 4 days for BVDV, or 7 days for BRSV.
- Fix the plates.

Fixation

- Shake media off plates into a biohazard bag.
- Dry plates for 10 – 20 minutes in a hood.
- Add 0.1 ml fixation buffer (PBS/20% acetone) per well.
- Incubate for 10 – 15 minutes at room temperature.
- Shake the fixation buffer off.
- Allow plates to dry overnight up side down.
- Detect viral antigen using Immunoperoxidase Staining.

Immunoperoxidase Staining (ELISA)

- Use fixed dry plates.
- Re-hydrate wells with 100 µl binding buffer/well for 2 – 4 minutes.

1. mAb (primary monoclonal antibody) **:

- Use anti-BVDV mAb 348 for BVDV isolates, and 8G12 for BRSV.
- Make a 1:1000 dilution of mAb in binding buffer.
- Shake the binding buffer off plates.
- Add 50 µl of the diluted mAb/well.
- Incubate at 37 ºC for 1 hour.

2. Biotinylated Horse anti-mouse IgG (secondary antibody) **:

- Make a 1:200 dilution of IgG in binding buffer with 60% chicken serum.
- Shake the mAb off plates.

- Wash plate three times: Shake off.
  Add 100 µl wash buffer/well.
  Shake off. Repeat three times.
  Drain on a towel.

- Add 50 µl of the diluted IgG/well.
- Incubate at 37 ºC for 1 hour.

3. HRP-Streptavidin **:

- Make a 1:500 dilution of HRP in binding buffer.
- Shake the IgG off plates.

- Wash plate three times with wash buffer.

- Add 50 µl of the diluted HRP/well.
- Incubate at 37 ºC for 1 hour.

Preparing a 3% H_2O_2 (Hydrogen peroxide) solution:
0.9 ml substrate buffer + 0.1 ml 30% H_2O_2
Use same day.

4. AEC (3-Amino-9-Ethyl-Carbozole) **:

- Use glassware with AEC always.
- For each 96-well plate, mix 5 ml substrate buffer with 20 µl 3% H_2O_2.
- Then add 0.3 ml AEC slowly while swirling the mixture.
- Shake the HRP off plates.

- Wash plate three times with wash buffer.

- Add 50 µl of the AEC/well. Incubate at room temperature for 2 – 4 minutes.
- When stained wells appear reddish brown color, shake off, rinse three times with tap water to stop the reaction.
- Let plate dry overnight, look for labeled viral antigen under the microscope and calculate the titer.

**See "table 1" for exact quantities/plate.

Growth Kinetics Assay

- Calculate the amount of virus needed at a m.o.i. of 0.01 using the following formula:

$$\frac{\text{Cells per well} \times \#\text{ of wells} \times \%\text{ confluency} \times \text{m.o.i.}}{TCID_{50}}$$

- Dilute viruses in DMEM to have a final volume of 1 ml/well.
- Use 90% confluent MDBK cell 6-well plates for BVDV2 isolates.
- Use two plates for each time-point.
- Infect two wells with 1 ml/well of BVDV2 NY93, BVDV2-NY93/c, or BVDV2-NY93/c-EGFP, or add DMEM as negative control.
- Incubate at 37 ºC with occasional rocking for 2 hours.

- Remove the inoculum and rinse with 1 ml DMEM.
- Add 3 ml 2%HS/DMEM/well.
- Freeze the two plates of the first time-point (2 hours).
- Incubate the remaining time-points at 37 ºC with 5% CO_2 for 1.5, 3, 6, 9, 12, 18, 24, 48, 72, 96 hours.
- Freeze plates of each time-point at –80 ºC for at least 24 hours.
- Thaw on ice.
- Aliquot 0.2 – 1 ml into four 2 ml cryovials and store at –80 ºC.
- Titer the viruses at each time-point.

Growth Kinetics of Concurrent Infections

- BVDV2-NY93 with BRSV (or BVDV2-NY93/c-EGFP with BRSV):
- Calculate the amount of virus needed at a m.o.i. of 0.6 for BVDV2-NY93, BVDV2-NY93/c N-N^{pro} 18 EGFP, and BRSV using the following formula:

$$\frac{\text{Cells per well} \times \#\text{ of wells} \times \%\text{ confluency} \times \text{m.o.i.}}{TCID_{50}}$$

- Dilute viruses in 2%HS/DMEM to have a final volume of 1 ml/well.
- Use 90% confluent BT cell 6-well plates.
- Use two plates for each time-point. Infect two wells with 1 ml/well of BRSV, BVDV2-NY93 (or BVDV2-NY93/c-EGFP), or BVDV2-NY93 with BRSV (or BVDV2-NY93/c-EGFP with BRSV), or add 2%HS/DMEM as negative control.
- Incubate at 37 ºC with occasional rocking for 90 minutes.
- Remove the inoculum and rinse with 1 ml DMEM.
- Add 3 ml 2%HS DMEM/well.
- Incubate at 37 ºC with 5% CO_2 for 1.5, 6, 12, 24, and 48 hours, and 3, 5, 7, and 9 days.
- Freeze plates of each time-point at –80 ºC for at least 24 hours.
- Thaw on ice and mix the two wells of each virus to have 6 ml.
- Aliquot 0.2 – 3 ml into five 2 ml cryovials and store at –80 ºC.
- Titer the viruses at each time-point.
- Extract the mRNAs and perform real-time RT-PCR.

RT-PCR Methods

RNA Extraction (Using Trizol® LS Reagent)

- Add 0.25 ml of the sample (cell-culture supernatant that has virus) into a 1.5 ml tube and add 0.75 ml Trizol LS reagent (the volume ratio should be 1:3). Pipette up and down to mix and lyse the cells.
  [Note: Trizol LS reagent is very dangerous and harmful to eyes and skin].
- Incubate at room temperature for 5 minutes.
- Add 0.2 ml chloroform into each tube.
- Cap tubes securely and shake vigorously for 15 seconds.
- Incubate samples at room temperature for 15 minutes.
- Centrifuge samples at no more than 12,000×g for 15 minutes at 2 – 8 °C.

- Now, there are three phases: clear aqueous phase at the top, white phase (like a membrane) as inter-phase, and phenol phase at the bottom.
- Transfer the upper aqueous phase to a clean 1.5-ml tube.
- Add 0.5 ml isopropyl alcohol (Isopropanol).
- Incubate at room temperature for 10 minutes.
- Centrifuge at no more than 12,000×g for 10 minutes at 2 – 8 °C. The RNA pellet may not be visible.
- Pour off the supernatant carefully.
- Add 1 ml 75% ethanol in DEPC-treated water (3 parts absolute ethanol + 1 part DEPC-treated water).
- Vortex samples and store at –80 °C.

RT-PCR Primers

For BVDV, the forward primer: 5' CAT GCC CAT AGT AGG AC 3'; and the reverse primer: 5' CCA TGT GCC ATG TAC AG 3' (Integrated DNA Technologies, Inc., Coralville, IA).

For EGFP, the forward primer: 5' GTG AGC AAG GGC GAG GAG CTG 3'; and the reverse primer: 5' CTT GTA CAG CTC GTC CAT GCC GAG AG 3' (Integrated DNA Technologies, Inc., Coralville, IA).

Reverse Transcription Polymerase Chain Reaction (RT-PCR)

Pellet the RNA:

- Using the extracted RNA in 1 ml 75% ethanol in DEPC.
- Centrifuge at 9,000×g for 10 minutes at 2 – 8 °C, and pour off the ethanol.
- Dry for 15 minutes in a speed-vac.
- Add 10 µl of DEPC-treated water and pipette up and down.
- Incubate at 55 °C for 15 minutes and on ice for a minute.

RT-PCR:

- Using thin-walled PCR tubes…

# of samples	one
Reverse primer (2 pmol/µl)	1 µl
10mM dNTP Mix	1 µl
DEPC-treated water	8 µl
RNA sample	2 µl
Final volume	12 µl

- Using PCR machine: perform the following cycle:

1 = 65 °C	for 5:00 minutes
2 = 4.0 °C	for 1:00 minute
3 = END	

- Add 8 µl of the following mixture to each RNA sample:

# of samples	one
5X First strand Buffer	4 µl
0.1 M DTT	1 µl
RNase Inhibitor (10 U/µl)	2 µl
Superscript III RT	1 µl
From last step	12 µl
Final volume	20 µl

- Perform the following cycle:

1 = 56 °C	for 1 hour
2 = 70 °C	for 15:00 minutes
3 = 4 °C	forever
4 = END	

- Now, the complementary DNA (cDNA) is formed.

- Add 2 µl cDNA to 48 µl of the following mixture:

# of samples	one
10X PCR Buffer (- $MgCl_2$)	5 µl
50mM $MgCl_2$	1.5 µl
10mM dNTP Mix	1 µl
Upstream primer (50 pmol/µl)	1 µl
Downstream primer (50 pmol/µl)	1 µl
Taq Polymerase	0.4 µl
DEPC-treated water	38.1 µl
cDNA	2 µl
Final volume	50 µl

- Perform the following cycle:

1 = 94 °C	for 2 minutes
2 = 94 °C	for 10 seconds
3 = 50 °C	for 15 seconds
4 = 72 °C	for 30 seconds
5 = Go to 2, 30 times	
6 = 72 °C	for 10 minutes
7 = 4 °C	forever
8 = END	

- Store at –20 °C, until performing an agarose gel electrophoresis.

Agarose Gel Electrophoresis

- To prepare a 1% agarose gel for a small gel apparatus, add 0.4 g of agarose to 40 ml of 0.5X TBE buffer.
- Microwave, cool, pour, and allow to solidify for 20 minutes.
- Mix 10 µl of RNA samples or 1KB ladder with 2 µl dye and load into wells of the gel.
- Run for approximately 90 minutes at 82V (voltage).
- Stain with 15 µl ethidium bromide (10 mg/ml) in 0.5X TBE buffer for 15 minutes.
- Destain in new 0.5X TBE buffer for 15 minutes.
- Visualize gel under ultraviolet light.

Viral RNA Extraction

(Using QIAamp® Viral RNA Mini kit, spin protocol, Cat. # 52904, Qiagen, Valencia, CA).

- Pipette 560 µl prepared buffer AVL (containing carrier RNA) into a 1.5-ml tube.
- Add 140 µl of the sample (cell-culture supernatant that has virus).
- Pulse-vortex for 15 seconds.
- Incubate at room temperature for at least 10 minutes, then briefly centrifuge.
- Add 560 µl of absolute (96 – 100%) ethanol (for molecular biology use).
- Pulse-vortex for 15 seconds, then briefly centrifuge.
- Apply 630 µl of the solution into a QIAamp Mini spin column (in a 2-ml tube), close lid.
- Centrifuge at 6,000×g (8,000 rpm) for 1 minute.
- Place the column into a new 2-ml tube.
- Apply the remaining 630 µl of the solution into the column, and repeat the last step. [At this step, the RNA is binding to the silica-gel-based membrane of the column].
- Apply 500 µl of buffer AW1 (wash buffer), close lid.
- Centrifuge at 8,000 rpm for 1 minute to wash the contaminants away (first wash).
- Place the column into a new 2-ml tube.
- Apply 500 µl of buffer AW2 (wash buffer), close lid.
- Centrifuge at full speed (14,000 rpm) for 3 minutes to wash the contaminants away (second wash).
- Place the column into a new 1.5-ml tube.
- Centrifuge at full speed for 1 minute.
- Place the column into a new 1.5-ml tube.
- Open the column and apply 60 µl of AVE, close lid.
- Incubate at room temperature for 1 minute.
- Centrifuge at 8,000 rpm for 1 minute to elute the RNA from the membrane into the 1.5-ml tube.
- Label the tubes and discard the columns.
- The RNA is stable for one year at –20 ºC or –80 ºC.
- Perform real-time RT-PCR.

Real-time RT-PCR Primers and Probe

For BVDV, the forward primer: 5'-GGGNAGTCGTCARTGGTTCG-3'; the reverse primer: 5'-GTGCCATGTACAGCAGAGWTTTT-3'; and probe: 5'-6-FAM-CCAYGTGGACGAGGGCAYGC-TAMRA-3'. The BVDV probe was labeled with a fluorescent reporter molecule (6-carboxy-fluorescein, 6-FAM) at the 5' end and with a quencher molecule (6-carboxy-tetra-methyl-rhodamine, TAMRA) at the 3' end. Primers and probe were based on sequences of the 5' UTR (Mahlum *et al.*, 2002).

For BRSV, the forward primer: 5'-GCA-ATG-CTG-CAG-GAC-TAG-GTA-TAA-T-3'; the reverse primer: 5'-ACA-CTG-TAA-TTG-ATG-ACC-CCA-TTC-T-3'; and probe: 5'-/5HEX/-ACC-AAG-ACT-TGT-ATG-ATG-CTG-CCA-AAG-CA-/31ABkFQ/-3'. The BRSV probe was labeled with a fluorescent reporter molecule (hexachlorofluorescein, HEX) at the 5' end and with a quencher molecule (31ABkFQ) at the 3' end. Primers and probe were based on conserved regions of the published sequences of the BRSV N gene (Boxus, 2005) (Integrated DNA Technologies, Inc., Coralville, IA).

Stock solutions of primers and probes are 100 µM/L (100 pmol/µl).

Real-Time RT-PCR

(Using BIO-RAD's iCycler iQ™).

- Prepare a table that shows which wells of the 96-well Real-time RT-PCR plate will be used. Use two wells for each RNA sample.
- Dilute the appropriate primers and probe of each virus in RNase-free water.
- Prepare the master mix for the RNA of BVDV2:

# of reactions	Pre reaction
2X QuantiTect Probe RT-PCR Mix	12.5 µl
Forward Primer (1:8 dilution)	1 µl
Reverse Primer (1:8 dilution)	1 µl
Probe (1:13.5 dilution)	1 µl
QuantiTect RT Mix	0.25 µl
RNase-Free Water	4.25 µl
Final Volume	20 µl

- Prepare the master mix for the RNA of BRSV 236-652:

# of reactions	Pre reaction
2X QuantiTect Probe RT-PCR Mix	12.5 µl
Forward Primer (1:10 dilution)	1 µl
Reverse Primer (1:10 dilution)	1 µl
Probe (1:20 dilution)	1 µl
QuantiTect RT Mix	0.25 µl
RNase-Free Water	4.25 µl
Final Volume	20 µl

- Apply 20 µl of the master mix into each well.
- Add 5 µl of RNA sample.
- Using BIO-RAD's iCycler iQ™, Optical System Software:
- For the mRNA of BVDV2, define FAM as fluorophore and perform this cycle:

Cycle **1**	1X	One step	50 ºC	For 30 minutes
Cycle **2**	1X	One step	95 ºC	For 15 minutes
Cycle **3**	40X	Step **1**	95 ºC	For 15 seconds
		Step **2**	55 ºC	For 30 seconds
		Data collection and Real-time analysis enabled		
		Step **3**	72 ºC	For 30 seconds
Cycle **4**	1X	One step	4 ºC	HOLD

- For the mRNA of BRSV236-652, define HEX as fluorophore and perform this cycle:

Cycle **1**	1X	One step	50 ºC	For 30 minutes
Cycle **2**	1X	One step	95 ºC	For 15 minutes
Cycle **3**	45X	Step **1**	94 ºC	For 15 seconds
		Step **2**	59 ºC	For 60 seconds
		Data collection and Real-time analysis enabled		
Cycle **4**	1X	One step	4 ºC	HOLD

- Copy the data and make a graph.

Interferon (IFN) Response Assay Methods

Interferon Expression Assay

BVDV2-NY93, BVDV2-NY93/c, and BVDV2-NY93/c-EGFP:

- Dilute viruses and poly I:C in 2%HS/DMEM to a final volume of 1 ml/well.
- Use 10 wells of three 90% confluent MDBK cell 6-well plates.
- Infect two wells with 1 ml/well of BVDV2-NY93, BVDV2-NY93/c, or BVDV2-NY93/c-EGFP, or add 2%HS/DMEM as negative control or poly I:C (100 µg/ml) as positive control.
- Incubate at 37 ºC with occasional rocking for 90 minutes.
- Add 2 ml 2%HS/DMEM/well.
- Incubate at 37 ºC with 5% CO_2 for 24 hours.
- Freeze plates at –80 ºC for at least 24 hours.
- Thaw on ice and place the cell lysate in 15-ml tubes.
- Centrifuge at 2,000×g for 30 minutes at 4 ºC.
- Transfer to new 15-ml tubes.
- Adjust pH to 2 with 2M HCl and test strips.
- Incubate at 4 ºC for 24 hours to inactive the viruses.
- Adjust pH to 7 with 2M NaOH and test strips.

Testing samples:

- Use 20 wells of three NCL1-ISRE-Luc-Hygro cell 12-well plates, which are seeded and incubated for 12 hours.
- Replace media of NCL1-ISRE-Luc-Hygro cell wells with 0.5 ml of each sample, using two wells for each sample.
- Incubate at 37 ºC with 5% CO_2 for 8 hours.
- Discard test sample, wash NCL1-ISRE-Luc-Hygro cells twice with 1 ml CMF-PBS.
- Apply 100 µl of 1X passive lysis buffer, and harvest the cells using scraper.
- Transfer cell debris and liquid into 1.5-ml tubes, vortex for 15 seconds.
- Centrifuge at 12,000×g at 4 ºC for 2 minutes.
- Transfer the supernatant to new 1.5-ml tubes.
- Store at –80 ºC for at least 24 hours.
- Perform luciferase assay.

IFN Standard Curve

Preparing 1:2 serial dilution of recombinant human IFN standard (Bio-source PHC 4045):

- Apply 200 µl of PBS with 0.1% BSA to 12 tubes (–1 to –12 tubes).
- Mix 5.4 µl of recombinant human IFN standard stock (100 units/µl, total 540 units) with 194.6 µl of PBS with 0.1% BSA to have 200 µl, vortex.
- Mix the 200 µl from last step (540 units) with the 200 µl of –1 tube, vortex, and then transfer 200 µl from –1 (270 units) to –2 tubes… until –12 tube.
- Now each tube has 200 µl.
- Add 1.8 ml DMEM to each tube to be 2 ml in each tube.
- Now, every 0.5 ml of –1 tube includes 67.5 units, every 0.5 ml of –2 tube includes 33.75 units, and every 0.5 ml of –12 tube includes 0.032959 units.
- Replace media of NCL1-ISRE-Luc-Hygro cell wells with 0.5 ml of each dilution sample, using three wells for each dilution sample (total 36 wells).
- Incubate and harvest just like previously described with other NCL1-ISRE-Luc-Hygro cell plates.

Luciferase Assay

- Using samples in 1X passive lysis buffer.
- Use opaque luminometer (dark) 96-well plate.

Preparing 1:50 serial dilution of Purified Luceferase standard:

- Apply 98 µl of 1X Reporter Lysis Buffer to 10 tubes (–1 to –10 tubes).
- Add 2 µl of Purified Luceferase standard to –1 to have 100 µl, vortex.
- Transfer 2 µl from –1 to –2 tubes until –10 tube.
- Equilibrate luciferase assay reagent and samples to room temperature.
- Leave the first two wells of the plate empty, and apply 20 µl/well from each sample into two wells. Use three wells for IFN standard curve samples. Use one well for Purified Luceferase standard dilution.
- Use FluoStar Optima luminometer, set to inject 100 µl luciferase assay buffer/well, and measure luminescence.

Interferon Inhibition Assay of Concurrent Infection

BVDV2-NY93 with BRSV & BVDV2-NY93/c-EGFP with BRSV:

- Dilute viruses and poly I:C in 2%HS/DMEM to a final volume of 1 ml/well.
- Use 14 wells of four 90% confluent BT cell 6-well plates.
- Infect two wells with 1 ml/well of BRSV, BVDV2-NY93, BVDV2-NY93 with BRSV, BVDV2-NY93/c-EGFP, or BVDV2-NY93/c-EGFP with BRSV, or add 2%HS/DMEM as negative control or poly I:C (100 µg/ml) as positive control.
- Incubate at 37 ºC with occasional rocking for 90 minutes.
- Add 2 ml 2%HS/DMEM/well.
- Incubate at 37 ºC with 5% CO_2 for 48 (or 72) hours.
- Wash wells with 1 ml DMEM, and replace with 3 ml fresh 2%HS/DMEM/well for one well for each, and replace with 3 ml fresh poly I:C in 2%HS/DMEM/well (50 µg/ml) for the another well of each.
- Incubate at 37 ºC with 5% CO_2 for 20 hours.
- Freeze plates at –80 ºC for at least 24 hours.
- Thaw on ice and place the cell lysate in 15-ml tubes.
- Centrifuge at 2,000×g for 30 minutes at 4 ºC, transfer to new 15-ml tubes.
- Adjust pH to 2 with 2M HCl and test strips.
- Incubate at 4 ºC for 24 hours to inactive the viruses.
- Adjust pH to 7 with 2M NaOH and test strips.
- Now, there are 14 different samples.

Testing samples:

- Use 28 wells of four NCL1-ISRE-Luc-Hygro cell 12-well plates, which are seeded and incubated for 12 hours.
- Replace media of NCL1-ISRE-Luc-Hygro cell wells with 0.5 ml of each sample, using two wells for each sample.
- Incubate at 37 ºC with 5% CO_2 for 8 hours.
- Discard test sample, wash NCL1-ISRE-Luc-Hygro cells twice with 1 ml CMF-PBS.
- Apply 100 µl of 1X passive lysis buffer, and harvest the cells using scraper.
- Transfer cell debris and liquid into 1.5-ml tubes.
- Vortex for 15 seconds.
- Centrifuge at 12,000×g at 4 ºC for 2 minutes.
- Transfer the supernatant to new 1.5-ml tubes.
- Store at –80 ºC for at least 24 hours.
- Perform luciferase assay.

Cellular Gene mRNA Extraction and Real-time Q-RT-PCR:

BT cells were infected and harvested. Total RNA was extracted from cell lysates. The cellular gene mRNA levels were quantified using real-time Q-RT-PCR.

Preparing 49 Flasks of BT Cells

- Using six 150 cm^2 flasks of NVSL-BT cells.
- Wash twice, trypsinize, re-suspend with 500 ml DMEM in one flask.
- Each flask has about 8 million BT cells. Total about 48 million.
- Pour 10 ml cells (≈ 1 million cells) into each 75 cm^2 flask.
- Add 15 ml media into each flask.
- After three days, the confluency became 90% (% confluency = 0.9).

Viral Inoculation

- Calculate the amount of virus needed at a m.o.i. of 0.05 using the following formula:

$$\frac{\text{Cells per well} \times \#\text{ of flasks} \times \%\text{ confluency} \times \text{m.o.i.}}{TCID_{50}}$$

- Dilute viruses in DMEM to have a final volume of 5 ml/flask.
- Label flasks for seven time-points. Seven flasks for each time-point.
- Infect seven flasks with 5 ml/flask of BVDV2-wt, BVDV2-E, BRSV, BRSV and BVDV2-wt, or BRSV and BVDV2-E at a m.o.i. of 0.05, stimulated with 5 ml/flask of poly I:C (100 µg/ml), or treated with 5 ml/flask of media as UI control.
- Incubate at 33 ºC for 2 hours.
- Discard the inoculum and rinse with 10 ml DMEM.
- Add 25 ml 2%HS/DMEM/flask.
- Harvest and lyse cells in the seven flasks for the first time-point (2 hour).
- Incubate other time-point flasks at 33 ºC for 1, 2, 3, 5, 7, or 9 Days.
- Harvest and lyse cells at other time-point flasks using RLT buffer (Qiagen).

Harvest (Trypsinize and Collect) Cells

- Completely discard the medium and wash with 10 ml PBS.
- Add 5 ml of 0.25% trypsin and remove 4.5 ml of it.
- After cells detach (5 – 10 minutes), tip the flask 2 – 3 times and add 4 ml DMEM.
- Transfer the 5 ml cells from each flask into a new 15-ml tube.
- Centrifuge the 15-ml tubes at 3000×g for 10 minutes and discard the supernatant.
- Centrifuge at 1000×g for 2 minutes and discard the rest of the supernatant.
- To disrupt the cells, add 0.75 ml of buffer Plus RLT/15-ml tube, pipet to mix.
- Homogenize the lysate by passing lysate at least 5 times through a 21-gauge needle (0.8 mm diameter). Do not reuse needle or syringe.
- Transfer the 0.75 ml lysate into a new 1.5-ml tube
- Store lysates at –20 °C.

Total RNA Extraction and gDNA Elimination

Using RNeasy Plus Mini Kit (Cat. # 74134, Qiagen, Valencia, CA, USA).
This kit includes gDNA Eliminator Mini Spin Columns specially designed to effectively remove genomic DNA (gDNA) contamination.

- Use 2 columns for each sample (total = 14 columns for each time-point).
- Thaw samples to room temperature.
- Transfer 0.35 ml of the sample to each of the 2 "gDNA Eliminator Mini Spin Columns" (uncolored) placed in 2-ml collection tubes.
- Centrifuge for 30 seconds at (or more than) 8000×g (10000 rpm), discard the columns.
- Save the flow-through within the 2-ml tube. This step removes the genomic DNA.
- Add 0.35 ml of 70% ethanol: mix well by pipetting. Do not centrifuge.
- Transfer the 0.7 ml (700 µl) to a new "RNeasy Mini Spin Column" (pink) placed in a 2-ml collection tube, close lid.
- Centrifuge for 15 seconds at (or more than) 8000×g (10000 rpm).
- Discard the flow-through and reuse the 2-ml tube.
- Add 0.7 ml buffer RW1 to the column, close lid.
- Centrifuge for 15 seconds at (or more than) 8000×g (10000 rpm) to wash the membrane.
- Discard the flow-through and reuse the 2-ml tube.
- Add 0.5 ml buffer RPE to the column, close lid.
- Centrifuge for 15 seconds at (or more than) 8000×g (10000 rpm) to wash the membrane for the second time.
- Discard the flow-through and reuse the 2-ml tube.
- Add 0.5 ml buffer RPE to the column, close lid.
- Centrifuge for 2 minutes at (or more than) 8000×g (10000 rpm) to wash (third time) and dry the membrane.
- Discard the flow-through and the 2-ml tube.
- Transfer the column into a new 2-ml tube, close lid.
- Centrifuge at full speed (17,000×g) for 1 minute to dry column completely.
- To elute the RNA, place the column in a new 1.5-ml tube, add 50 µl RNase-free water directly to the membrane, close lid.
- Centrifuge for 1 minute at (or more than) 8000×g (10000 rpm).
- Repeat the last step using another 50 µl RNase-free water.
- Discard the columns, label the RNA tubes.
- Mix the total RNAs of the two columns of each sample in one of them to have 200 µl RNA sample.
- Using the Nanodrop, analyze the purified RNA for quantity.
- Dilute RNA samples to be 20 ng/µl using nuclease-free water.
- Aliquot the diluted RNAs (20 ng/µl) into labeled ten 0.6-ml tubes.
- Aliquot 45 µl/tube.
- Store the RNAs at –80 °C.

Common RNA Sample (Inter-Run Calibration) for Real-time Q-RT-PCR

- BT cells were passed into three 162 cm^2 flasks with 10% HS DMEM.
- Incubate at 37 ºC with 5% CO_2.
- Three days later, the cell monolayer became 100% confluent.
- Cells were harvested and lysed as described previously.
- Total RNA was extracted using twelve columns of RNeasy Plus Mini Kit (Cat. # 74134, Qiagen).
- Mix the total RNA from the twelve columns of each sample into one of them to have 1200 µl.
- Using the Nanodrop, analyze the purified RNA for quantity.
- Dilute common RNA sample to 40 ng/µl using nuclease-free water.
- Aliquot the diluted RNA (40 ng/µl) into labeled ten 0.6-ml tubes.
- Aliquot 100 µl/tube.
- More than 80 tubes of common RNA sample.
- Store the RNAs at –80 °C.
- This common RNA sample needs to be diluted before use to 20 ng/µl by adding 100 µl nuclease-free water before using.
- Used common RNA sample tube should not be used again. Each tube must be discarded when it is thawed.

Determination of the Appropriate Two Reference Genes

<u>Preparing BRSV samples at two time-points:</u>

- Two flasks of 75 cm^2 of BT cells 90% confluency were used.
- Cells were infected with BRSV at a m.o.i. of 0.05.
- Incubate at 33 ºC with 5% CO_2 for 2 hours.
- Discard the inoculum and rinse with 10 ml DMEM.
- Add 25 ml 2%HS/DMEM/flask.
- Incubate at 33 ºC with 5% CO_2.
- Cells were harvested and lysed at two time-points: 1 and 5 days.
- Total RNA was extracted using RNeasy Plus Mini Kit (Cat. # 74134, Qiagen).
- Using the Nanodrop, analyze the purified RNA for quantity.
- RNA was diluted to 20 ng/µl using nuclease-free water.
- Aliquot 280 µl/tube (three tubes).
- Store RNA at –80 °C.

Real-time Q-RT-PCR for determination of the two reference genes:

Use a prime PCR Custom 96-well plate with 19 genes (Cow B96 reference plate, 20X, Bio-Rad, Hercules, CA, USA). This plate includes forward and reverse primes for 19 cow genes. One half (columns # 1 - 6) of this plate will be used with BRSV sample at one day and the other half will be used with BRSV sample at 5 days.

Product: PrimePCR Custom Plate 96 Well, 19 genes
Plate Name: Cow B96 Reference Plate, Cow
Concentration: 20×
Purification: Desalted
Format: 96-wells × 20µl reactions
Item: 10025217
Instrument: CFX96
Quantity: 3

	1	2	3	4	5	6	7	8	9	10	11	12
A	ACTB	ACTB	ACTB	RPL13A	RPL13A	RPL13A	ACTB	ACTB	ACTB	RPL13A	RPL13A	RPL13A
B	AMBP	AMBP	AMBP	RPLPO	RPLPO	RPLPO	AMBP	AMBP	AMBP	RPLPO	RPLPO	RPLPO
C	G6PD	G6PD	G6PD	RPS18	RPS18	RPS18	G6PD	G6PD	G6PD	RPS18	RPS18	RPS18
D	G3PDH	G3PDH	G3PDH	TBP	TBP	TBP	G3PDH	G3PDH	G3PDH	TBP	TBP	TBP
E	GUSB	GUSB	GUSB	TFRC	TFRC	TFRC	GUSB	GUSB	GUSB	TFRC	TFRC	TFRC
F	HMBS	HMBS	HMBS	YWHAZ	YWHAZ	YWHAZ	HMBS	HMBS	HMBS	YWHAZ	YWHAZ	YWHAZ
G	HPRT1	HPRT1	HPRT1	gDNA	RQ1	RQ2	HPRT1	HPRT1	HPRT1	gDNA	RQ1	RQ2
H	PGK1	PGK1	PGK1	PCR	RT		PGK1	PGK1	PGK1	PCR	RT	

Using EXPRESS One-Step SYBR® GreenER™ Kit for one-step qRT-PCR using EXPRESS SYBR® GreenER™ qPCR SuperMixes (Cat. # 11784-200, Invitrogen, Carlsbad, CA, USA).

- Prepare the master mix:

# of reactions	Per reaction	52 + 52 = 104
EXPRESS SYBR® GreenER™ qPCR SuperMix Universal	10 µl	1040 µl
EXPRESS SuperScript® Mix for One-Step SYBR® GreenER™	0.5 µl	52 µl
RNase-Free Water	4.1 µl	426.4 µl
ROX Reference Dye (25µM)	0.4 µl	41.6 µl
BRSV Samples (Day 1 or 5)	5 µl	
Sub-Total	20 µl	1560 µl
Mix 780 µl with 260 µl of BRSV samples Day 1. Mix 780 µl with 260 µl of BRSV samples Day 5.		

- Apply 20 µl of the (1040 µl) master mixture into each well (48 wells + 4) of each half of the 96-well plate.
- Using C1000 Touch™ Thermal Cycler (Bio-Rad):

- The protocol:

Cycle **1**	1X	One step	50 ºC	For 15 minutes
Cycle **2**	1X	One step	95 ºC	For 2 minutes
Cycle **3**	40X	Step **1**	95 ºC	For 15 seconds
		Step **2**	60 ºC	For 60 seconds
		+ Plate Read		
Cycle **4**	1X	One step	4 ºC	HOLD

- Copy the data and determine reference genes.
- Glyceraldehyde 3-phosphate dehydrogenase (GAPDH) and bovine ribosomal protein S18 (RPS18) were chosen as endogenous controls to normalize all gene expression results.

Real-time Q-RT-PCR of Cellular Signals

The cellular genes (MAVS, PKR, TBK-1, NF-κB, IRF-3, IRF-7, IFN-β, and PIN-1) were detected using commercially available primer and probe sets specific for bovine genes (TaqMan Gene Expression Assays, Applied Biosystems, Foster City, CA, USA). Three wells were used for each sample. Therefore, two plates (plate 1 and 2) were used for each gene.

Step 1: *designing the Real-time Q-RT-PCR plates:*

- Plate # 1: See table 2.
- Plate # 2: See table 3.
- One well was used with water instead of RNA sample as negative control.
- One well was used for common RNA sample with the gene of the plate as positive control.
- Two wells were used with common RNA sample and the gene of the plate, but without reverse transcriptase (No-RT) as negative control.
- The reading of No-RT wells should be at least 35 cycles or no reading, indicating no detection of gDNA contamination.
- Three wells were used as inter-run calibration, using the common RNA sample with GAPDH on every single plate for all signals. Wells are H5, H6, and H7.
- Five wells were used for standard curve using dilution (0 to dilution – 4) of common RNA sample with GAPDH on every single plate for all signals. Wells are H8, H9, H10, H11, and H12.
- For other genes, use primers and probes of the gene instead of GAPDH in all wells except wells on row # H from column 5 to 12.

Step 2: *The protocol:*

Cycle **1**	1X	One step	50 ºC	For 15 minutes
Cycle **2**	1X	One step	95 ºC	For 2 minutes
Cycle **3**	40X	Step **1**	95 ºC	For 15 seconds
		Step **2**	60 ºC	For 60 seconds
		+ Plate Read		
Cycle **4**	1X	One step	4 ºC	HOLD

Step 3: *Mix the master mixtures:*

- Using 0.4 µl ROX/reaction:

# of reactions	Per reaction	190 reactions
EXPRESS SuperScript® qPCR SuperMix Universal	10 µl	1900 µl
EXPRESS SuperScript® Mix for one-Step qPCR (RT)		
RNase-Free Water	1.6 µl	304 µl
ROX Reference Dye (25µM)	0.4 µl	76 µl
GAPDH Primers and Probe (TaqMan® Gene Expression Assays)	1 µl	190 µl
Sub-Total	13 µl	2470 µl

In 0.5-ml tube, mix 65 µl (for 5 wells) of the master mixtures with 10 µl water = 75 µl → two No-RT reactions (Wells # 3-H and 4-H) for each plate.
The rest will be enough for about 180 wells (2340 µl).

# of reactions	Per reaction	180 reactions
Master mixtures	13 µl	2340 µl
EXPRESS SuperScript® Mix for one-Step qPCR (RT)	2 µl	360 µl
Total	15 µl	2700 µl

Apply 15 µl of the master mixture into labeled wells on the two 96-well plates.

- The plate should be kept in the ice box → cover the plate.
- Add 5 µl from each sample into its labeled three wells.
- Cover the plate. Take it to the real-time qRT-PCR machine.
- Leave the cover on the plate in the machine.

Step 4: *result calculation:*

The ΔCq value was calculated by normalizing each sample to the average of GAPDH and RPS18 using the equation ΔCq = Cq (target gene) – Cq ((GAPDH + RPS18) / 2). Then, ΔΔCq was calculated by subtracting the ΔCq of the control (UI at 2 HPI) sample from the ΔCq of each experimental and control sample using the equation ΔΔCq = ΔCq (a normalized sample) – ΔCq (the control sample). Lastly, the relative values to the control sample were calculated by using the formula $2^{-(\Delta\Delta Cq)}$, where the control sample = $2^{-(0)}$ = 2^0 = 1.

Genomic DNA Extraction from BT Cells

Using DNeasy Blood & Tissue Kit, (Cat. # 69504, QIAGEN).

Step 1: Preparing the BT cells

- Use a 75 cm^2 flask of NVSL-BT cells.
- Wash twice with 12 ml of PBS.
- Use 5 ml trypsin and remove it.
- Incubate for 5 – 8 minutes in the 37 °C incubator.
- Re-suspend cells with 2.6 ml PBS and transfer 1.3 ml (~ 2 million) cells to tube # 1.
- Add new 1.3 ml PBS to the flask, mix.
- Transfer 1.3 ml (~ 1 million) cells to tube # 2.
- Add new 1.3 ml PBS to the flask, mix.
- Transfer 1.3 ml (~ 0.5 million) cells to tube # 3.
- At room temperature, centrifuge the three tubes at 2,000 rpm for 5 minutes to make cell pellets.

Step 2: Preparing the mixtures

- Remove the supernatant. Re-suspend the cell pellets with 200 µl PBS.
- Add 20 µl of proteinase K.
- Add 200 µl of Buffer AL.
- Mix thoroughly by vortexing for 5 seconds.
- Incubate in 56 °C water bath for 10 minutes.
- Then, add 200 µl of absolute ethanol (99%).
- Mix thoroughly by vortexing for 5 seconds.

Step 3: Extract the genomic DNA

- Use three columns of kit # 69504 (QIAGEN) and label them as # 1 – 3.
- Transfer the mixtures (620 µl) to the columns.
- Centrifuge the three columns at 8,000 rpm for 1 minute.
- Discard the flow-through and collection tubes.
- Transfer the columns to new 2-ml tubes.
- Add 500 µl Buffer AW1.
- Centrifuge the three columns at 8,000 rpm for 1 minute.
- Discard the flow-through and collection tubes.
- Transfer the columns to new 2-ml tubes.
- Add 500 µl Buffer AW2.
- Centrifuge the three columns at 14,000 rpm for 3 minutes.
- Discard the flow-through and collection tubes.
- Transfer the columns to new 1.5-ml tubes.
- Add 100 (not 200) µl Buffer AE.
- Incubate for 1 minute.
- Centrifuge the three columns at 8,000 rpm for 1 minute.
- Close the 1.5-ml tubes (A set) which include the eluate DNA (high concentration of DNA). Label the three tubes.

- Transfer the columns to new 1.5-ml tubes.
- Add 100 (not 200) µl Buffer AE.
- Incubate for 1 minute.
- Centrifuge the three columns at 8,000 rpm for 1 minute.
- Close the 1.5-ml tubes (B set) which include the eluate DNA (low concentration of DNA). Label the three tubes.

Step 4: Measuring the quantity

- Using the Nanodrop, analyze the genomic DNA for quantity.
- Use the sample type: "DNA-50".
- Use B set tubes to dilute the DNA in A set tubes to prepare tubes with 100 ng/µl DNA.
- Store at –20 °C.
- Genomic DNA was sent to the "Active Motif" company to make plasmids, including: IRF-3, IRF-7, PKR, TBK1, and ACTB.

Plasmid Clones

Plasmids for different genes were received from different labs and companies. Plasmids were amplified in E. coli DH5α in our lab to make a stock for each plasmid.
NF-kB plasmid: pGL4.32[luc2P/NF-κB-RE/Hygro] Vector (Promega, Cat. # E8491).

Using *Escherichia coli* (DH5α) bacteria (Invitrogen, Cat. # 18265-017, store at –80 °C).

Day 1.

- Thaw the bacteria on ice. Do not touch the bottom of the bacteria tube.
- Leave the bacteria on ice for 10 – 15 minutes to thaw.
- Put a new 15-ml tube on ice.
- The plasmid concentration should not be more than 50 ng within 1 – 5 µl.
- Dilute the plasmid to 20 ng/µl.
- Transfer 60 µl of bacteria to the 15-ml tube.
- Add 2.5 µl (50 ng) plasmid and gently mix one time.
- Incubate the bacteria on ice for 30 minutes.
- Re-freeze the unused bacteria using dry ice with 70% ethanol. Store at –80 °C.
- Heat shock: at 42 °C for 30 – 40 seconds.
- This "heat shock" will increase the diameter of the pores to allow the plasmids to go inside the bacteria.
- Then incubate the bacteria on ice for 2 minutes to close the pores.
- Add 940 µl of LB broth (with no ampicillin).
- Do not tighten the lid of the 15-ml tube to allow air exchange. You can replace the lid with foil.
- Incubate the tube at 37 °C with shaking at 225 RPM for one hour in a shaking incubator.
- After the one-hour incubation, the LB broth should change from very clear to slightly cloudy (turbid).

- After this point, do not put the bacteria on ice.
- Incubate six LB plates with Ampicillin (an antibiotic) for an hour at 37 °C.
- Use two plates with 30 µl of bacteria per plate, two plates with 50 µl, and two plates with 100 µl.
- Mix 60 µl of bacteria with 140 µl new LB broth for the 30 µl of bacteria plates.
- Mix 100 µl of bacteria with 100 µl new LB broth for the 50 µl of bacteria plates.
- Incubate them at 37 °C for 10 minutes upside up, then for 14 hours (overnight) upside down with or without CO_2.
- Store the rest of the 1 ml bacteria at 4 °C for one week.

Day 2. After 14 hours

- Mix 10 ml LB broth with 100 µl Ampicillin (10µg/µl). [Final: 100 µg/ml].
- Aliquot it into four 12-ml tubes (2.5 ml/tube).
- Take (pick) one colony using a pipette tip, and put the tip inside the tube with broth.
- The best colony is a large one and separated from other colonies.
- Note: small colonies may not have the plasmid.
- Incubate the tube at 37 °C with shaking at 260 – 300 RPM for 7 – 8 hours in a shaking incubator.

- After 7 – 8 hours:
- Mix 56 ml LB broth with 560 µl Ampicillin (10 µg/µl).
- Aliquot it into four 125-ml flasks (14 ml/flask).
- Add 28 µl bacteria from one 12-ml tube into one flask. Use one flask with each tube (dilution 1:500).
- Incubate the flasks at 37 °C with shaking at 260 – 300 RPM for 18 hour (overnight) in a shaking incubator.

Day 3. After 18 hours

Use the Wizard Plus Minipreps DNA Purification System (Promega, Cat. # A7100).
- Transfer the 14 ml of each flask into 15-ml tube on ice.
- Centrifuge the four 15-ml tube at 3000 RPM for 15 minutes at 4 °C.
- Pour off the supernatant (media) completely or use vacuum.
- Resuspend the cell pellet in 400 µl of cell resuspension solution.
- Transfer the resuspended cells to a 1.5-ml tube.
- Add 400 µl of cell lysis solution and mix well by inverting the tube several times.
- Incubate for 3 – 5 minutes for efficient lysis.
- Add 400 µl of neutralization solution and mix by inverting the tube several times.
- Centrifuge the lysate at 10,000×*g* for 6 minutes.
- Using a laboratory vacuum manifold, prepare four Wizard® Miniprep Columns (syringe barrels with minicolumns).
- Pipet 1 ml of the resuspended resin into each barrel with minicolumn.
- Transfer all of the cleared lysate from 1.5-ml tubes to the miniprep column.
- Apply the vacuum.
- Add 2 ml of the Column Wash Solution (with ethanol).

- Apply the vacuum.
- Dry the resin by continuing to draw a vacuum for 30 seconds, but not longer.
- Discard the syringe and transfer the minicolumns to new 1.5-ml tubes.
- Centrifuge the minicolumn at 10,000×*g* for 2 minutes to remove any residual column wash solution.
- Transfer the minicolumns to new 1.5-ml tubes.
- Add 50 µl of nuclease-free water to each minicolumn and wait for 1 minute.
- Centrifuge the tubes (with minicolumns) at 10,000×*g* for 20 seconds to elute the plasmids.
- Discard the minicolumns.
- Using the Nanodrop, analyze the plasmid (DNA) for quantity.
- Label the tubes and store at –20 °C.

Western Blotting

Cell Harvesting from 75 cm^2 Flasks

- Completely discard media.
- Wash once with 10 ml PBS.
- Add 5 ml of 0.25% trypsin and remove 4 ml of it.
- (Optional) you can incubate at 37 °C.
- After cells detach (5 – 10 minutes) add 9 ml media (2% HS).
- Transfer 5 ml/tube into two 15-ml tubes on ice.
- Centrifuge the tubes at 2000 rpm (1900×g) 4 °C for 5 minutes.
- Completely discard the supernatant.
- Prepare RIPA with 1% Halt protease inhibitors.
- Homogenize samples for 5 seconds. Clean between samples with 70% alcohol swab.
- Transfer the samples into 1.5-ml tubes and label them.
- Store for at least 15 minutes to break bubbles at –80 °C or until they are needed.
- Take proteins (samples) out of the freezer on ice to thaw.
- Centrifuge the protein at 10,000 rpm (9,500×g) 4 °C for 5 minutes.
- Place on ice.

Protein Quantification

- In a 15-ml tube, prepare 50:1 ratio reagent A&B from BCA Pierce Kit (Pierce® BCA Protein Assay Kit (Prod # 23225, Lot # NC171236, Thermo scientific).
- Pour 200 µl of reagent mixture in each well of the 26 wells of a 96-well plate.
- Load 2 µl of each sample and standard (Albumin) into each well.
- Tap the plates gently to mix.
- Incubate at 37 °C for 20 minutes in dry or humid incubator with gentle shaking.
- Read the protein concentrations on the plate reader.

4x NUPAGE (LDS Sample buffer (4X), 10 ml, Cat. # NP0007):

Using DTT: DL-1,4-Dithiothiothreitol, for molecular biology, 1M solution in water (code: 426380100, 10 ml, Acros Organics).

- Mix 3 volume of sample + 1 volume of NUPAGE + 1x of DTT (20x).
- Pour 85 µl of sample into 1.5-ml tube.
- Add 34.3 µl of the mixture [85 + 34.3 = 119.3 µl].
- Discard the Debris (cell membranes).
- Vortex and spin for 1 second.
- Incubate samples at 70 °C for 10 minutes to denaturing proteins.
- Place samples on ice immediately for 10 – 20 minutes.
- Store at –80 °C for years.

Preparing the Western Gels

Using Pierce® ECL Western Blotting Substrate (Prod # 32106, Lot # OC182119, Thermo scientific).

- Use clean and dry glass plates (spacer plate and short plate). Place them in the clamp and then on the casting stander with gasket.
- Fill with ultrapure water (upH_2O) to make sure that there is no leaking.
- Discard the water.
- Dry plates by using filter paper.
- Mark a line 2 cm from the top of the short plate.
- Prepare the gel (8%).
- Pour the gel until the line.
- Add isopropanol on the gel to make the top of the gel equal.
- Allow to solidify for 20 – 30 minutes.
- Use filter paper to remove isopropanol.
- Pour the stacking gel.
- Insert a 10-well comb.
- Allow to solidify for 20 – 30 minutes.
- Remove the comb.
- Incubate the protein sample on ice for 30 minutes.
- Centrifuge the samples at 10,000 rpm at 4 °C for 5 minutes, then on ice.

When the gel is solidified:

- Put the solidified gel within the two glass plates on the "electrode assembly." Then in the Mini tank.
- Fill the tank with 1X running buffer with sodium bisulfite as antioxidant (5 mM final).
- Wash wells with the running buffer to make sure they are clean.
- Load 10 µl ladder in the first well, samples in their wells, and RIPA in the empty wells. Use the same amount of samples (proteins).
- Cover the Mini tank with the lid.
- Contact to the electrophoresis device.
- Start with 80 volts (Amps max).
- Once the samples reach the line between the upper and lower gels, and they are migrating in an even, well defined, and compact band, you can increase the voltage to 100 and then to 120 volts.

Transferring the Proteins from the Gel to the Membrane (Wet Transfer)

- Cut PVDF membrane (6×9 cm) and label.
- Treat it with methanol for 1 – 10 minutes (recycle methanol for one month only).
- Use a small tray with some of 1X Transfer buffer.
- Place one filter paper.
- Place the membrane onto the filter paper.
- Discard the well section of the gel (stacking gel).
- Remove the gel from the glass onto the membrane.
- Remove the air bubbles from between the gel and the membrane.
- Place another filter paper onto the gel.
- Incubate at room temperature for 5 minutes.
- Assemble the sandwiches and place it into the tank.
- Fill the tank with transfer buffer,
- Add the ice box.
- Incubate them in for 10 – 20 minutes.
- Transfer with stirring.
- Use 63 volts for 2 hours at room temperature or 22 volts overnight in cool room.

–
Black
sponge
filter paper
gel
PVDF membrane
filter paper
sponge
Clear
+

- The gel sandwich (wet transfer) order (look at the table):

-Black ← black - sponge - filter- Gel - membrane - filter - sponge - Clear → Red+

Membrane Incubation with Antibodies

1. *Block the membrane:*

The membrane needs to be blocked before adding the antibodies. Use the same solution recommended by the primary antibody datasheet.

- Wash membrane three times for 5 minutes/each with TBS-T.
- In plastic bag, put 5 ml of blocking solution and the membrane.
- Put the bag on rocker for 2 hours. Or overnight in cool room.
- Wash three times for 5 minutes/each with TBS-T.
- Wash the bag with upH_2O.

2. *Incubation with the primary antibody:*

Use primary antibody (e.g. β-Actin, # 4967S, from Cell Signaling).

- Use 5% BSA in TBS-T.
- Use 1:1000 dilution = 10 µl antibody with 10 ml 5% BSA in TBS-T solution.
- Using the same plastic bag, add diluted antibody and the membrane.
- Put the bag on rocker overnight in cool room.
- Then, wash three times for 5 minutes/each with TBS-T.
- Wash the bag with upH_2O.

3. *Incubation with the secondary antibody:*

Use secondary antibody (e.g. β-Actin, cat. # 7074S, from Cell Signaling).
- Use 5% BSA in TBS-T.
- Use 1:2400 dilution = 5 µl antibody with 12 ml 5% BSA in TBS-T solution.
- Using the same plastic bag, add 6 ml of diluted antibody and the membrane.
- Put the bag on rocker for 2 hours at room temperature.
- Then, wash three times for 5 minutes/each with TBS-T.
- Wash the bag with upH_2O.

Developing the Membrane

Use Pierce ECL Western Blotting Substrate (Prod # 32106, Lot # OC182119, Thermo scientific).
- Just before leaving to the scanning machine (VersaDoc), Mix 0.5 ml of reagent # 1 with 0.5 ml of reagent # 2.
- Take the membranes in the washing buffer to the scanning machine.
- Take the first membrane out of the washing buffer and transfer to an empty tray.
- Apply the developing solution to the membrane at least 5 times and then transfer the solution back to its tube.
- Put the developed membrane in the scanning machine (VersaDoc).
- To check that the membrane is in the right place, click on "Preview".
- Change the time: 10, 20, 30, 40, 50, 60, 70, 80 seconds.
- Click on "Acquire", name the file, and wait.
- When you see the image, click on "file", then Transfer to your file.
- In the end, use your flash memory (USP) to transfer your result to your computer.

Image J

Use the Image J program to calculate the density of the bands:
- Open the program.
- File → Open → then, open you file.
- Choose your first band and locate it.

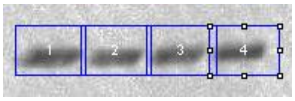

- Label the first band as # 1 by clicking "analyze" then "Gels" then "Select First Lane".
- Use the arrows to locate the second band.
- Label the second band as # 2 by clicking "analyze" then "Gels" then "Select Next Lane".
- Use the arrows to locate the third band.
- Label the third band as # 3 by clicking "analyze" then "Gels" then "Select Next Lane".
- When you end, click "analyze" then "Gels" then "Plot Lanes".
- Make lines between the background and the rest.
- Use the 'Wand Tool" to calculate the bands.
- Transfer the results to Excel and make your figure.

Table 1: BVDV and BRSV isolation microtiter assay:

Immunoperoxidase Staining for BVDV-1 & 2
Enzyme-Linked Immunosorbent Assay (ELISA)

# of Plates		1	**2**	3	**4**	5	**6**	7	**8**	9	**10**
mAb*	Binding Buffer	6 ml	**10 ml**	15 ml	**20 ml**	25 ml	**30 ml**	35 ml	**40 ml**	45 ml	**50 ml**
	348[#] (or 8G12[¶])	6 µl	**10 µl**	15 µl	**20 µl**	25 µl	**30 µl**	35 µl	**40 µl**	45µl	**50 µl**
Biotinylated Horse α-mouse Ig	Binding Buffer	2 ml	**4 ml**	6 ml	**8 ml**	10 ml	**12 ml**	14 ml	**16 ml**	18ml	**20 ml**
	Chicken Serum	3 ml	**6 ml**	9 ml	**12 ml**	15 ml	**18 ml**	21 ml	**24 ml**	27 ml	**30 ml**
	Biotinylated horse α-mouse Ig	25 µl	**50 µl**	75 µl	**100µl**	125µl	**150µl**	175µl	**200µl**	225µl	**250µl**
HRP-Streptavidin	Binding Buffer	5 ml	**10 ml**	15 ml	**20 ml**	25 ml	**30 ml**	35 ml	**40 ml**	45 ml	**50 ml**
	HRP-Streptavidin	10 µl	**20 µl**	30 µl	**40 µl**	50 µl	**60 µl**	70 µl	**80 µl**	90 µl	**100µl**
AEC	Substrate Buffer	5 ml	**10 ml**	15 ml	**20 ml**	25 ml	**30 ml**	35 ml	**40 ml**	45 ml	**50 ml**
	3% H_2O_2 Solution	20 µl	**40 µl**	60 µl	**80 µl**	100 µl	**120µl**	140µl	**160µl**	180µl	**200µl**
	AEC Solution	0.3ml	**0.6ml**	0.9ml	**1.2ml**	1.5ml	**1.8ml**	2.1ml	**2.4ml**	2.7ml	**3 ml**

* Final dilution of monoclonal antibody (mAb) is 1:1000

[#] Primary Monoclonal antibody (mAb 348) directed against BVDV-1 & BVDV-2 E2 (gp53).

[¶] Primary Monoclonal antibody (mAb 8G12) directed against BRSV F protein.

Table 2: Real-time Q-RT-PCR designed plate of cellular signals:

Detecting the GAPDH mRNA: Q-RT-PCR plate # 1.

#1	1	2	3	4	5	6	7	8	9	10	11	12
A	U.I. Time # 1	U.I. Time # 1	U.I. Time # 1	U.I. Time # 2	U.I. Time # 2	U.I. Time # 2	U.I. Time # 3	U.I. Time # 3	U.I. Time # 3	U.I. Time # 4	U.I. Time # 4	U.I. Time # 4
B	Poly I:C Time # 1	Poly I:C Time # 1	Poly I:C Time # 1	Poly I:C Time # 2	Poly I:C Time # 2	Poly I:C Time # 2	Poly I:C Time # 3	Poly I:C Time # 3	Poly I:C Time # 3	Poly I:C Time # 4	Poly I:C Time # 4	Poly I:C Time # 4
C	BVDV-wt Time # 1	BVDV-wt Time # 1	BVDV-wt Time # 1	BVDV-wt Time # 2	BVDV-wt Time # 2	BVDV-wt Time # 2	BVDV-wt Time # 3	BVDV-wt Time # 3	BVDV-wt Time # 3	BVDV-wt Time # 4	BVDV-wt Time # 4	BVDV-wt Time # 4
D	BVDV-EGFP Time # 1	BVDV-EGFP Time # 1	BVDV-EGFP Time # 1	BVDV-EGFP Time # 2	BVDV-EGFP Time # 2	BVDV-EGFP Time # 2	BVDV-EGFP Time # 3	BVDV-EGFP Time # 3	BVDV-EGFP Time # 3	BVDV-EGFP Time # 4	BVDV-EGFP Time # 4	BVDV-EGFP Time # 4
E	BRSV Time # 1	BRSV Time # 1	BRSV Time # 1	BRSV Time # 2	BRSV Time # 2	BRSV Time # 2	BRSV Time # 3	BRSV Time # 3	BRSV Time # 3	BRSV Time # 4	BRSV Time # 4	BRSV Time # 4
F	BVDV-wt/BRSV Time # 1	BVDV-wt/BRSV Time # 1	BVDV-wt/BRSV Time # 1	BVDV-wt/BRSV Time # 2	BVDV-wt/BRSV Time # 2	BVDV-wt/BRSV Time # 2	BVDV-wt/BRSV Time # 3	BVDV-wt/BRSV Time # 3	BVDV-wt/BRSV Time # 3	BVDV-wt/BRSV Time # 4	BVDV-wt/BRSV Time # 4	BVDV-wt/BRSV Time # 4
G	BVDV-EGFP/BRSV Time # 1	BVDV-EGFP/BRSV Time # 1	BVDV-EGFP/BRSV Time # 1	BVDV-EGFP/BRSV Time # 2	BVDV-EGFP/BRSV Time # 2	BVDV-EGFP/BRSV Time # 2	BVDV-EGFP/BRSV Time # 3	BVDV-EGFP/BRSV Time # 3	BVDV-EGFP/BRSV Time # 3	BVDV-EGFP/BRSV Time # 4	BVDV-EGFP/BRSV Time # 4	BVDV-EGFP/BRSV Time # 4
H	15 µl + 5 µl Water	C.S. + RT U.I. GAPDH	C.S. No-RT U.I. GAPDH	C.S. No-RT U.I. GAPDH	Com. Sam. U.I. GAPDH	Com. Sam. U.I. GAPDH	Com. Sam. U.I. GAPDH	Com. Sam. U.I. - 0 GAPDH	Com. Sam. U.I. - 1 GAPDH	Com. Sam. U.I. - 2 GAPDH	Com. Sam. U.I. - 3 GAPDH	Com. Sam. U.I. - 4 GAPDH

Com. Sam. = the common samples; C.S. + RT = the common samples with reverse transcriptase; C.S. No-RT = the common samples without reverse transcriptase.
The H5, H6, and H7 wells are used in every single Q-RT-PCR plate of every single gene as inter-run calibration, using the same common samples and GAPDH primers and probe throughout the experiment.
The H8, H9, H10, H11, and H12 wells are used for standard curve without any change throughout the experiment.

Table 3: Real-time Q-RT-PCR designed plate of cellular signals:

Detecting the GAPDH mRNA: Q-RT-PCR plate # 2.

#2	1	2	3	4	5	6	7	8	9	10	11	12
A	U.I. Time # 5	U.I. Time # 5	U.I. Time # 5	U.I. Time # 6	U.I. Time # 6	U.I. Time # 6	U.I. Time # 7	U.I. Time # 7	U.I. Time # 7	Empty	Empty	Empty
B	Poly I:C Time # 5	Poly I:C Time # 5	Poly I:C Time # 5	Poly I:C Time # 6	Poly I:C Time # 6	Poly I:C Time # 6	Poly I:C Time # 7	Poly I:C Time # 7	Poly I:C Time # 7	Empty	Empty	Empty
C	BVDV-wt Time # 5	BVDV-wt Time # 5	BVDV-wt Time # 5	BVDV-wt Time # 6	BVDV-wt Time # 6	BVDV-wt Time # 6	BVDV-wt Time # 7	BVDV-wt Time # 7	BVDV-wt Time # 7	Empty	Empty	Empty
D	BVDV-EGFP Time # 5	BVDV-EGFP Time # 5	BVDV-EGFP Time # 5	BVDV-EGFP Time # 6	BVDV-EGFP Time # 6	BVDV-EGFP Time # 6	BVDV-EGFP Time # 7	BVDV-EGFP Time # 7	BVDV-EGFP Time # 7	Empty	Empty	Empty
E	BRSV Time # 5	BRSV Time # 5	BRSV Time # 5	BRSV Time # 6	BRSV Time # 6	BRSV Time # 6	BRSV Time # 7	BRSV Time # 7	BRSV Time # 7	Empty	Empty	Empty
F	BVDV-wt/BRSV Time # 5	BVDV-wt/BRSV Time # 5	BVDV-wt/BRSV Time # 5	BVDV-wt/BRSV Time # 6	BVDV-wt/BRSV Time # 6	BVDV-wt/BRSV Time # 6	BVDV-wt/BRSV Time # 7	BVDV-wt/BRSV Time # 7	BVDV-wt/BRSV Time # 7	Empty	Empty	Empty
G	BVDV-EGFP/BRSV Time # 5	BVDV-EGFP/BRSV Time # 5	BVDV-EGFP/BRSV Time # 5	BVDV-EGFP/BRSV Time # 6	BVDV-EGFP/BRSV Time # 6	BVDV-EGFP/BRSV Time # 6	BVDV-EGFP/BRSV Time # 7	BVDV-EGFP/BRSV Time # 7	BVDV-EGFP/BRSV Time # 7	Empty	Empty	Empty
H	15 µl + 5 µl Water	C.S. + RT U.I. GAPDH	C.S. No-RT U.I. GAPDH	C.S. No-RT U.I. GAPDH	Com. Sam. U.I. GAPDH	Com. Sam. U.I. GAPDH	Com. Sam. U.I. GAPDH	Com. Sam. U.I. - 0 GAPDH	Com. Sam. U.I. - 1 GAPDH	Com. Sam. U.I. - 2 GAPDH	Com. Sam. U.I. - 3 GAPDH	Com. Sam. U.I. - 4 GAPDH

Com. Sam. = the common samples; C.S. + RT = the common samples with reverse transcriptase; C.S. No-RT = the common samples without reverse transcriptase.
The H5, H6, and H7 wells are used in every single Q-RT-PCR plate of every single gene as inter-run calibration, using the same common samples and GAPDH primers and probe throughout the experiment.
The H8, H9, H10, H11, and H12 wells are used for standard curve without any change throughout the experiment.

BIBLIOGRAPHY

Adler, B., Adler, H., Pfister, H., Jungi, T.W., Peterhans, E., 1997. Macrophages infected with cytopathic bovine viral diarrhea virus release a factor(s) capable of priming uninfected macrophages for activation-induced apoptosis. J Virol 71(4):3255-8.

Achenbach, J.E., Topliff, C.L., Vassilev, V.B., Donis, R.O., Eskridge, K.M., Kelling, C.L., 2004. Detection and quantitation of bovine respiratory syncytial virus using real-time quantitative RT-PCR and quantitative competitive RT-PCR assays. J Virol Methods 121(1):1-6.

Akhtar, L.N., Benveniste, E.N., 2011. Viral exploitation of host SOCS protein functions. J Virol 85(5):1912-21.

Alexopoulou, L., Holt, A.C., Medzhitov, R., Flavell, R.A., 2001. Recognition of double-stranded RNA and activation of NF-kappaB by Toll-like receptor 3. Nature 413(6857):732-8.

Alkheraif, A.A., Topliff, C.L., Reddy, J., Massilamany, C., Donis, R.O., Meyers, G., Eskridge, K.M., Kelling, C.L., 2017. Type 2 BVDV N(pro) suppresses IFN-1 pathway signaling in bovine cells and augments BRSV replication. Virology 507:123-34.

Ames, T.R., 1986. The causative agent of BVD: its epidemiology and pathogenesis. Vet Med 81:848-69.

Baigent, S.J., Goodbourn, S., McCauley, J.W., 2004. Differential activation of interferon regulatory factors-3 and -7 by non-cytopathogenic and cytopathogenic bovine viral diarrhoea virus. Vet Immunol Immunopathol 100(3-4):135-44.

Baigent, S.J., Zhang, G., Fray, M.D., Flick-Smith, H., Goodbourn, S., McCauley, J.W., 2002. Inhibition of beta interferon transcription by noncytopathogenic bovine viral diarrhea virus is through an interferon regulatory factor 3-dependent mechanism. J Virol 76(18):8979-88.

Baker, J.C., 1995. The clinical manifestations of bovine viral diarrhea infection. Vet Clin North Am Food Anim Pract 11(3):425-45.

Barber, D.M., Nettleton, P.F., Herring, J.A., 1985. Disease in a dairy herd associated with the introduction and spread of bovine virus diarrhoea virus. Vet Rec 117(18):459-64.

Bartlett, N.W., Buttigieg, K., Kotenko, S.V., Smith, G.L., 2005. Murine interferon lambdas (type III interferons) exhibit potent antiviral activity in vivo in a poxvirus infection model. J Gen Virol 86(Pt 6):1589-96.

Bauhofer, O., Summerfield, A., McCullough, K.C., Ruggli, N., 2005. Role of double-stranded RNA and Npro of classical swine fever virus in the activation of monocyte-derived dendritic cells. Virology 343(1):93-105.

Bautista, E.M., Ferman, G.S., Gregg, D., Brum, M.C., Grubman, M.J., Golde, W.T., 2005. Constitutive expression of alpha interferon by skin dendritic cells confers resistance to infection by foot-and-mouth disease virus. J Virol 79(8):4838-47.

Becher, P., Orlich, M., König, M., Thiel, H.J., 1999. Nonhomologous RNA recombination in bovine viral diarrhea virus: molecular characterization of a variety of subgenomic RNAs isolated during an outbreak of fatal mucosal disease. J Virol 73(7):5646-53.

Becher, P., Orlich, M., Thiel, H.J., 2001. RNA recombination between persisting pestivirus and a vaccine strain: generation of cytopathogenic virus and induction of lethal disease. J Virol 75(14):6256-64.

Beer, M., Wolf, G., Pichler, J., Wolfmeyer, A., Kaaden, O.R., 1997. Cytotoxic T-lymphocyte responses in cattle infected with bovine viral diarrhea virus. Vet Microbiol 58(1):9-22.

Belák, S., Ballagi-Pordány, A., 1991. Bovine viral diarrhea virus infection: rapid diagnosis by the polymerase chain reaction. Arch Virol Suppl 3:181-90.

Belknap, E.B., Collins, J.K., Larsen, R.S., Conrad, K.P., 2000. Bovine viral diarrhea virus in New World camelids. J Vet Diagn Invest 12(6):568-70.

Bendfeldt, S., Grummer, B., Greiser-Wilke, I., 2003. No caspase activation but overexpression of Bcl-2 in bovine cells infected with noncytopathic bovine virus diarrhoea virus. Vet Microbiol 96(4):313-26.

Bhudevi, B., Weinstock, D., 2001. Fluorogenic RT-PCR assay (TaqMan) for detection and classification of bovine viral diarrhea virus. Vet Microbiol 83(1):1-10.

Bielefeldt-Ohmann, H., 1983. Pathogenesis of bovine viral diarrhea-mucosal disease: distribution and significance of BVDV antigen in diseased calves. Res Vet Sci 34:5-10.

Bielefeldt-Ohmann, H., 1987. Double-immunolabeling systems for phenotyping of immune cells harboring bovine viral diarrhea virus. J Histochem Cytochem 35(6):627-33.

Bielefeldt-Ohmann, H., 1988. BVD virus antigens in tissues of persistently viraemic, clinically normal cattle: implications for the pathogenesis of clinically fatal disease. Acta Vet Scand 29(1):77-84.

Bielefeldt-Ohmann, H., 1995. The pathologies of bovine viral diarrhea virus infection. A window on the pathogenesis. Vet Clin North Am Food Anim Pract 11(3):447-76.

Biron, C.A., 2001. Interferons alpha and beta as immune regulators--a new look. Immunity 14(6):661-4.

Blount, R.E., Morris, J.A., Savage, R.E., 1956. Recovery of cytopathogenic agent from chimpanzees with coryza. Proc Soc Exp Biol Med 92(3):544-9.

Bogdan, C., 2000. The function of type I interferons in antimicrobial immunity. Curr Opin Immunol 12(4):419-24.

Bolin, S.R., 1990. The current understanding about the pathogenesis and clinical forms of BVD. Vet. Med 85:1124-32.

Bolin, S.R., 1995a. Control of bovine viral diarrhea infection by use of vaccination. Vet Clin North Am Food Anim Pract 11(3):615-25.

Bolin, S.R., 1995b. The pathogenesis of mucosal disease. Vet Clin North Am Food Anim Pract 11(3):489-500.

Bolin, S.R., McClurkin, A.W., Cutlip, R.C., Coria, M.F., 1985a. Response of cattle persistently infected with noncytopathic bovine viral diarrhea virus to vaccination for bovine viral diarrhea and to subsequent challenge exposure with cytopathic bovine viral diarrhea virus. Am J Vet Res 46(12):2467-70.

Bolin, S.R., McClurkin, A.W., Cutlip, R.C., Coria, M.F., 1985b. Severe clinical disease induced in cattle persistently infected with noncytopathic bovine viral diarrhea virus by superinfection with cytopathic bovine viral diarrhea virus. Am J Vet Res 46(3):573-6.

Bollini, M., Leal, E.S., Adler, N.S., Aucar, M.G., Fernández, G.A., Pascual, M.J., Merwaiss, F., Alvarez, D.E., Cavasotto, C.N., 2018. Discovery of novel bovine viral diarrhea inhibitors using structure-based virtual screening on the envelope protein E2. Front Chem 6:79.

Booker, C.W., Abutarbush, S.M., Morley, P.S., Guichon, P.T., Wildman, B.K., Jim, G.K., Schunicht, O.C., Pittman, T.J., Perrett, T., Ellis, J.A., Appleyard, G., Haines, D.M., 2008. The effect of bovine viral diarrhea virus infections on health and performance of feedlot cattle. Can Vet J 49(3):253-60.

Bossert, B., Conzelmann, K.K., 2002. Respiratory syncytial virus (RSV) nonstructural (NS) proteins as host range determinants: a chimeric bovine RSV with NS genes from human RSV is attenuated in interferon-competent bovine cells. J Virol 76(9):4287-93.

Bossert, B., Marozin, S., Conzelmann, K.K., 2003. Nonstructural proteins NS1 and NS2 of bovine respiratory syncytial virus block activation of interferon regulatory factor 3. J Virol 77(16):8661-8.

Boxus, M., Letellier, C., Kerkhofs, P., 2005. Real Time RT-PCR for the detection and quantitation of bovine respiratory syncytial virus. J Virol Methods 125(2):125-30.

Brock, K.V., 2004. Strategies for the control and prevention of bovine viral diarrhea virus. Vet Clin North Am Food Anim Pract 20(1):171-80.

Brodersen, B.W., Kelling, C.L., 1998. Effect of concurrent experimentally induced bovine respiratory syncytial virus and bovine viral diarrhea virus infection on respiratory tract and enteric diseases in calves. Am J Vet Res 59(11):1423-30.

Brownlie, J., 1990a. Pathogenesis of mucosal disease and molecular aspects of bovine virus diarrhoea virus. Vet Microbiol 23(1-4):371-82.

Brownlie, J., 1990b. The pathogenesis of bovine virus diarrhoea virus infections. Rev Sci Tech 9(1):43-59.

Brownlie, J., Clarke, M.C., Howard, C.J., 1984. Experimental production of fatal mucosal disease in cattle. Vet Rec 114(22):535-6.

Bryson, D.G., McNulty, M.S., Logan, E.F., Cush, P.F., 1983. Respiratory syncytial virus pneumonia in young calves: clinical and pathologic findings. Am J Vet Res 44(9):1648-55.

Caidi, H., Miao, C., Thornburg, N.J., Tripp, R.A., Anderson, L.J., Haynes, L.M., 2018. Anti-respiratory syncytial virus (RSV) G monoclonal antibodies reduce lung inflammation and viral lung titers when delivered therapeutically in a BALB/c mouse model. Antiviral Res 154:149-57.

Caldas, L.A., Freitas, T.R.P., Azevedo, R.C., de Souza, W., 2018. Prostaglandin A(1) inhibits the replication of bovine viral diarrhea virus. Braz J Microbiol. pii: S1517-8382(17)30910-3.

Carman, S., van Dreumel, T., Ridpath, J., Hazlett, M., Alves, D., Dubovi, E., Tremblay, R., Bolin, S., Godkin, A., Anderson, N., 1998. Severe acute bovine viral diarrhea in Ontario, 1993-1995. J Vet Diagn Invest 10(1):27-35.

Castelli, J.C., Hassel, B.A., Wood, K.A., Li, X.L., Amemiya, K., Dalakas, M.C., Torrence, P.F., Youle, R.J., 1997. A study of the interferon antiviral mechanism: apoptosis activation by the 2-5A system. J Exp Med 186(6):967-72.

Chanock, R., Roizman, B., Myers, R., 1957. Recovery from infants with respiratory illness of a virus related to chimpanzee coryza agent (CCA). I. Isolation, properties and characterization. Am J Hyg 66(3):281-90.

Chapman, J.R., Waldenström, J., 2015. With reference to reference genes: a systematic review of endogenous controls in gene expression studies. PLoS One 10(11):e0141853.

Charleston, B., Brackenbury, L.S., Carr, B.V., Fray, M.D., Hope, J.C., Howard, C.J., Morrison, W.I., 2002. Alpha/beta and gamma interferons are induced by infection with noncytopathic bovine viral diarrhea virus in vivo. J Virol 76(2):923-7.

Chawla-Sarkar, M., Lindner, D.J., Liu, Y.F., Williams, B.R., Sen, G.C., Silverman, R.H., Borden, E.C., 2003. Apoptosis and interferons: role of interferon-stimulated genes as mediators of apoptosis. Apoptosis 8(3):237-49.

Chen, Z., Rijnbrand, R., Jangra, R.K., Devaraj, S.G., Qu, L., Ma, Y., Lemon, S.M., Li, K., 2007. Ubiquitination and proteasomal degradation of interferon regulatory factor-3 induced by Npro from a cytopathic bovine viral diarrhea virus. Virology 366(2):277-92.

Clemens, M.J., Elia, A., 1997. The double-stranded RNA-dependent protein kinase PKR: structure and function. J Interferon Cytokine Res 17(9):503-24.

Cockcroft, P.D., Dornin, L.E., Lambert, R.C., Perry, J., Reichel, M.P., 2015. Serological survey for antibodies against bovine viral diarrhoea virus and Neospora caninum in a population of South Australian alpacas (Vicugna pacos). Aust Vet J 93(12):476-8.

Colitti, B., Nogarol, C., Bertolotti, L., Rosati, S., 2018. Complete genome sequence of bovine viral diarrhea virus subgenotype 2a strain CN10.2015.821, isolated in Piedmont, Italy. Genome Announc 6(11).

Collett, M.S., Larson, R., Belzer, S.K., Retzel, E., 1988. Proteins encoded by bovine viral diarrhea virus: the genomic organization of a pestivirus. Virology 165(1):200-8.

Collett, M.S., Wiskerchen, M., Welniak, E., Belzer, S.K., 1991. Bovine viral diarrhea virus genomic organization. Arch Virol Suppl 3:19-27

Confer, A.W., Fulton, R.W., Step, D.L., Johnson, B.J., Ridpath, J.F., 2005. Viral antigen distribution in the respiratory tract of cattle persistently infected with bovine viral diarrhea virus subtype 2a. Vet Pathol 42(2):192-9.

Cornish, T.E., van Olphen, A.L., Cavender, J.L., Edwards, J.M., Jaeger, P.T., Vieyra, L.L., Woodard, L.F., Miller, D.R., O'Toole, D., 2005. Comparison of ear notch immunohistochemistry, ear notch antigen-capture ELISA, and buffy coat virus isolation for detection of calves persistently infected with bovine viral diarrhea virus. J Vet Diagn Invest 17(2):110-7.

Dabak, M., Karapinar, T., Gulacti, I., Bulut, H., Kizil, O., Aydin, S., 2007. Hemorrhagic syndrome-like disease in calves with bovine viral diarrhea and mucosal disease complex. J Vet Intern Med 21(3):514-8.

den Hartog, G., Jacobino, S., Bont, L., Cox, L., Ulfman, L.H., Leusen, J.H., van Neerven, R.J., 2014. Specificity and effector functions of human RSV-specific IgG from bovine milk. PLoS One 9(11):e112047.

Deregt, D., van Rijn, P.A., Wiens, T.Y., van den Hurk, J., 1998. Monoclonal antibodies to the E2 protein of a new genotype (type 2) of bovine viral diarrhea virus define three antigenic domains involved in neutralization. Virus Res 57(2):171-81.

Dittmer, K.E., Hinkson, J.A., Dwyer, C., Adlington, B., van Andel, M., 2018. Prevalence of Candidatus Mycoplasma haemolamae, bovine viral diarrhoea virus, and gastrointestinal parasitism in a sample of adult New Zealand alpaca (Vicugna pacos). N Z Vet J 66(1):9-15.

Done, J.T., Terlecki, S., Richardson, C., Harkness, J.W., Sands, J.J., Patterson, D.S., Sweasey, D., Shaw, I.G., Winkler, C.E., Duffell, S.J., 1980. Bovine virus diarrhoea-mucosal disease virus: pathogenicity for the fetal calf following maternal infection. Vet Rec 106(23):473-9.

Donis, R.O., Corapi, W., Dubovi, E.J., 1988. Neutralizing monoclonal antibodies to bovine viral diarrhoea virus bind to the 56K to 58K glycoprotein. J Gen Virol 69 (Pt 1):77-86.

Duffell, S.J., Harkness, J.W., 1985. Bovine virus diarrhoea-mucosal disease infection in cattle. Vet Rec 117(10):240-5.

Edmondson, M.A., Givens, M.D., Walz, P.H., Gard, J.A., Stringfellow, D.A., Carson, R.L., 2007. Comparison of tests for detection of bovine viral diarrhea virus in diagnostic samples. J Vet Diagn Invest 19(4):376-81.

Evans, C.A., Hemmatzadeh, F., Reichel, M.P., Cockcroft, P.D., 2018. Natural transmission of bovine viral diarrhoea virus-1c from a persistently infected neonate lamb to naïve sheep and cattle. Vet Rec 182(12):352.

Foster, G.R., Masri, S.H., David, R., Jones, M., Datta, A., Lombardi, G., Runkell, L., de Dios, C., Sizing, I., James, M.J., Marelli-Berg, F.M., 2004. IFN-alpha subtypes differentially affect human T cell motility. J Immunol 173(3):1663-70.

Fray, M.D., Mann, G.E., Charleston, B., 2001. Validation of an Mx/CAT reporter gene assay for the quantification of bovine type-I interferon. J Immunol Methods 249(1-2):235-44.

Fredericksen, F., Carrasco, G., Villalba, M., Olavarría, V.H., 2015. Cytopathic BVDV-1 strain induces immune marker production in bovine cells through the NF-κB signaling pathway. Mol Immunol 68(2 Pt A):213-22.

Fredericksen, F., Villalba, M., Olavarría, V.H., 2016. Characterization of bovine A20 gene: Expression mediated by NF-κB pathway in MDBK cells infected with bovine viral diarrhea virus-1. Gene 581(2):117-29.

Fredriksen, B., Press, C.M., Løken, T., Odegaard, S.A., 1999. Distribution of viral antigen in uterus, placenta and foetus of cattle persistently infected with bovine virus diarrhoea virus. Vet Microbiol 64(2-3):109-22.

Fritzemeier, J., Greiser-Wilke, I., Haas, L., Pituco, E., Moennig, V., Liess, B., 1995. Experimentally induced "late-onset" mucosal disease--characterization of the cytopathogenic viruses isolated. Vet Microbiol 46(1-3):285-94.

Fritzemeier, J., Haas, L., Liebler, E., Moennig, V., Greiser-Wilke, I., 1997. The development of early vs. late onset mucosal disease is a consequence of two different pathogenic mechanisms. Arch Virol 142(7):1335-50.

Frölich, K., Hofmann, M., 1995. Isolation of bovine viral diarrhea virus-like pestiviruses from roe deer (Capreolus capreolus). J Wildl Dis 31(2):243-6.

Fulton, R.W., Briggs, R.E., Ridpath, J.F., Saliki, J.T., Confer, A.W., Payton, M.E., Duff, G.C., Step, D.L., Walker, D.A., 2005. Transmission of bovine viral diarrhea virus 1b to susceptible and vaccinated calves by exposure to persistently infected calves. Can J Vet Res 69(3):161-9.

Fulton, R.W., Cook, B.J., Step, D.L., Confer, A.W., Saliki, J.T., Payton, M.E., Burge, L.J., Welsh, R.D., Blood, K.S., 2002a. Evaluation of health status of calves and the impact on feedlot performance: assessment of a retained ownership program for postweaning calves. Can J Vet Res 66(3):173-80.

Fulton, R.W., Ridpath, J.F., Saliki, J.T., Briggs, R.E., Confer, A.W., Burge, L.J., Purdy, C.W., Loan, R.W., Duff, G.C., Payton, M.E., 2002b. Bovine viral diarrhea virus (BVDV) 1b: predominant BVDV subtype in calves with respiratory disease. Can J Vet Res 66(3):181-90.

Gabel, F., Wang, D., Madern, D., Sadler, A., Dayie, K., Daryoush, M.Z., Schwahn, D., Zaccai, G., Lee, X., Williams, B.R., 2006. Dynamic flexibility of double-stranded RNA activated PKR in solution. J Mol Biol 359(3):610-23.

Gabriele, L., Ozato, K., 2007. The role of the interferon regulatory factor (IRF) family in dendritic cell development and function. Cytokine Growth Factor Rev 18(5-6):503-10.

Gagea, M.I., Bateman, K.G., Shanahan, R.A., van Dreumel, T., McEwen, B.J., Carman, S., Archambault, M., Caswell, J.L., 2006. Naturally occurring Mycoplasma bovis-associated pneumonia and polyarthritis in feedlot beef calves. J Vet Diagn Invest 18(1):29-40.

García-Sastre, A., Biron, C.A., 2006. Type 1 interferons and the virus-host relationship: a lesson in détente. Science 312(5775):879-82.

García, M.A., Gil, J., Ventoso, I., Guerra, S., Domingo, E., Rivas, C., Esteban, M., 2006. Impact of protein kinase PKR in cell biology: from antiviral to antiproliferative action. Microbiol Mol Biol Rev 70(4):1032-60.

García, M.A., Meurs, E.F., Esteban, M., 2007. The dsRNA protein kinase PKR: virus and cell control. Biochimie 89(6-7):799-811.

Gard, J.A., Givens, M.D., Stringfellow, D.A., 2007. Bovine viral diarrhea virus (BVDV): epidemiologic concerns relative to semen and embryos. Theriogenology 68(3):434-42.

Gershwin, L.J., 2012. Immunology of bovine respiratory syncytial virus infection of cattle. Comp Immunol Microbiol Infect Dis 35(3):253-7.

Gil, J., Esteban, M., 2000. Induction of apoptosis by the dsRNA-dependent protein kinase (PKR): mechanism of action. Apoptosis 5(2):107-14.

Gil, L.H., Ansari, I.H., Vassilev, V., Liang, D., Lai, V.C., Zhong, W., Hong, Z., Dubovi, E.J., Donis, R.O., 2006a. The amino-terminal domain of bovine viral diarrhea virus Npro protein is necessary for alpha/beta interferon antagonism. J Virol 80(2):900-11.

Gil, L.H., van Olphen, A.L., Mittal, S.K., Donis, R.O., 2006b. Modulation of PKR activity in cells infected by bovine viral diarrhea virus. Virus Res 116(1-2):69-77.

Givens, M.D., Heath, A.M., Brock, K.V., Brodersen, B.W., Carson, R.L., Stringfellow, D.A., 2003. Detection of bovine viral diarrhea virus in semen obtained after inoculation of seronegative postpubertal bulls. Am J Vet Res 64(4):428-34.

Glew, E.J., Carr, B.V., Brackenbury, L.S., Hope, J.C., Charleston, B., Howard, C.J., 2003. Differential effects of bovine viral diarrhoea virus on monocytes and dendritic cells. J Gen Virol 84(Pt 7):1771-80.

Gottipati, K., Holthauzen, L.M., Ruggli, N., Choi, K.H., 2016. Pestivirus Npro directly interacts with interferon regulatory factor 3 monomer and dimer. J Virol 90(17):7740-7.

Greiser-Wilke, I., Dittmar, K.E., Liess, B., Moennig, V., 1992. Heterogeneous expression of the non-structural protein p80/p125 in cells infected with different pestiviruses. J Gen Virol 73(Pt 1):47-52.

Grummer, B., Moennig, V., Greiser-Wilke, I., 1998. Cytopathogenic bovine viral diarrhea viruses induce apoptosis in bovine cell cultures. Dtsch Tierarztl Wochenschr 105(1):29-31.

Guzman, E., Taylor, G., 2015. Immunology of bovine respiratory syncytial virus in calves. Mol Immunol 66(1):48-56.

Hägglund, S., Hu, K., Vargmar, K., Poré, L., Olofson, A.S., Blodörn, K., Anderson, J., Ahooghalandari, P., Pringle, J., Taylor, G., Valarcher, J.F., 2011. Bovine respiratory syncytial virus ISCOMs-Immunity, protection and safety in young conventional calves. Vaccine 29(47):8719-30.

Hansen, T.R., Smirnova, N.P., Webb, B.T., Bielefeldt-Ohmann, H., Sacco, R.E., Van Campen, H., 2015. Innate and adaptive immune responses to in utero infection with bovine viral diarrhea virus. Anim Health Res Rev 16(1):15-26.

Harding, M.J., Cao, X., Shams, H., Johnson, A.F., Vassilev, V.B., Gil, L.H., Wheeler, D.W., Haines, D., Sibert, G.J., Nelson, L.D., Campos, M., Donis, R.O., 2002. Role of bovine viral diarrhea virus biotype in the establishment of fetal infections. Am J Vet Res 63(10):1455-63.

Hellemans, J., Mortier, G., De Paepe, A., Speleman, F., Vandesompele, J., 2007. qBase relative quantification framework and software for management and automated analysis of real-time quantitative PCR data. Genome Biol 8(2):R19.

Henningson, J.N., Steffen, D.J., Topliff, C.L., Kurth, K.L., Dubielzig, R.R., Brodersen, B.W., Bedenice, D., Eskridge, K.M., Callan, R.J., Reggiardo, C., Rupp, G.P., Kelling, C.L., 2013. Systemic distribution of viral antigen in alpacas persistently infected with bovine pestivirus. Vet Pathol 50(2):308-17.

Henningson, J.N., Topliff, C.L., Gil, L.H., Donis, R.O., Steffen, D.J., Charleston, B., Eskridge, K.M., Kelling, C.L., 2009. Effect of the viral protein N(pro) on virulence of bovine viral diarrhea virus and induction of interferon type I in calves. Am J Vet Res 70(9):1117-23.

Hertig, C., Pauli, U., Zanoni, R., Peterhans, E., 1991. Detection of bovine viral diarrhea (BVD) virus using the polymerase chain reaction. Vet Microbiol 26(1-2):65-76.

Hewicker, M., Wöhrmann, T., Fernandez, A., Trautwein, G., Liess, B., Moennig, V., 1990. Immunohistological detection of bovine viral diarrhoea virus antigen in the central nervous system of persistently infected cattle using monoclonal antibodies. Vet Microbiol 23(1-4):203-10.

Hewicker-Trautwein, M., Trautwein, G., 1994. Porencephaly, hydranencephaly and leukoencephalopathy in ovine fetuses following transplacental infection with bovine virus diarrhoea virus: distribution of viral antigen and characterization of cellular response. Acta Neuropathol 87(4):385-97.

Hiscott, J., Pitha, P., Genin, P., Nguyen, H., Heylbroeck, C., Mamane, Y., Algarte, M., Lin, R., 1999. Triggering the interferon response: the role of IRF-3 transcription factor. J Interferon Cytokine Res 19(1):1-13.

Hilton, L., Moganeradj, K., Zhang, G., Chen, Y.H., Randall, R.E., McCauley, J.W., Goodbourn, S., 2006. The N^{pro} product of bovine viral diarrhea virus inhibits DNA binding by interferon regulatory factor 3 and targets it for proteasomal degradation. J Virol 80(23):11723-32.

Hoff, H.S., Donis, R.O., 1997. Induction of apoptosis and cleavage of poly (ADP-ribose) polymerase by cytopathic bovine viral diarrhea virus infection. Virus Res 49(1):101-13.

Honda, K., Taniguchi, T., 2006. IRFs: master regulators of signalling by Toll-like receptors and cytosolic pattern-recognition receptors. Nat Rev Immunol 6(9):644-58.

Honda, K., Yanai, H., Takaoka, A., Taniguchi, T., 2005. Regulation of the type I IFN induction: a current view. Int Immunol. 17(11):1367-78.

Horscroft, N., Bellows, D., Ansari, I., Lai, V.C., Dempsey, S., Liang, D., Donis, R., Zhong, W., Hong, Z., 2005. Establishment of a subgenomic replicon for bovine viral diarrhea virus in Huh-7 cells and modulation of interferon-regulated factor 3-mediated antiviral response. J Virol 79(5):2788-96.

Houe, H., 1993. Survivorship of animals persistently infected with bovine virus diarrhea virus (BVDV). Prev Vet Med 15:275-83.

Houe, H., 1995. Epidemiology of bovine viral diarrhea virus. Vet Clin North Am Food Anim Pract 11(3):521-47.

Houe, H., 1999. Epidemiological features and economical importance of bovine viral diarrhoea virus (BVDV) infections. Vet Microbiol 64(2-3):89-107.

Houe, H., 2003. Economic impact of BVDV infection in dairies. Biologicals 31(2):137-43.

Hsu, W.L., Chen, C.L., Huang, S.W., Wu, C.C., Chen, I.H., Nadar, M., Su, Y.P., Tsai, C.H., 2014. The untranslated regions of classic swine fever virus RNA trigger apoptosis. PLoS One 9(2):e88863.

Huang, Y.T., Wertz, G.W., 1982. The genome of respiratory syncytial virus is a negative-stranded RNA that codes for at least seven mRNA species. J Virol 43(1):150-7.

Jacobs, J.L., Coyne, C.B., 2013. Mechanisms of MAVS regulation at the mitochondrial membrane. J Mol Biol 425(24):5009-19.

Jacobs, J.L., Zhu, J., Sarkar, S.N., Coyne, C.B., 2014. Regulation of mitochondrial antiviral signaling (MAVS) expression and signaling by the mitochondria-associated endoplasmic reticulum membrane (MAM) protein Gp78. J Biol Chem 289(3):1604-16.

Jamaluddin, M., Casola, A., Garofalo, R.P., Han, Y., Elliott, T., Ogra, P.L., Brasier, A.R., 1998. The major component of IkappaBalpha proteolysis occurs independently of the proteasome pathway in respiratory syncytial virus-infected pulmonary epithelial cells. J Virol 72(6):4849-57.

Jego, G., Palucka, A.K., Blanck, J.P., Chalouni, C., Pascual, V., Banchereau, J., 2003. Plasmacytoid dendritic cells induce plasma cell differentiation through type I interferon and interleukin 6. Immunity 19(2):225-34.

Jordan, R., Wang, L., Graczyk, T.M., Block, T.M., Romano, P.R., 2002. Replication of a cytopathic strain of bovine viral diarrhea virus activates PERK and induces endoplasmic reticulum stress-mediated apoptosis of MDBK cells. J Virol 76(19):9588-99.

Kelling, C.L., 2004. Evolution of bovine viral diarrhea virus vaccines. Vet Clin North Am Food Anim Pract 20(1):115-29.

Kelling, C.L., Grotelueschen, D.M., Smith, D.R., Brodersen, B.W., 2000. Testing and management strategies for effective beef and dairy herd BVDV biosecurity programs. The Bovine Pract 34(1):13-22.

Kelling, C.L., Hunsaker, B.D., Steffen, D.J., Topliff, C.L., Abdelmagid, O.Y., Eskridge, K.M., 2005. Characterization of protection from systemic infection and disease by use of a modified-live noncytopathic bovine viral diarrhea virus type 1 vaccine in experimentally infected calves. Am J Vet Res 66(10):1785-91.

Kelling, C.L., Steffen, D.J., Cooper, V.L., Higuchi, D.S., Eskridge, K.M., 2002a. Effect of infection with bovine viral diarrhea virus alone, bovine rotavirus alone, or concurrent infection with both on enteric disease in gnotobiotic neonatal calves. Am J Vet Res 63(8):1179-86.

Kelling, C.L., Steffen, D.J., Topliff, C.L., Eskridge, K.M., Donis, R.O., Higuchi, D.S., 2002b. Comparative virulence of isolates of bovine viral diarrhea virus type II in experimentally inoculated six- to nine-month-old calves. Am J Vet Res 63(10):1379-84.

Kimman, T.G., Straver, P.J., Zimmer, G.M., 1989. Pathogenesis of naturally acquired bovine respiratory syncytial virus infection in calves: morphologic and serologic findings. Am J Vet Res 50(5):684-93.

Kirkbride, C.A., 1992. Etiologic agents detected in a 10-year study of bovine abortions and stillbirths. J Vet Diagn Invest 4(2):175-80.

Kirkland, P.D., Mackintosh, S.G., Moyle, A., 1994. The outcome of widespread use of semen from a bull persistently infected with pestivirus. Vet Rec 135(22):527-9.

Kotenko, S.V., Gallagher, G., Baurin, V.V., Lewis-Antes, A., Shen, M., Shah, N.K., Langer, J.A., Sheikh, F., Dickensheets, H., Donnelly, R.P., 2003. IFN-lambdas mediate antiviral protection through a distinct class II cytokine receptor complex. Nat Immunol 4(1):69-77.

Kotla, S., Gustin, K.E., 2015. Proteolysis of MDA5 and IPS-1 is not required for inhibition of the type I IFN response by poliovirus. Virol J 12:158.

Lai, V.C., Zhong, W., Skelton, A., Ingravallo, P., Vassilev, V., Donis, R.O., Hong, Z., Lau, J.Y., 2000. Generation and characterization of a hepatitis C virus NS3 protease-dependent bovine viral diarrhea virus. J Virol 74(14):6339-47.

Lambot, M., Hanon, E., Lecomte, C., Hamers, C., Letesson, J.J., Pastoret, P.P., 1998. Bovine viral diarrhoea virus induces apoptosis in blood mononuclear cells by a mechanism largely dependent on monocytes. J Gen Virol 79(Pt 7):1745-9.

Le Bon, A., Etchart, N., Rossmann, C., Ashton, M., Hou, S., Gewert, D., Borrow, P., Tough, D.F., 2003. Cross-priming of CD8+ T cells stimulated by virus-induced type I interferon. Nat Immunol 4(10):1009-15.

Lee, S.B., Rodríguez, D., Rodríguez, J.R., Esteban, M., 1997. The apoptosis pathway triggered by the interferon-induced protein kinase PKR requires the third basic domain, initiates upstream of Bcl-2, and involves ICE-like proteases. Virology 231(1):81-8.

Lerch, R.A., Stott, E.J., Wertz, G.W., 1989. Characterization of bovine respiratory syncytial virus proteins and mRNAs and generation of cDNA clones to the viral mRNAs. J Virol 63(2):833-40.

Liebler-Tenorio, E.M., Lanwehr, A., Greiser-Wilke, I., Loehr, B.I., Pohlenz, J., 2000. Comparative investigation of tissue alterations and distribution of BVD-viral antigen in cattle with early onset versus late onset mucosal disease. Vet Microbiol 77(1-2):163-74.

Liebler-Tenorio, E.M., Ridpath, J.E., Neill, J.D., 2004. Distribution of viral antigen and tissue lesions in persistent and acute infection with the homologous strain of noncytopathic bovine viral diarrhea virus. J Vet Diagn Invest 16(5):388-96.

Liess, B., Moennig, V., 1990. Ruminant pestivirus infection in pigs. Rev Sci Tech 9(1):151-61.

Litinskiy, M.B., Nardelli, B., Hilbert, D.M., He, B., Schaffer, A., Casali, P., Cerutti, A., 2002. DCs induce CD40-independent immunoglobulin class switching through BLyS and APRIL. Nat Immunol 3(9):822-9.

Løken, T., 1995. Ruminant pestivirus infections in animals other than cattle and sheep. Vet Clin North Am Food Anim Pract 11(3):597-614.

Loneragan, G.H., Thomson, D.U., Montgomery, D.L., Mason, G.L., Larson, R.L., 2005. Prevalence, outcome, and health consequences associated with persistent infection with bovine viral diarrhea virus in feedlot cattle. J Am Vet Med Assoc 226(4):595-601.

Lopez, O.J., Osorio, F.A., Kelling, C.L., Donis, R.O., 1993. Presence of bovine viral diarrhoea virus in lymphoid cell populations of persistently infected cattle. J Gen Virol 74 (Pt 5):925-9.

Lussi, C., Schweizer, M., 2016. What can pestiviral endonucleases teach us about innate immunotolerance? Cytokine Growth Factor Rev 29:53-62.

Mahlum, C.E., Haugerud, S., Shivers, J.L., Rossow, K.D., Goyal, S.M., Collins, J.E., Faaberg, K.S., 2002. Detection of bovine viral diarrhea virus by TaqMan reverse transcription polymerase chain reaction. J Vet Diagn Invest 14(2):120-5.

Mahony, R., Ahmed, S., Diskin, C., Stevenson, N.J., 2016. SOCS3 revisited: a broad regulator of disease, now ready for therapeutic use? Cell Mol Life Sci 73(17):3323-36.

Mallipeddi, S.K., Samal, S.K., 1993. Analysis of the ovine respiratory syncytial virus (RSV) G glycoprotein gene defines a subgroup of ungulate RSV. J Gen Virol 74(Pt 12):2787-91.

Malmquist, W.A., 1968. Bovine viral diarrhea-mucosal disease: Etiology, pathogenesis and applied immunity. J Am Vet Med Assoc 152:763-8.

Marshall, D.J., Moxley, R.A., Kelling, C.L., 1996. Distribution of virus and viral antigen in specific pathogen-free calves following inoculation with noncytopathic bovine viral diarrhea virus. Vet Pathol 33(3):311-8.

Meurs, E., Chong, K., Galabru, J., Thomas, N.S., Kerr, I.M., Williams, B.R., Hovanessian, A.G., 1990. Molecular cloning and characterization of the human double-stranded RNA-activated protein kinase induced by interferon. Cell 62(2):379-90.

McClurkin, A.W., Littledike, E.T., Cutlip, R.C., Frank, G.H., Coria, M.F., Bolin, S.R., 1984. Production of cattle immunotolerant to bovine viral diarrhea virus. Can J Comp Med 48(2):156-61.

McGill, J.L., Kelly, S.M., Kumar, P., Speckhart, S., Haughney, S.L., Henningson, J., Narasimhan, B., Sacco, R.E., 2018. Efficacy of mucosal polyanhydride nanovaccine against respiratory syncytial virus infection in the neonatal calf. Sci Rep 8(1):3021.

McGoldrick, A., Bensaude, E., Ibata, G., Sharp, G., Paton, D.J., 1999. Closed one-tube reverse transcription nested polymerase chain reaction for the detection of pestiviral RNA with fluorescent probes. J Virol Methods 79(1):85-95.

Mendez, E., Ruggli, N., Collett, M.S., Rice, C.M., 1998. Infectious bovine viral diarrhea virus (strain NADL) RNA from stable cDNA clones: a cellular insert determines NS3 production and viral cytopathogenicity. J Virol 72(6):4737-45.

Menzo, S., Bagnarelli, P., Giacca, M., Manzin, A., Varaldo, P.E., Clementi, M., 1992. Absolute quantitation of viremia in human immunodeficiency virus infection by competitive reverse transcription and polymerase chain reaction. J Clin Microbiol 30(7):1752-7.

Meyers, G., Thiel, H.J., 1996. Molecular characterization of pestiviruses. Adv Virus Res 47:53-118.

Mitra, N., Cernicchiaro, N., Torres, S., Li, F., Hause, BM., 2016. Metagenomic characterization of the virome associated with bovine respiratory disease in feedlot cattle identified novel viruses and suggests an etiologic role for influenza D virus. J Gen Virol 97(8):1771-84.

Moennig, V., Eicken, K., Flebbe, U., Frey, H.R., Grummer, B., Haas, L., Greiser-Wilke, I., Liess, B., 2005. Implementation of two-step vaccination in the control of bovine viral diarrhoea (BVD). Prev Vet Med 72(1-2):109-14.

Moennig, V., Frey, H.R., Liebler, E., Pohlenz, J., Liess, B., 1990. Reproduction of mucosal disease with cytopathogenic bovine viral diarrhoea virus selected in vitro. Vet Rec 127(8):200-3.

Moerman, A., Straver, P.J., de Jong, M.C., Quak, J., Baanvinger, T., van Oirschot, J.T., 1994. Clinical consequences of a bovine virus diarrhoea virus infection in a dairy herd: a longitudinal study. Vet Q 16(2):115-9.

Montgomery, D.L., 2007. Distribution and cellular heterogeneity of bovine viral diarrhea viral antigen expression in the brain of persistently infected calves: a new perspective. Vet Pathol 44(5):643-54.

Munder, M., Mallo, M., Eichmann, K., Modolell, M., 1998. Murine macrophages secrete interferon gamma upon combined stimulation with interleukin (IL)-12 and IL-18: A novel pathway of autocrine macrophage activation. J Exp Med 187(12):2103-8.

Muñoz-Zanzi, C.A., Hietala, S.K., Thurmond, M.C., Johnson, W.O., 2003. Quantification, risk factors, and health impact of natural congenital infection with bovine viral diarrhea virus in dairy calves. Am J Vet Res 64(3):358-65. Erratum in: Am J Vet Res 64(5):568.

Murphy, F.A., Famfuet, C.M., Bishop, D.H.L., Ghabrial, S.A., Jarvis, A.W., Martelli, G.P., Mayo, M.A., Summers, M.D., 1995. Virus Taxonomy, Sixth report on taxonomy of the international committee on taxonomy of viruses. Archives of Virology. Supplement 10.

Niskanen, R., Alenius, S., Belák, K., Baule, C., Belák, S., Voges, H., Gustafsson, H., 2002. Insemination of susceptible heifers with semen from a non-viraemic bull with persistent bovine virus diarrhoea virus infection localized in the testes. Reprod Domest Anim 37(3):171-5.

Nogarol, C., Decaro, N., Bertolotti, L., Colitti, B., Iotti, B., Petrini, S., Lucente, M.S., Elia, G., Perona, G., Profiti, M., Buonavoglia, C., Rosati, S., 2017. Pestivirus infection in cattle dairy farms: E2 glycoprotein ELISA reveals the presence of bovine viral diarrhea virus type 2 in northwestern Italy. BMC Vet Res 13(1):377.

Oberst, R.D., Hays, M.P., Evermann, J.F., Kelling, C.L., 1993. Characteristic differences in reverse transcription-polymerase chain reaction products of ovine, bovine, and human respiratory syncytial viruses. J Vet Diagn Invest 5(3):322-8.

Olafson, P., MacCallum, A.D., Fox, F.H., 1946. An apparently new transmissible disease of cattle. Cornell Vet 36:205-13.

Onomoto, K., Jogi, M., Yoo, J.S., Narita, R., Morimoto, S., Takemura, A., Sambhara, S., Kawaguchi, A., Osari, S., Nagata, K., et al., 2012. Critical role of an antiviral stress granule containing RIG-I and PKR in viral detection and innate immunity. PLoS One 7:e43031.

Ophuis, R.J., Morrissy, C.J., Boyle, D.B., 2006. Detection and quantitative pathogenesis study of classical swine fever virus using a real time RT-PCR assay. J Virol Methods 131(1):78-85.

Osburn, B.I., Castrucci, G., 1991. Diaplacental infections with ruminant pestiviruses. Arch Virol Suppl 3:71-8.

Otsuka, M., Kato, N., Moriyama, M., Taniguchi, H., Wang, Y., Dharel, N., Kawabe, T., Omata, M., 2005. Interaction between the HCV NS3 protein and the host TBK1 protein leads to inhibition of cellular antiviral responses. Hepatology 41(5):1004-12.

Paccaud, M.F., Jacquier, C., 1970. A respiratory syncytial virus of bovine origin. Arch Gesamte Virusforsch 30(4):327-42.

Palomares, R.A., Walz, H.G., Brock, K.V., 2013. Expression of type I interferon-induced antiviral state and pro-apoptosis markers during experimental infection with low or high virulence bovine viral diarrhea virus in beef calves. Virus Res 173(2):260-9.

Paquette, R.L., Hsu, N., Said, J., Mohammed, M., Rao, N.P., Shih, G., Schiller, G., Sawyers, C., Glaspy, J.A., 2002. Interferon-alpha induces dendritic cell differentiation of CML mononuclear cells in vitro and in vivo. Leukemia 16(8):1484-9.

Pascual, M.J., Merwaiss, F., Leal, E., Quintana, M.E., Capozzo, A.V., Cavasotto, C.N., Bollini, M., Alvarez, D.E., 2018. Structure-based drug design for envelope protein E2 uncovers a new class of bovine viral diarrhea inhibitors that block virus entry. Antiviral Res 149:179-90.

Pathak, V.K., Schindler, D., Hershey, J.W., 1988. Generation of a mutant form of protein synthesis initiation factor eIF-2 lacking the site of phosphorylation by eIF-2 kinases. Mol Cell Biol 8(2):993-5.

Paton, D.J., Brockman, S., Wood, L., 1990. Insemination of susceptible and preimmunized cattle with bovine viral diarrhoea virus infected semen. Br Vet J 146(2):171-4.

Pellerin, C., van den Hurk, J., Lecomte, J., Tussen, P., 1994. Identification of a new group of bovine viral diarrhea virus strains associated with severe outbreaks and high mortalities. Virology 203(2):260-8.

Perler, L., Schweizer, M., Jungi, T.W., Peterhans, E., 2000. Bovine viral diarrhoea virus and bovine herpesvirus-1 prime uninfected macrophages for lipopolysaccharide-triggered apoptosis by interferon-dependent and –independent pathways. J Gen Virol 81(Pt 4):881-7.

Peterhans, E., Schweizer, M., 2013. BVDV: a pestivirus inducing tolerance of the innate immune response. Biologicals 41(1):39-51.

Philippou, S., Otto, P., Reinhold, P., Elschner, M., Streckert, H.J., 2000. Respiratory syncytial virus-induced chronic bronchiolitis in experimentally infected calves. Virchows Arch 436(6):617-21.

Pollock, N., Taylor, G., Jobe, F., Guzman, E., 2017. Modulation of the transcription factor NF-κB in antigen-presenting cells by bovine respiratory syncytial virus small hydrophobic protein. J Gen Virol 98(7):1587-99.

Qi, F., Ridpath, J.F., Lewis, T., Bolin, S.R., Berry, E.S., 1992. Analysis of the bovine viral diarrhea virus genome for possible cellular insertions. Virology 189(1):285-92.

Raizman, E.A., Pogranichniy, R., Lévy, M., Negron, M., Langohr, I., Van Alstine, W., 2009. Experimental infection of white-tailed deer fawns (Odocoileus virginianus) with bovine viral diarrhea virus type-1 isolated from free-ranging white-tailed deer. J Wildl Dis 45(3):653-60.

Ridpath, J., 2010. The contribution of infections with bovine viral diarrhea viruses to bovine respiratory disease. Vet Clin North Am Food Anim Pract 26(2):335-48.

Ridpath, J.F., Bolin, S.R., 1995. Delayed onset postvaccinal mucosal disease as a result of genetic recombination between genotype 1 and genotype 2 BVDV. Virology 212(1):259-62.

Ridpath, J.F., Bolin, S.R., 1998. Differentiation of types 1a, 1b and 2 bovine viral diarrhea virus (BVDV) by PCR. Mol Cell Probes 12(2):101-6.

Ridpath, J.F., Bolin, S.R., Dubovi, E.J., 1994. Segregation of bovine viral diarrhea virus into genotypes. Virology 205(1):66-74.

Roberts, N.J. Jr, Douglas, R.G. Jr, Simons, R.M., Diamond, M.E., 1979. Virus-induced interferon production by human macrophages. J Immunol 123(1):365-9.

Rogge, L., D'Ambrosio, D., Biffi, M., Penna, G., Minetti, L.J., Presky, D.H., Adorini, L., Sinigaglia, F., 1998. The role of Stat4 in species-specific regulation of Th cell development by type I IFNs. J Immunol 161(12):6567-74.

Ruggli, N., Tratschin, J.D., Schweizer, M., McCullough, K.C., Hofmann, M.A., Summerfield, A., 2003. Classical swine fever virus interferes with cellular antiviral defense: evidence for a novel function of N(pro). J Virol 77(13):7645-54.

Rumenapf, T., Stark, R., Heimann, M., Thiel, H.J., 1998. N-terminal protease of pestiviruses: identification of putative catalytic residues by site-directed mutagenesis. J Virol 72(3):2544-7.

Sacco, R.E., McGill, J.L., Pillatzki, A.E., Palmer, M.V., Ackermann, M.R., 2014. Respiratory syncytial virus infection in cattle. Vet Pathol 51(2):427-36.

Saitoh, T., Tun-Kyi, A., Ryo, A., Yamamoto, M., Finn, G., Fujita, T., Akira, S., Yamamoto, N., Lu, K.P., Yamaoka, S., 2006. Negative regulation of interferon-regulatory factor 3-dependent innate antiviral response by the prolyl isomerase Pin1. Nat Immunol 7(6):598-605.

Saliki, J.T., Dubovi, E.J., 2004. Laboratory diagnosis of bovine viral diarrhea virus infections. Vet Clin North Am Food Anim Pract 20(1):69-83.

Samson, H.C., Topliff, C.L., Donis, R.O., Kelling, C.L., 2011. Comparison of viral replication and IFN response in alpaca and bovine cells following bovine viral diarrhea virus infection. Virology 413(1):111-7.

Sandvik, T., 2005. Selection and use of laboratory diagnostic assays in BVD control programmes. Prev Vet Med 72(1-2):3-16.

Sato, K., Hida, S., Takayanagi, H., Yokochi, T., Kayagaki, N., Takeda, K., Yagita, H., Okumura, K., Tanaka, N., Taniguchi, T., Ogasawara, K., 2001. Antiviral response by natural killer cells through TRAIL gene induction by IFN-alpha/beta. Eur J Immunol 31(11):3138-46.

Schlender, J., Bossert, B., Buchholz, U., Conzelmann, K.K., 2000. Bovine respiratory syncytial virus nonstructural proteins NS1 and NS2 cooperatively antagonize alpha/beta interferon-induced antiviral response. J Virol 74(18):8234-42.

Schroeder, B.A., Balassu-Chan, T.C., 1990. Specific sequence amplification of bovine viral diarrhoea virus nucleic acid. Arch Virol 111(3-4):239-46.

Schmitt, B.J., Lopez, O.J., Ridpath, J.F., Galeota-Wheeler, J., Osorio, F.A., 1994. Evaluation of PCR for diagnosis of bovine viral diarrhea virus in tissue homogenates. J Vet Diagn Invest 6(1):44-7.

Schweizer, M., Peterhans, E., 1999. Oxidative stress in cells infected with bovine viral diarrhoea virus: a crucial step in the induction of apoptosis. J Gen Virol 80(Pt 5):1147-55.

Schweizer, M., Peterhans, E., 2001. Noncytopathic bovine viral diarrhea virus inhibits double-stranded RNA-induced apoptosis and interferon synthesis. J Virol 75(10):4692-8.

Seago, J., Hilton, L., Reid, E., Doceul, V., Jeyatheesan, J., Moganeradj, K., McCauley, J., Charleston, B., Goodbourn, S., 2007. The N^{pro} product of classical swine fever virus and bovine viral diarrhea virus uses a conserved mechanism to target interferon regulatory factor-3. J Gen Virol 88(Pt 11):3002-6.

Sharan, R.N., Vaiphei, S.T., Nongrum, S., Keppen, J., Ksoo, M., 2015. Consensus reference gene(s) for gene expression studies in human cancers: end of the tunnel visible? Cell Oncol (Dordr) 38(6):419-31.

Shin, T., Acland, H., 2001. Tissue distribution of bovine viral diarrhea virus antigens in persistently infected cattle. J Vet Sci 2(2):81-4.

Silveira, S., Falkenberg, S.M., Elderbrook, M.J., Sondgeroth, K.S., Dassanayake, R.P., Neill, J.D., Ridpath, J.F., Canal, C.W., 2018. Serological survey for antibodies against pestiviruses in Wyoming domestic sheep. Vet Microbiol 219:96-9.

Simmonds, P., Becher, P., Bukh, J., Gould, E.A., Meyers, G., Monath, T., Muerhoff, S., Pletnev, A., Rico-Hesse, R., Smith, D.B., Stapleton, J.T., ICTV Report Consortium. 2017. ICTV Virus Taxonomy Profile: *Flaviviridae*. J Gen Virol 98(1):2-3.

Smirnova, N.P., Bielefeldt-Ohmann, H., Van Campen, H., Austin, K.J., Han, H., Montgomery, D.L., Shoemaker, M.L., van Olphen, A.L., Hansen, T.R., 2008. Acute non-cytopathic bovine viral diarrhea virus infection induces pronounced type I interferon response in pregnant cows and fetuses. Virus Res 132(1-2):49-58.

Smirnova, N.P., Webb, B.T., McGill, J.L., Schaut, R.G., Bielefeldt-Ohmann, H., Van Campen, H., Sacco, R.E., Hansen, T.R., 2014. Induction of interferon-gamma and downstream pathways during establishment of fetal persistent infection with bovine viral diarrhea virus. Virus Res 183:95-106.

Smith, D.B., Meyers, G., Bukh, J., Gould, E.A., Monath, T., Scott Muerhoff, A., Pletnev, A., Rico-Hesse, R., Stapleton, J.T., Simmonds, P., Becher, P., 2017. Proposed revision to the taxonomy of the genus Pestivirus, family *Flaviviridae*. J Gen Virol 98(8):2106-12.

Snowder, G.D., Van Vleck, L.D., Cundiff, L.V., Bennett, G.L., 2006. Bovine respiratory disease in feedlot cattle: environmental, genetic, and economic factors. J Anim Sci 84(8):1999-2008.

Stark, R., Meyers, G., Rümenapf, T., Thiel, H.J., 1993. Processing of Pestivirus polyprotein: cleavage site between autoprotease and nucleocapsid protein of classical swine fever virus. J Virol 67(12):7088-95

Steck, F., Lazary, S., Fey, H., Wandeler, A., Huggler, C., Oppliger, G., Baumberger, H., Kaderli, R., Martig, J., 1980. Immune responsiveness in cattle fatally affected by bovine virus diarrhea-mucosal disease. Zentralbl Veterinarmed B 27(6):429-45.

St-Louis, M.C., Massie, B., Archambault, D., 2005. The bovine viral diarrhea virus (BVDV) NS3 protein, when expressed alone in mammalian cells, induces apoptosis which correlates with caspase-8 and caspase-9 activation. Vet Res 36(2):213-27.

Stoffregen, B., Bolin, S.R., Ridpath, J.F., Pohlenz, J., 2000. Morphologic lesions in type 2 BVDV infections experimentally induced by strain BVDV2-1373 recovered from a field case. Vet Microbiol 77(1-2):157-62.

Stokstad, M., Løken, T., 2002. Pestivirus in cattle: experimentally induced persistent infection in calves. J Vet Med B Infect Dis Vet Public Health 49(10):494-501.

Tajima, M., Kirisawa, R., Taguchi, M., Iwai, H., Kawakami, Y., Hagiwara, K., Ohtsuka, H., Sentsui, H., 1995. Takahashi K. Attempt to discriminate between bovine viral-diarrhoea virus strains using polymerase chain reaction. Zentralbl Veterinarmed B 42(5):257-65.

Taniguchi, T., Ogasawara, K., Takaoka, A., Tanaka, N., 2001. IRF family of transcription factors as regulators of host defense. Annu Rev Immunol 19:623-55.

Tautz, N., Tews, B.A., Meyers, G., 2015. The Molecular Biology of Pestiviruses. Adv Virus Res 93:47-160.

Tautz, N., Thiel, H.J., Dubovi, E.J., Meyers, G., 1994. Pathogenesis of mucosal disease: a cytopathogenic pestivirus generated by an internal deletion. J Virol 68(5):3289-97.

Taylor, G., Wyld, S., Valarcher, J.F., Guzman, E., Thom, M., Widdison, S., Buchholz, U.J., 2014. Recombinant bovine respiratory syncytial virus with deletion of the SH gene induces increased apoptosis and pro-inflammatory cytokines in vitro, and is attenuated and induces protective immunity in calves. J Gen Virol 95(Pt 6):1244-54.

Taylor, K.E., Mossman, K.L., 2013. Recent advances in understanding viral evasion of type I interferon. Immunology 138(3):190-7.

Taylor, S.S., Haste, N.M., Ghosh, G., 2005. PKR and eIF2alpha: integration of kinase dimerization, activation, and substrate docking. Cell 122(6):823-5.

Thiel, H.J., Stark, R., Weiland, E., Rümenapf, T., Meyers, G., 1991. Hog cholera virus: molecular composition of virions from a pestivirus. J Virol 65(9):4705-12.

Thwaites, R.S., Coates, M., Ito, K., Ghazaly, M., Feather, C., Abdulla, F., Tunstall, T., Jain, P., Cass, L., Rapeport, G., Hansel, T.T., Nadel, S., Openshaw, P.J., 2018. Reduced Nasal Viral Load and IFN Responses in Infants with RSV Bronchiolitis and Respiratory Failure. Am J Respir Crit Care Med. doi: 10.1164/rccm.201712-2567OC.

Topliff, C.L., Alkheraif, A.A., Kuszynski, C.A., Davis, W.C., Steffen, D.J., Schmitz, J.A., Eskridge, K.M., Charleston, B., Henningson, J.N., Kelling, C.L., 2017. Experimental acute infection of alpacas with bovine viral diarrhea virus 1 subgenotype b alters peripheral blood and GALT leukocyte subsets. J Vet Diagn Invest 29(2):186-192.

Topliff, C.L., Kelling, C.L., 1998. Virulence markers in the 5' untranslated region of genotype 2 bovine viral diarrhea virus isolates. Virology 250(1):164-72.

Topliff, C.L., Smith, D.R., Clowser, S.L., Steffen, D.J., Henningson, J.N., Brodersen, B.W., Bedenice, D., Callan, R.J., Reggiardo, C., Kurth, K.L., Kelling, C.L., 2009. Prevalence of bovine viral diarrhea virus infections in alpacas in the United States. J Am Vet Med Assoc 234(4):519-29.

Tough, D.F., 2004. Type I interferon as a link between innate and adaptive immunity through dendritic cell stimulation. Leuk Lymphoma 45(2):257-64.

Tratschin, J.D., Moser, C., Ruggli, N., Hofmann, M.A., 1998. Classical swine fever virus leader proteinase Npro is not required for viral replication in cell culture. J Virol 72(9):7681-4.

Tsukimoto, A., Sugiyama, R., Abe, M., Nishitsuji, H., Shimizu, Y., Shimotohno, K., Kawai, G., Takaku, H., 2015. A new role for PGA1 in inhibiting hepatitis C virus-IRES-mediated translation by targeting viral translation factors. Antiviral Res 117:1-9.

Valarcher, J.F., Furze, J., Wyld, S., Cook, R., Conzelmann, K.K., Taylor, G., 2003. Role of alpha/beta interferons in the attenuation and immunogenicity of recombinant bovine respiratory syncytial viruses lacking NS proteins. J Virol 77(15):8426-39.

Valarcher, J.F., Taylor, G., 2007. Bovine respiratory syncytial virus infection. Vet Res 38(2):153-80.

Van der Poel, W.H., Kramps, J.A., Middel, W.G., Van Oirschot, J.T., Brand, A., 1993. Dynamics of bovine respiratory syncytial virus infections: a longitudinal epidemiological study in dairy herds. Arch Virol 133(3-4):309-21.

Villalba, M., Fredericksen, F., Otth, C., Olavarría, V., 2016. Transcriptomic analysis of responses to cytopathic bovine viral diarrhea virus-1 (BVDV-1) infection in MDBK cells. Mol Immunol 71:192-202.

Villalba, M., Fredericksen, F., Otth, C., Olavarría, V.H., 2017. Molecular characterization of the bovine IER3 gene: Down-regulation of IL-8 by blocking NF-κB activity mediated by IER3 overexpression in MDBK cells infected with bovine viral diarrhea virus-1. Mol Immunol 92:169-79.

Walz, P.H., Bell, T.G., Grooms, D.L., Kaiser, L., Maes, R.K., Baker, J.C., 2001. Platelet aggregation responses and virus isolation from platelets in calves experimentally infected with type I or type II bovine viral diarrhea virus. Can J Vet Res 65(4):241-7.

Wang, C., Pflugheber, J., Sumpter, R. Jr, Sodora, D.L., Hui, D., Sen, G.C., Gale, M. Jr., 2003. Alpha interferon induces distinct translational control programs to suppress hepatitis C virus RNA replication. J Virol 77(7):3898-912.

Wengler, G., 1991. Family *Flaviviridae*. In: Francki, R.I.B., Fauquet, C.M., Knudson, D.L., Brown, F. (Eds.), Classification and Nomenclature of Viruses. Fifth Report of the International Committee on Taxonomy of Viruses. Springer, Berlin. 223-33.

Wong, A.H., Tam, N.W., Yang, Y.L., Cuddihy, A.R., Li, S., Kirchhoff, S., Hauser, H., Decker, T., Koromilas, A.E., 1997. Physical association between STAT1 and the interferon-inducible protein kinase PKR and implications for interferon and double-stranded RNA signaling pathways. EMBO J 16(6):1291-304.

Wu, H., Zhang, X., Liu, C., Liu, D., Liu, J., Wang, G., Tian, J., Qu, L., 2016. Molecular cloning and functional characterization of feline MAVS. Immunol Res 64(1):82-92.

Xia, C., Dan, W., Wen-Xue, W., Jian-Qing, W., Li, W., Tian-Yao, Y., Qin, W., Yi-Bao, N., 2005. Cloning and expression of interferon-alpha/gamma from a domestic porcine breed and its effect on classical swine fever virus. Vet Immunol Immunopathol 104(1-2):81-9.

Yamane, D., Kato, K., Tohya, Y., Akashi, H., 2006. The double-stranded RNA-induced apoptosis pathway is involved in the cytopathogenicity of cytopathogenic Bovine viral diarrhea virus. J Gen Virol 87(Pt 10):2961-70.

Yamane, D., Kato, K., Tohya, Y., Akashi, H., 2008. The relationship between the viral RNA level and upregulation of innate immunity in spleen of cattle persistently infected with bovine viral diarrhea virus. Vet Microbiol 129(1-2):69-79.

Yamane, D., Nagai, M., Ogawa, Y., Tohya, Y., Akashi, H., 2005. Enhancement of apoptosis via an extrinsic factor, TNF-alpha, in cells infected with cytopathic bovine viral diarrhea virus. Microbes Infect 7(15):1482-91.

Yeşilbağ, K., Güngör, B., 2009. Antibody prevalence against respiratory viruses in sheep and goats in North-Western Turkey. Trop Anim Health Prod 41(4):421-5.

Yoneyama, M., Onomoto, K., Jogi, M., Akaboshi, T., Fujita, T., 2015. Viral RNA detection by RIG-I-like receptors. Curr Opin Immunol 32:48-53.

Zhang, G., Aldridge, S., Clarke, M.C., McCauley, J.W., 1996. Cell death induced by cytopathic bovine viral diarrhoea virus is mediated by apoptosis. J Gen Virol 77 (Pt 8):1677-81.

Zhang, P., Wu, S., Li, L., Liang, Z., Li, Y., Feng, L., Huang, X., 2013. Adjuvant PIKA protects hepatoma cells from dengue virus infection by promoting a TBK-1-dependent innate immune response. Arch Virol 158(4):829-38.

Zhang, X., Diraviyam, T., Li, X., Yao, G., Michael, A., 2016. Preparation of chicken IgY against recombinant E2 protein of bovine viral diarrhea virus (BVDV) and development of ELISA and ICA for BVDV detection. Biosci Biotechnol Biochem 80(12):2467-72.

Zhao, W., 2013. Negative regulation of TBK1-mediated antiviral immunity. FEBS Lett 587(6):542-8.

Zheng, J., Yang, P., Tang, Y., Pan, Z., Zhao, D., 2015. Respiratory syncytial virus nonstructural proteins upregulate SOCS1 and SOCS3 in the different manner from endogenous IFN signaling. J Immunol Res 738547.